People's Democratic Republic of Algeria
Ministry of Higher Education and Scientific Research
Hassiba Benbouali University of Chlef -UHBC
Faculty of Exact Sciences and Informatics
Department of Physics

THESIS

Presented for obtaining the degree of

DOCTORATE Es-Sciences

In PHYSICS

Option: MaterialsPhysics

Submitted by:

Moustafa TADJINE

Titled:

Plasma Effect on Adsorbed Biomolecules

Defended on 20/06/2024 in front of the jury composed of:

Prof. Habib RACHED	Hassiba Benbouali University - Chlef	Chairman
Dr. Abderrezak BERBRI	Hassiba Benbouali University - Chlef	Supervisor
Prof. Ahmed BOUHEKKA	Tissemsilt University - Tissemsilt	Co- Supervisor
Prof. Taïeb SEDDIK	Mustapha Stambouli University - Mascara	Examiner
Dr. Kaddour RAKRAK	Ibn Khaloun University- Tiaret	Examiner
Dr. Larbi FILALI	Higher school of Elec. and Ener. Engi. - Oran	Examiner
Dr. Halima BOUCHENAFA	Hassiba Benbouali University - Chlef	Invited
Dr. Hamida BOUHANI BENZIANE	Hassiba Benbouali University - Chlef	Invited

University year: 2023-2024

Acknowledgements

Elhamdolillah and thanks to ALLAH the Almighty for the blessings throughout my life and being to complete this scientific research of my PhD with success.

This thesis evolved with the generous help of a lot people to whom I feel greatly indebted. I would like to express my sincere thanks and deepest gratitude to my two supervisors, Prof. A. BOUHEKKA and Dr. A. BERBRI. I am deeply grateful to Prof. A. BOUHEKKA for the long insightful discussions and scientific advice about my research, I would thank him for his constant guidance, and for his patience and support that helped me overcome many crisis situations and finish this work, besides he gave me the independence to explore my research, and at the same time guided from the beginning to find the right way.

I will never forget that you used to come from the state of Tissemsilt to the University of Chlef in order to work with us for a full day, despite the hardship of travel.

I am also thankful to Dr. A. BERBRI for encouraging the use of correct and consistent notation in my writings and for carefully reading and commenting on countless revisions of this manuscript. More importantly, I am deeply grateful for the understanding, support and encouragement during the whole periods of time. I feel very fortunate for this opportunity to work under the supervision of two incredible mentors.

Many thanks for all the jury members who accepted to judge my thesis. I thank the president of the jury Prof. Habib RACHED from Chlef university and all the examiners: Prof. Taïeb SEDDIK from the university of Mascara, Dr. Larbi FILALI from the higher school of electrical and energy engineering of Oran, Dr. Kaddour RAKRAK from Tiaret university, Dr. Hamida BOUHANI BENZIANE and Dr. Halima BOUCHENAFA from Chlef university.

I have been fortunate to learn from many inspiring teachers over my school career. I also thank all the administration staff of our department, faculty and university for their help.

Many thanks to my colleagues at the lab and friends F.BOUZIDI, H.NEHMAR, for sharing with me this experience and I'm grateful for their support, I also thank all my friends who work at Algeria Telecom.

I thank my father MOHAMED for all things he has done for me. He sacrificed a lot to give me all the necessary conditions so that I can become what I am. My gratitude to him is inexpressible. I thank my dear mother for her love and support during all these years and thanks a lot dear brothers and sisters; you who always pushed me forward and believed in me.

At the end, I thank everybody who helped me directly or indirectly during this period of time to achieve this work.

Table of contents

Acknowledgements..... ii
Table of contents iii
Abstract..... vi
Nomenclature..... ix
List of figures xi
List of tables.....xvii
General introduction 18
References 20
I. The structure of protein and solid surface
I.1. Introduction..... 22
I.2. Amino acids..... 22
I.3. Classification of amino acids..... 23
I.3.1.Non polar aliphatic amino acids..... 23
I.3.2.Amino acids with aromatic R groups 23
I.3.3. Amino acids with polar, uncharged R groups 23
I.3.4. Amino acids with positively charged (basic) R groups..... 23
I.3.5. Amino acids with negatively charged (acidic) R groups..... 24
I.4.Peptide bond and polypeptide backbone..... 25
I.5. Proteins structure 26
I.5.1. Primary structure..... 27
I.5.2. Secondary structure..... 27
I.5.3. Tertiary structure..... 29
I.5.4.Quaternary structure..... 30
I.6.Some proteins..... 31
I.6.1. Fibrinogen protein..... 31
I.6.2. Human serum albumin..... 31
I.6.3.Bovine serum albumin..... 31
I.7. Solution pH effect on BSA form..... 34
I.8. Titanium dioxide TiO_2..... 36
I.9. Defects of TiO_2 solid surface..... 37
I.10.pH effect on TiO_2 surface..... 38
I.11. Protein-surface interactions under pH effect 38
I.12.Conclusion 39

References…….…….....…….…….....40

II. Proteins-solid surface interactions

II.1. Introduction ……..…….....…….…….....44

II.2.Phenomena of protein adsorption …….....…….…….....44

II.3. Factors controlling protein adsorption……..…….....46

II.3.1. Influence of external parameters on protein adsorption…….....47

II.3.1.1. Ionic strength……..….....47

II.3.1.2. Temperature…….....47

II.3.1.3. Concentration of proteins…….....48

II.3.2. Influence of protein properties on its adsorption ……..…….....48

II.3.2.1. Size……..…….....49

II.3.2.2.Charge……..…….....49

II.3.2.3.Structure stability……..…….....49

II.3.3.Influence of surface properties on protein adsorption…….....50

II.3.3.1. Topography……..…….....50

II.3.3.2.Composition……..…….....50

II.3.3.3.Hydrophobic interaction……..…….....50

II.4. Protein adsorption on flat surface……..…….....51

II.4.1. Impact of protein structures…….....51

II.4.2. Change of hydration state and reorganization of electric charges.....52

II.4.3. Adsorption and conformational changes of proteins….....53

II.5. Multilayer adsorption, reversibility and desorption….....53

II.6. Adsorption isotherm….....….....55

II.7. Plasma surface cleaning process…....….....56

II.7.1. Definition of plasma….....….....56

II.7.2. Internal reflection element….....56

II.7.3. Oxygen plasma and IRE cleaning….....….....59

II.8. Methods for measuring protein adsorption….....….....60

II.8.1. Attenuated total reflection FTIR-ATR spectroscopy….....….....61

II.8.2. FTIR Spectroscopy and protein structure….....….....62

II.8.3. FTIR spectrum of protein…..... …..…….....63

II.8.4.The correspondence between protein secondary structure and amide bonds.....63

II.9. Native and unfolded states of protein……..…….....64

II.10.Conclusion……..…….....…….…….....65

References ……..……..... …..……..... 66

III. In situ ATR-FTIR and two state kinetics model of BSA adsorption on TiO_2 surface

III.1. Introduction…..……..... …..……..……..……..... 72

III.2. Materials and methods…..……..... …..……..……..... 72

III.2.1. TiO_2 thin film preparation on germanium substrate…..……..... 72

III.2.2. In situ attenuated total reflection infrared spectroscopy…..……..... 73

III.3.ATR-FTIR results…..…….. ……..... …..……..... 73

III.3.1. The pH effect on the adsorption of BSA onto TiO_2anatase…..... 73

III.4. Kinetics model of BSA protein adsorption at a solid surface…..... 76

III.4.1Modeling of expanded BSA protein adsorbed at pH = 1.7……..... 89

III.5. Conclusion……..……..... …..……..... 90

References……..……..... …..……..... 92

IV. The effect of available space during unfolding process: A comparison study

IV.1. Introduction……..……..... …..……..... 95

IV.2. The effect of concentration and adsorption rate constant in case of equilibrium between adsorption and desorption ……..……..... 95

IV.2.1.Case of steady state……..……..... ……..... 101

IV.2.2. Case of steady state ($K_a = K_f + K_{d_1}$ and $K_{d_2} = K_f$) ……..…..... 103

IV.3. The effect of available space during unfolding in the case of steady state…..... 104

IV.4. Comparison between the two models in steady state case……..…..... 108

IV.4.1. Effect of available space in the case of time dependence of model B ($K_a = K_f + K_{d_1}$ and $K_f = K_{d_2}$)..... ……..……..... 109

IV.4.2.Comparison between the two models in the case of time dependence……..…… 110

IV.5. Application on FN adsorption and desorption processes……..……..... 112

IV.6. Conclusion...……...…...……..... 113

References ...……...……...……..... 114

General conclusion and perspectives...……...……...……..……..... 118

Abstract

It is well known that the study of protein interactions with solid surfaces is still a big challenge for scientists, due to the parameters that control this type of adsorption. Both structures (protein and surface) are very complicated, to be well identified especially when they become in contact. The aim of the present research of thesis is to investigate the adsorption of Bovine Serum Albumin protein with the surface of titanium dioxide (TiO_2) by modeling, and using in Situ attenuated total reflection spectroscopy.

An extended two states kinetics model was proposed and solved analytically then applied on the case of expanded BSA protein at TiO_2anatase surface at a pH value of 1.7 where the adsorption rate constant was evaluated and the using the model, we could determine the surface coverage of the native and unfolding states of protein. Another important thing was the study of the free available space effect during the unfolding process, and to compare it with the extended model where it was ignored. The findings of this research clearly demonstrated necessity of modeling to complete the experimental weakness, and it illustrated also the difference between the two models with and without taking into account the free space.

Keywords: Proteins adsorption, TiO_2 surface, In Situ FTIR-IR, Modeling, Kinetics model.

Résumé

Il est bien connu que l'étude des interactions des protéines avec les surfaces solides reste un défi de taille pour les scientifiques, en raison des paramètres qui contrôlent ce type d'adsorption. Les deux structures (protéine et surface) sont très compliquées, à bien identifier surtout lorsqu'elles entrent en contact. L'objectif de la présente recherche de thèse est d'étudier l'adsorption de la protéine d'albumine sérique bovine avec la surface du dioxyde de titane (TiO_2) en modélisant, et en utilisant la spectroscopie de réflexion totale atténuée in situ.

Un modèle cinétique étendu à deux états a été proposé et résolu analytiquement puis appliqué au cas de la protéine BSA expansée à la surface de l'anatase TiO_2 à une valeur de pH de 1.7. où la constante du taux d'adsorption a été évaluée et en utilisant le modèle, nous avons pu déterminer la couverture de surface des états natifs et de déploiement des protéines. Une autre chose importante était l'étude de l'effet d'espace disponible libre pendant le processus de déploiement, et sa comparaison avec le modèle étendu où il était ignoré. Les résultats de cette recherche ont clairement démontré la nécessité d'une modélisation pour compléter la faiblesse expérimentale, et ont également illustré la différence entre les deux modèles avec et sans prise en compte de l'espace libre.

Mots clés : Adsorption de protéines, surface TiO_2, In Situ FTIR-IR, Modélisation, Modèle cinétique.

ملخص.

من المعروف أن دراسة تفاعلات البروتين مع الأسطح الصلبة لا تزال تشكل تحدياً كبيراً للعلماء، بسبب العوامل التي تتحكم في هذا النوع من الامتزاز. كلا الهيكلين (البروتين والسطح) معقدان للغاية، بحيث لا يمكن التعرف عليهما بشكل جيدًا خاصة عندما يصبحان على اتصال.

الهدف من هذا البحث هو دراسة امتزاز بروتين ألبومين المصل البقري مع سطح ثاني أكسيد التيتانيوم (TiO_2) عن طريق النمذجة، واستخدام التحليل الطيفي للانعكاس الكلي الموهن في الموقع.

تم اقتراح نموذج حركي ممتد للحالتين وحله تحليليا ثم تطبيقه على حالة بروتين BSA الموسع على سطح TiO_2 Anatase عند قيمة pH = 1.7. بحيث تم تقييم ثابت معدل الامتزاز، وباستخدام النموذج تمكنا من تحديد التغطية السطحية للسطح، الحالات الأصلية والمتكشفة للبروتين. والأمر المهم الآخر هو دراسة تأثير المساحة الحرة المتاحة أثناء عملية الكشف ومقارنتها بالنموذج الموسع الذي تم تجاهله. وقد أظهرت نتائج هذا البحث بوضوح ضرورة النمذجة لاستكمال الضعف التجريبي، كما أوضحت الفرق بين النموذجين مع الأخذ بعين الاعتبار المساحة الحرة وبدونها.

الكلمات المفتاحية: امتزاز البروتينات، سطح TiO_2، في الموقع FTIR-IR، النمذجة، النموذج الحركي.

.

Nomenclature

FTIR-ATR : Fourier Transform Infrared Attenuated Total Reflection

PH : Potential Hydrogen.

FN : Fibrinogen.

HAS :Human Serum Albumin.

BSA :Bovine Serum Albumin.

TiO_2 : Titanium Dioxide.

V_O : Oxygen Vacancy.

OH_{br} : Bridging Hydroxyl Group

5f-Ti: Titanium Fivefold Coordinate.

6f-Ti : Titanium Six fold Coordinate.

UV : Ultraviolet.

σs :Surface Charge.

pI : Isoelectric Point.

BET : Brunauer-Emmett-Teller.

Ge : Germanium.

Si : Silicon.

IRE : Internal Reflection Element.

CO: Carbon Monoxide.

CO_2 : Carbon Dioxide.

H_2O : Water.

SPR : Surface Plasmon Resonance.

OWLS : Optical Waveguide Light Mode Spectroscopy.

XPS : X-ray Photoelectron Spectroscopy.

FITC : Fluoresce in isothiocyanate.

TIRF : Total Internal Reflection Fluorescence.

FRET : Förster Resonance Energy Transfer.

AFM : Atomic Force Microscopy.

ATR-IR : Attenuated Total Reflectance-Infrared.

IR : Infrared.

CD: Circular Dichroism Spectroscopy.

K_a : Rate constant of adsorption.

K_f : Rate constant of transformation.

K_{d_1}: Rate constant of desorption from native state.

K_{d_2}: Rate constant of desorption from unfolding state.

C_0 : Concentration.

θ_1 : The surface area occupied by protein in native state (surface coverage of native state).

θ_2 : The surface area occupied by protein in unfolded state (surface coverage of unfolded state).

θ: The full surface coverage occupied by protein in both states.

List of figures

Figure I.1: General form of amino acid.

FigureI.2: The 20 common amino acids of proteins: (a) Structure of non-polar aliphatic amino acids, (b) Structure of aromatic amino acids, (c) Structure of polar uncharged amino acids, (d) Structure of polar uncharged amino acids, (e) Structure of polar uncharged amino acids.

Figure I.3: Peptide formation.

Figure I.4: Geometry of backbone atoms.

Figure I.5: Protein in the four predominant structures.

Figure I.6: α-helix structure.

Figure I.7: Key to Structure β Sheets. (a) An antiparallel β sheet. (b) A parallel β sheet.

Figure I.8: Tertiary structure.

Figure I.9: Structure of BSA.

Figure I.10: A schematic diagram of conformational changes of BSA structure as a function of pH, a) N form = Native, b) F form = Fast and c) E form = Expanded).

Figure I.11: Crystallographic structures of TiO_2.

Figure I.12: Two models of the TiO_2 (110) surface. Both models show different defects and species discussed in the text. Large red balls represent O atoms, and small grey or yellow balls represent T_i atoms. Fivefold (5f-T_i) and sixfold (6f-T_i) coordinated T_i atoms, bridge bonded O species (O_{br}), single oxygen vacancies (V_o), bridging hydroxyl group (OH_{br}), and the on-top bonded O species (O_{ot}) are indicated.

Figure I.13: Charge surface of TiO_2 at different pH. (a) pH<pHpzc, (b) pH=pHpzc and (c) pH>pHpzc.

Figure I.14: Schematic representation of: The theoretical variation of the surface charge (σs) vs pH curves for (a) HAS in solution and (b) TiO_2 colloidal particles. (c) Representation of protein molecules adsorbed under different electrostatics conditions.

Figure II.1: Schematic representation of protein- solid surface interactions mechanism (adapted from Norde and Haynes).

Figure II.2: Schematic illustration of (a) a globular protein, whose conformation may be distorted on interaction with the surface and (b) a rod-like protein undergoing multistage process where (i) initially the protein adsorbs with its long axis parallel to the surface and (ii) rearrangement of protein molecules occurs to increase a protein-protein interaction (reproduced from).

Figure II.3: Schematic representation of protein monolayer to show difference between high and low concentration on protein adsorption on flat surface.

Figure II.4: Schematic representation of interaction between a surface and a hard protein and soft protein.

Figure II.5: Schematic representation of the change of hydration state to an interaction between negative charged surface and proteins. Ions in solution are represented by negative and positive charges.

Figure II.6: Illustration of the development of an adsorbed protein layer formed when a surface is exposed to a single-component protein solution of constant concentration.

Figure II.7: Shape of different adsorption isotherms: Plot of surface concentration (q) vs solution concentration (C) with (a) Langmuir isotherm (——), (b) BET isotherm (-.-), (c) Freundlich isotherm (---).

Figure II.8: Schematic representation of the four states of matter.

Figure II.9: (a) Ge surface with organic contamination (black). (b) Atomic oxygen (red) reacts with carbon on the surface and forms volatile CO, CO_2 and H_2O leaving behind a carbon-free Ge surface (c).

Figure II.10: (a) Harrick plasma cleaning machine, and (b) Germanium substrates cleaned in oxygen plasma unde around 890 mtorr (pictures kindly given by A. Bouhekka).

Figure II.11: A multiple reflection ATR system.

Figure II.12: Time-dependent molecular spreading of a protein on a surface.

Figure II.13: Effect of protein unfolding on interaction with a surface.

Figure III.1: (a) The equilibrium spectra of BSA protein adsorption onto TiO_2anatase thin films surface under various pH values (water is used as a solvent at 10-6 mol/l of BSA concentration). (b) Maximum of amide I band versus pH

values (Experiments were done by A. Bouhekka who kindly gave these graphs).

Figure III.2:(a) ATR-IR spectra collected in situ recorded during adsorption of BSA protein onto TiO_2anatase surface at pH = 1.7 where the difference between each two successive spectra was around 7.5 min. (b) Absorbance variation of amide I band versus time and the difference between the first spectrum and background was taken as the origin of time (Experiments were done by A. Bouhekka who kindly gave these graphs).

Figure III.3: The normalized absorption intensity of amide I (full surface coverage (Θ)) of BSA adsorbed onto TiO_2anatase surface versus time at pH = 1.7.

Figure III.4: A schematic illustrating the adsorption model of BSA protein on a solid surface presented in terms of the dependence of relative surface coverage by BSA.

Figure III.5: The time dependence of the native (Θ_1), unfolding (Θ_2) states and full surface coverage (Θ) calculated for BSA adsorption on a gold surface using data from where $C_0 = 3 \times 10^{-6}$ mol/l, $K_a = 1.57 \times 10^5$ mol^{-1} l min^{-1}, $K_f = 0.80 \times 10^{-2}$ min^{-1} and $K_{d_1} = 0.74 \times 10^{-1}$ min^{-1}. $K_{d_2}$was chosen slightly different from K_{d_1} ($K_{d_2} = 0.1 \times 10^{-1}$ min^{-1}).

Figure III.6: The time dependence of the native (Θ_1), unfolding (Θ_2) states and full surface coverage (Θ) calculatedfor BSA adsorption on a gold surface using data from where $C_0 = 3 \times 10^{-6}$ mol/l, $K_a = 1.57 \times 10^5$ mol^{-1} l min^{-1}, $K_f = 0.80 \times 10^{-2}$ min^{-1} and $K_{d_1} = 0.74 \times 10^{-1}$ min^{-1}.

Figure III.7: The time dependence of surface coverage of BSA where (Θ_1) indicated by dashed lines (— —) and continuous lines (——) for (Θ_2) for different values of rate transformation constant K_f. The parameters used are: $K_a = 1.57 \times 10^5$ mol^{-1} l $min^{-1}$and $C_0 = 3 \times 10^{-6}$ mol/l.

Figure III.8: The time dependence of surface coverage of BSA where (Θ_1) indicated by dashed lines (— —) and continuous lines (——) for (Θ_2) for different values of rate adsorption constant K_a. The parameters used are: $K_f = 0.8 \times 10^{-2}$ $min^{-1}$and $C_0 = 3 \times 10^{-6}$ mol/l.

Figure III.9: The time dependence of full surface coverage of BSA (Θ) for different values of rate adsorption constant K_a. The parameters used are: K_f = 0.8 x 10^{-2} $min^{-1}$and C_0 = 3 x 10^{-6} mol/l.

Figure III.10: The time dependence of native and unfolding states of BSA for different concentrations (same color for each value of C_0).Θ_1 dashed lines (— —) and $\Theta_2$continuous lines (——). The parameters used areK_a= 1.57 x 10^5 mol^{-1} l min^{-1} and K_f= 0.8 x $10^{-2}min^{-1}$.

Figure III.11: The time dependence of full surface coverage of BSA (Θ) for different concentrations. The parameters used areK_a=1.57 x 10^5 mol^{-1} l $min^{-1}$and K_f = 0.8x $10^{-2}min^{-1}$.

Figure III.12: Three dimensions 3D kinetic curves of: (a) the native state (Θ_1), (b) unfolding state (Θ_2) and (c) full surface coverage (Θ) versus time and concentration. The parameters used are K_a= 1.57 x 10^5 mol^{-1} l $min^{-1}$and K_f= 0.8 x $10^{-2}min^{-1}$.

Figure III.13: Fitting of experimental data of the full surface coverage of BSA protein adsorbed onto TiO_2anatase surface at pH = 1.7.

Figure IV.1: The time dependence of native and unfolding states of BSA for different concentrations (same color for each value of C_0).$\Theta_1$dashed lines (— —) and $\Theta_2$continuous lines (——). The parameters used areK_a= K_f+ K_{d_1}= 0.082 mol^{-1} l min^{-1}, K_{d_2}= K_f = 0.8 x $10^{-2}min^{-1}$ and K_{d_1}= 0.74 x $10^{-1}min^{-1}$.

Figure IV.2: Represent the variation of the surface rate coverage as a function of temperature (K), a) for OH and O_b and b) for H_2O.

Figure IV.3: The time dependence of surface coverage of BSA where (Θ_1) indicated by dashed lines (— —) and continuous lines (——) for (Θ_2) for different values of rate adsorption constant K_a. The parameters used are: C_0 = 3 x $10^{-0.5}$ mol/l, K_a= K_f+ $K_{d_1}$and K_{d_2}= K_f.

Figure IV.4: The time dependence of full surface coverage of BSA (Θ) for different values of rate adsorption constant K_a. The parameters used are: C_0 = 3 x $10^{-0.5}$ mol/l, K_a= K_f+ $K_{d_1}$and K_{d_2}= K_f.

Figure IV.5: (Model A = 0). The versus concentrations of the native (Θ_1), unfolding (Θ_2) states and full surface coverage (Θ) calculated for BSA adsorption on a surface using data from [10] where, K_a= 1.57 x10^5 $mol^{-1}lmin^{-1}$, K_f = 0.80 x10^{-2} min^{-1}, K_{d_1}= 0.74 x10^{-1} min^{-1} and K_{d_2}= 0.1x 10^{-1} min^{-1}.

Figure IV.6: (Model A = 0).The versus concentrations of the native (Θ_1), unfolding (Θ_2) states and full surface coverage (Θ) calculated for BSA adsorption on a surface. The parameters used areK_a=K_f+ K_{d_1}= 0.082 mol^{-1} l min^{-1}, K_{d_2}= K_f = 0.8 x $10^{-2}min^{-1}$ and K_{d_1}= 0.74 x $10^{-1}min^{-1}$.

Figure IV.7: The concentration dependence of surface coverage of BSA where (Θ_1) indicated by dashed lines (— —) and continuous lines (———) for (Θ_2) for different values of rate adsorption constant K_a. The parameters used are K_f= 0.8 x $10^{-2}min^{-1}$, K_{d_1}= 0.74 x $10^{-1}min^{-1}$ and K_{d_2}= 0.1x 10^{-1} min^{-1}.

Figure IV.8: The concentration dependence of full surface coverage of BSA (Θ) for different concentrations. The parameters used are K_a= 1.57 x 10^5 mol^{-1} l min^{-1}, K_f = 0.8 x $10^{-2}min^{-1}$, K_{d_1}= 0.74 x $10^{-1}min^{-1}$ and K_{d_2}= 0.1x 10^{-1} min^{-1}.

Figure IV.9: The concentration dependence of surface coverage of BSA where (Θ_1) indicated by dashed lines (— —) and continuous lines (———) for (Θ_2) for different values of rate transformation constant K_f. The parameters used are K_a= 1.57 x 10^5 mol^{-1} l min^{-1}, K_{d_1}= 0.74 x $10^{-1}min^{-1}$ and K_{d_2}= 0.1x 10^{-1} min^{-1}.

Figure IV.10: The versus concentrations of the native (Θ_1), unfolding (Θ_2) states and full surface coverage (Θ) of BSA where(Model A = 0) indicated by dashed lines (— —) and continuous lines (———) for (Model B = 0). The parameters used areK_a= 1.57 x 10^5 mol^{-1} l min^{-1},K_f= 0.8 x $10^{-2}min^{-1}$, K_{d_1}= 0.74 x $10^{-1}min^{-1}$ and K_{d_2}= 0.1x 10^{-1} min^{-1}.

Figure IV.11: The time dependence of surface coverage of BSA where (Θ_1) indicated by dashed lines (— —) and continuous lines (———) for (Θ_2) for different concentrations (same color for each value of C_0). The parameters used are:

$K_a = K_f + K_{d_1} = 0.082$ mol^{-1} l min^{-1}, $K_{d_2} = K_f = 0.8 \times 10^{-2} min^{-1}$ and $K_{d_1} = 0.74 \times 10^{-1} min^{-1}$.

Figure IV.12: The time dependence of the native (Θ_1) and unfolding (Θ_2) states calculated for BSA adsorption on a gold surface using data from,(a) Model B VARIABLE and (b) Model A VARIABLE. The parameters used are $C_0 = 3 \times 10^{-6}$ mol/l, $K_a = 1.57 \times 10^5$ mol^{-1} l min^{-1}, $K_f = 0.8 \times 10^{-2} min^{-1}$, $K_{d_1} = 0.74 \times 10^{-1} min^{-1}$ and $K_{d_2} = 0.1 \times 10^{-1}$ min^{-1}.

Figure IV.13: The time dependence of the native (Θ_1), unfolding (Θ_2) states and full surface coverage (Θ) calculated for FN adsorption on a surface using data from **[37]** where $C_0 = 0.2$ g/l, $K_a = 8.03 \times 10^3$ mol^{-1} l s^{-1}, $K_f = 5.32 \times 10^{-4}$ s^{-1} and $K_{d_1} = 6.76 \times 10^{-3}$ s^{-1}.

List of tables

Table I.1: The composition in amino acids of BSA protein (presence of S in the molecule).

Table I.2: Atomic composition of BSA protein.

Table II.1: Chemical bond energies of organic molecules found on the Ge surface.

Table II.2: Band assignments in the amide I region of FTIR spectrum.

General introduction

Understanding the interactions of bio-molecules with surfaces of solid is of great interest in several fields of industrial and medical applications, such as reparatory implants, biosensors, biofouling, food and biochemical processing**[1-5]**.

Several experimental techniques are used to investigate this complex process to get necessary information about the mechanism of interactions and the behavior of adsorbed molecules. There are several methods commonly used to measure protein adsorption, each with its own advantages and limitations. some of the most common methods**[6,7]**:infrared spectroscopy (IR), X-ray photoelectron spectroscopy (XPS) , circular dichroism (CD) spectroscopy **[8-10]**, atomic force microscopy (AFM),total internal reflection fluorescence (TIRF), surface plasmon resonance (SPR) and attenuated total internal reflectance-infrared spectroscopy (ATR-IR)**[6, 11-14]**.

Using the previous methods to study this complex phenomenon is not always a good option where modeling and simulation are mandatory because of the parameters that control these interactions. One of the most important knowledge we are looking for is the coverage of the surface during the adsorption process; where mathematical models are necessary and they can be valid only if we compare them with experimental results.

The aim of this thesis goes in this last point. We are interested to determine the coverage of BSA protein at TiO_2surface taking into account the two states of adsorption where we have native and unfolding states. To achieve this goal we extended the two states kinetics model that was applied on experimental results of expanded BSA (PH< 2.7) taken by in Situ FTIR-IR. Proteins are huge molecules that have so many functional groups and their adsorption is driven by different forces including van der Waals, electrostatic and hydrophilicity. This kind of adsorption happens on the surface and is still not well understood.

To make things clear for future readers; this dissertation contains, after this general introduction, four chapters and general conclusion:

The first chapter is devoted to presenting protein composition and its four levels of structure. It also illustrates some proteins like Fibrinogen; Human Serum Albumin; Bovine

Serum Albumin. The pH parameter is the most important one which affects the structure of the protein and determines the electrostatic state of proteins. We will also give three structures of the surface Titanium dioxide TiO_2 and its characteristics and defects.

The second chapter introduces the structure and the physical characteristics of proteins. It presents also the phenomenon of protein adsorption on solid surfaces and the parameters that influence it. We will present the methods for oxygen plasma cleaning involves exposing a substrate or surface to a plasma formed from oxygen gas. This plasma contains highly reactive oxygen species such as ions, radicals, and atoms. This process effectively cleans the surface and removes organic residues, improving surface wettability and adhesion properties.

We will present several methods for measuring protein adsorption, the method Attenuated total reflection spectroscopy FTIR-ART used as a main technique in our work to investigate the interfaces phenomena.

Results of our study are in the tow last chapters III and IV. In the third we give the method for preparing thin layers of TiO_2 substrate; the results clearly elucidate the effect of pH on the adsorption of BSA onto TiO_2anatase surface. The model proposed and its application to calculate the full surface coverage (Θ), the native state (θ_1)and unfolding state (θ_2) plus the adsorption rate constant for several parameters like concentration C_0 and K_a, K_f, K_{d_1} and K_{d_2}which are the rate constants of adsorption, transformation and desorption from native and unfolding states, respectively. In chapter IV, we did a comparison study of the model with another one when taking into account free available space during the unfolding process which was neglected in the calculation of chapter III.

It is very important to conclude this thesis by a general conclusion in which we resume the most important efforts and results of our research contribution and the recommendations for future research in the field of bio-molecule adsorption onto solid surfaces.

References

[1] R.A. Latour, "Fundamental principles of the thermodynamics and kinetics of protein adsorption to material surfaces". Colloids and Surfaces B: Biointerfaces**191**, 110992(2020).

[2]A. Bratek-Skicki, P.Żeliszewska and Z. Adamczyk, "Tuning conformations offibrinogen monolayers on latex particles by pH of adsorption". Colloids and Surfaces B: Biointerfaces **103**, 482–488 (2013).

[3]S. Gonand M.M. Santore,"Sensitivity of protein adsorption to architectural variations in a protein-resistant polymer brush containing engineered nanoscaleadhesive sites".Langmuir**27**(24), 15083–15091 (2011).

[4]C.J. Nonckreman, S. Fleith, P.G. Rouxhet and C.C. Dupont-Gillain,"Competitiveadsorption of fibrinogen and albumin and blood platelet adhesion on surfaces modifiedwithnanoparticles and/or PEO.Colloids Surf B Biointerfaces**77**(2), 139–149 (2010).

[5] J.Y. Yoon, J.H. Kimand W.S. Kim,"Interpretation of protein adsorption phenomenaonto functional microspheres". Colloids and Surfaces B: Biointerfaces**12**(1), 15–22(1998).

[6] S.D. Stuchebryukov,"Attenuated total refection spectroscopy under conditions weakabsorption: New method for determination of integrated intensities". Protection of Metals and Physical Chemistry of Surfaces**46**,366–374(2010).

[7] J. Saikia, M. Yazdimamaghani, S.P. HadipourMoghaddamand H. Ghandehari,"Differential protein adsorption and cellular uptake of silica nanoparticles based on size and porosity". ACS applied materials and interfaces **8**(50), 34820-34832 (2016).

[8] Y. Brahmi, L. Filali, J.D. Sib, A. Bouhekka, D. Benlakehal, Y. Bouizem, A.Kebaband L.Chahed, "Conformational study of protein interactions with hydrogen-passivatedamorphous silicon surfaces: effect of pH". Appl. Surf. Sci.**423**, 394–402(2017).

[9] L. Filali,"Protein adsorption on hydrogenated silicon surfaces". Doctoral thesis, University of Oran 1, Algeria (2018).

[10] Y. Brahmi, "Electrostatic interactions effect on the adsorption of proteins on hydrogenated amorphous and nanocrystalline silicon at the solid/liquid interface". Doctoralthesis, University of Oran, Algeria (2018).

[11] S. Tunc, M.F. Maitz, G. Steiner, L. Vázquez, M.T. Pham and R. Salzer, "In situconformational analysis of fibrinogen adsorbed on Si surfaces". Colloids and Surfaces B: Biointerfaces**42**, 219-225(2005).

[12]B. Stuart, "Infrared Spectroscopy: Fundamentals and Applications", Book Series:Analytical Techniques in the Sciences (2004).

[13]T.F. Kumosinki and J.J. Unruh,"Quantization of the global secondary structure ofglobular proteins by FTIR spectroscopy: comparison with X-ray crystallographicstructure". Talanta**43**, 199-219(1996).

[14]A. Bouhekka,"Adsorption of BSAprotein on silicon, germanium and titanium dioxide investigated by In Situ ATR-IR spectroscopy". Doctoral thesis, University of Oran, Algeria (2013).

Chapter I

The structure of protein and solid surface

I.1 Introduction

Biomolecules like proteins are considered one of the most abundant organic molecules in living systems. They have the most diverse range of functions of all macromolecules. Proteins may be structural, regulatory, contractile, or protective; they may serve in transport, storage, or membranes; or they may be toxins or enzymes **[1]**. Each cell in a living system can contain thousands of different proteins, each with a unique function. Their structures, like their functions, vary greatly. They are polymers of alpha amino acids, arranged in a linear sequence and connected together by covalent bonds **[2]**.

We have more than 80 amino acids in the nature but only some of them (20) can contribute in the constitution of proteins.

I.2. Amino acids

The building blocks of proteins are amino acids. Twenty types of amino acids have been found in protein structures. A typical amino acid has an amine functional group ($-NH_2$) and a carboxyl functional group (-COOH). In an amino acid, these two groups are attached to a C atom, which is referred to as C_α (Figure I.1) **[3]**.

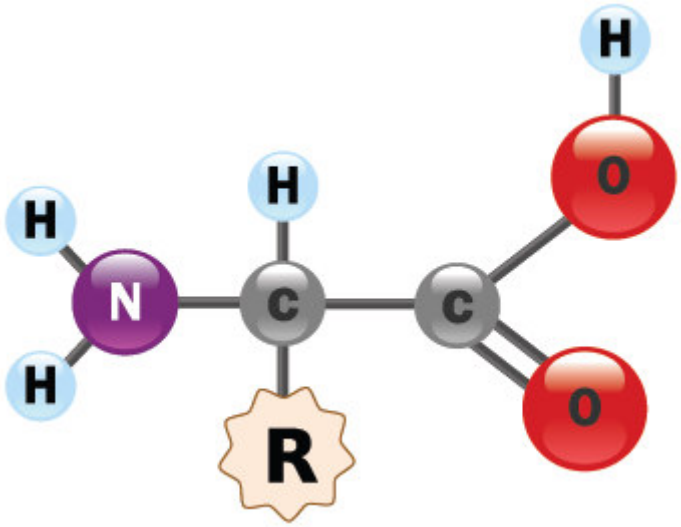

Figure I.1: General form of amino acid **[4]**.

In addition, an R group is attached to the C_α in the amino acid, and is referred to as the side chain of the amino acid. The amino acids differ mainly by the types of their side chains. An R group can be as simple as an H atom, or as complex as to contain aromatic

substructure. Twenty formulas for the side chains have been found in protein structures, resulting in twenty types of amino acids **[3]**.

I.3. Classification of amino acids

Classification of amino acids according to the polarities of R group is the most common way of classification. According to this classification there are five types of amino acids.

I.3.1. Non polar aliphatic amino acids

This group contains seven amino acids. Four amino acids glycine, alanine, valine, leucine and isoleucine have are R groups of aliphatic hydrocarbon (Figure I.2-a). Methionine, one of the two sulfur containing amino acids has a slightly non polar thiol ether side chain. Proline has a cyclic secondary amino (imino) group **[5]**.

I.3.2. Amino acids with aromatic R groups

Three amino acids namely phenylalanine, tyrosine and tryptophan have aromatic side chain that makes them slightly non polar (hydrophobic) and hence participate in hydrophobic interactions (Figure I.2-b). Tyrosine and tryptophan are relatively more polar than phenylalanine due to presence of –OH group in tyrosine and the nitrogen atom in the indole ring of tryptophan **[6]**.

I.3.3. Amino acids with polar, uncharged R groups

The amino acids that belong to this class are serine, threonine, cycteine, asparagine and glutamine (Figure I.2-c). The R groups of these amino acids are polar (hydrophilic) and therefore they are more soluble in water. Polarity in these amino acids is because they contain functional groups like -OH (serine and threonine), -$CONH_2$ (glutamine and asparagine), -SH (cysteine) **[5]**.

I.3.4. Amino acids with positively charged (basic) R groups

In this class of amino acids R groups have positive charge at physiological pH (Figure I.2-d). Lysine has a second primary amino group at the ε position on its aliphatic chain. Arginine has a positively charged guanidium group and histidine has an aromatic imidazole group **[7]**.

I.3.5. Amino acids with negatively charged (acidic) R groups

There are two amino acids having a negative charge at pH 7.0 (Figure I.2-e). These are aspartate and glutamate; both contain a second -COOH group **[8]**.

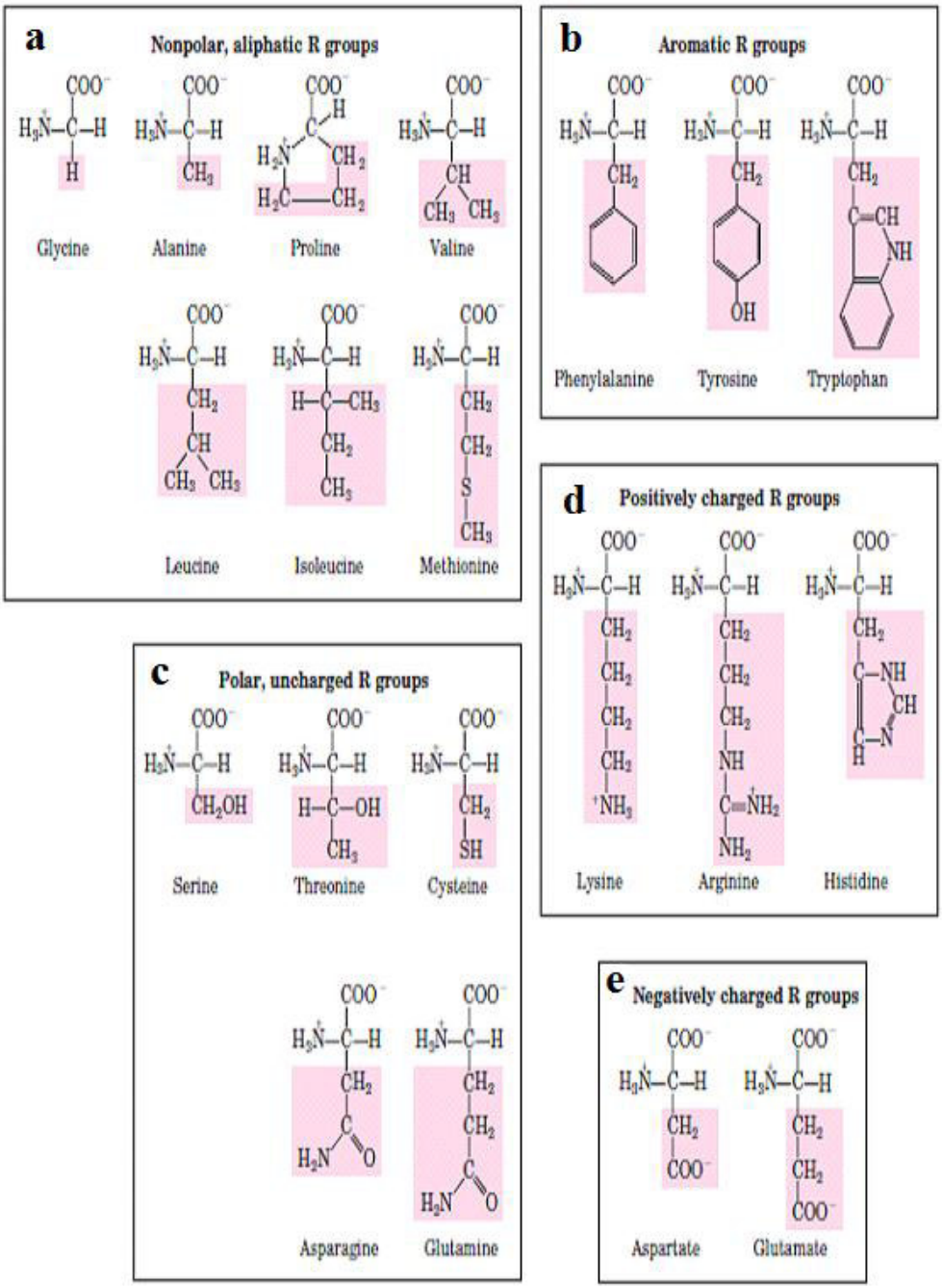

Figure I.2: The 20 common amino acids of proteins: (a) Structure of non-polar aliphatic amino acids, (b) Structure of aromatic amino acids, (c) Structure of polar uncharged amino acids, (d) Structure of polar uncharged amino acids, (e) Structure of polar uncharged amino acids **[9]**.

I.4. Peptide bond and polypeptide backbone

Two amino acids can react to form a peptide bond. In particular, the amine group of one amino acid reacts with the other amino acid's carboxyl group to create a new peptide bond, releasing one water molecule in the process (Figure I.3). One end of this new molecule is an amine group, and the other end is a carboxyl group. This enables the molecule to continually react with other amino acids to form a polymerization of amino acids. A protein is a polymerization of amino acids **[3, 10, 11]**.

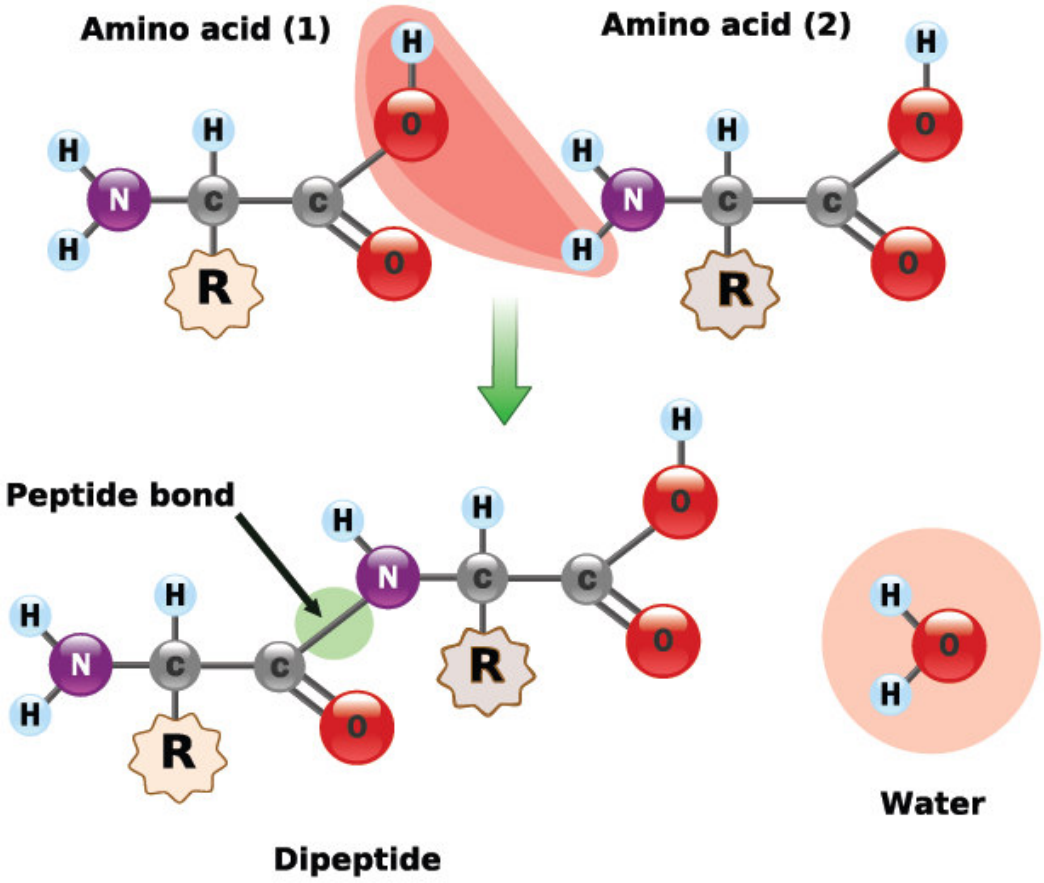

Figure I.3: Peptide formation **[4]**.

The backbone or main chain of a protein refers to the atoms that participate in peptide bonds, ignoring the side chains of the amino acid residues. The backbone is drawn as a linked sequence of rigid planar peptide groups. Its conformation can be described by the torsion angles (also called dihedral angles or rotation angles) around the Cα−N bond (ϕ) and the Cα−C bond (ψ) of each residue (Figure I.4). Rotation around the Cα−N and Cα−C bonds to make (form) certain combinations of ϕ and ψ angles may cause the amide

hydrogen, the carbonyl oxygen, or the substituent of Cα of adjacent residues to collide. Certain conformations of longer polypeptides can similarly produce collisions between residues that are far apart in sequence **[12]**.

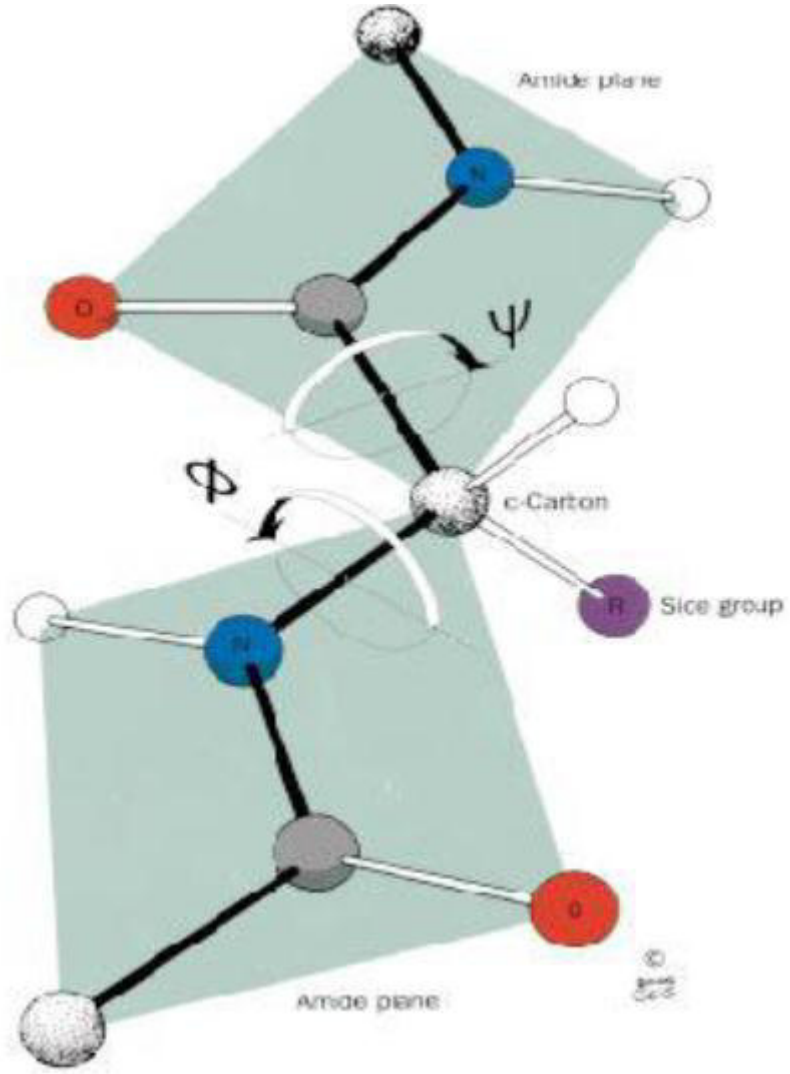

Figure I.4: Geometry of backbone atoms **[10]**.

I.5. Proteins structure

The 20 standard amino acids join through peptide bonds to form proteins. Protein has four levels of structure namely primary, secondary, tertiary and quaternary (Figure I.5).

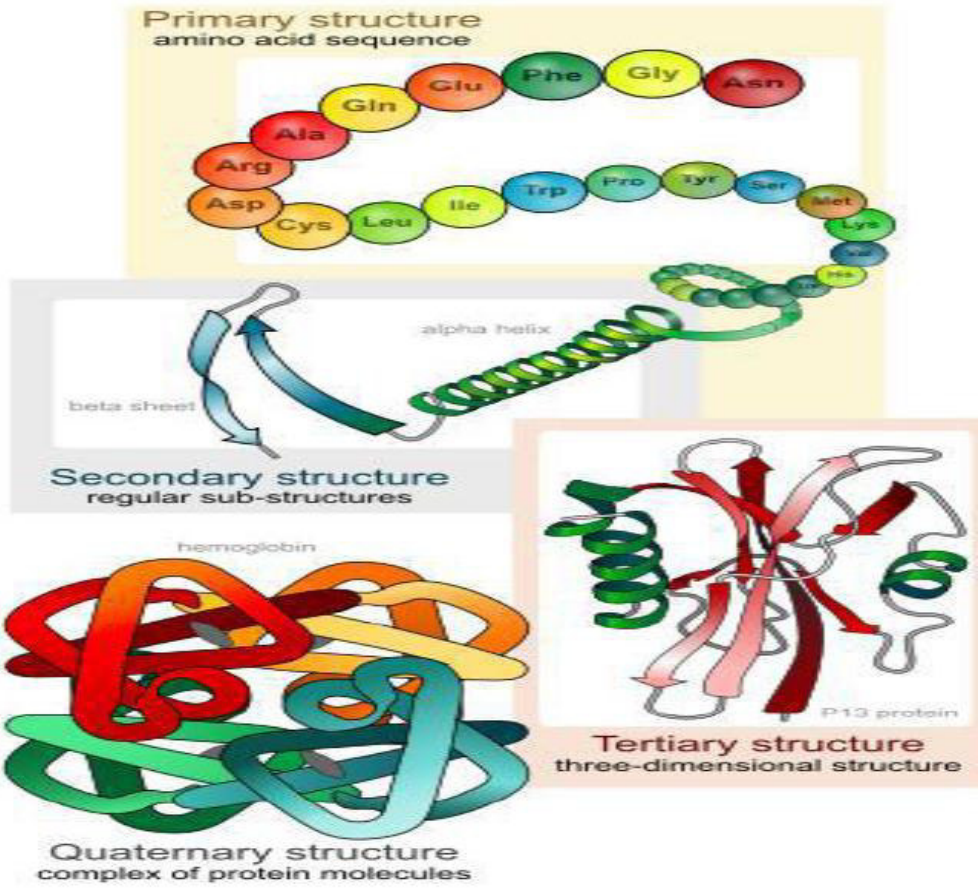

Figure I.5: Protein in the four predominant structures **[13]**.

I.5.1. Primary structure

Refers to the linear sequence of amino acids which is genetically determined and often modelled as beads on a string, where each bead represents one amino acid unit.

I.5.2. Secondary structure

Amino acids can rotate around bonds within a protein. This is the reason why proteins are flexible and can fold into a variety of shapes. Folding can be irregular or certain regions can have a repeating folding pattern.

Folding of polypepeptide chain is possible because of the presence of hydrogen bond. A regular secondary structure occurs when each dihedral angle φ and ψ remains the same or nearly same throughout the segment. Because of the planar nature of the peptide bonds, only certain types of secondary structure exist. The most important secondary structures are α-helix, β-sheets.

α Helix: As illustrated by figure I.6; Pauling and Corey observed that a polypeptide chain with planar peptide bonds would build a right handed helical structure by simple twists about the Cα–N and the Cα–C bonds. They called this helical structure as α helix. An α helix is a rod like structure **[14]**. The inner part of helix is made up of the tightly coiled backbone and the side chains extend outward in the helix. The protruding side chains determine the interaction of α helix both with other parts of the folded protein chain and with other protein molecules. The helix is stabilized by hydrogen bonds between NH and CO groups of the main chain. The α helix contains 3.6 amino acids per turn of the helix. All known polypeptides contain right handed α helix. The occurrence of α helical content in proteins ranges widely. For example in ferritin, that helps storage of iron, has 75% of its amino acid residues form α helix **[15]**.

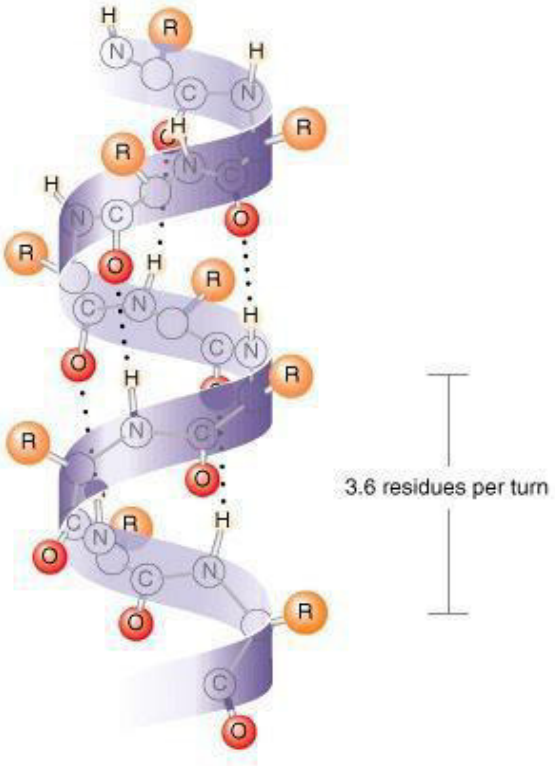

Figure I.6: α-helix structure **[15]**.

β sheet: The second type of periodic structure is β sheet. The β sheet involves hydrogen bonds between groups from residues distant from each other in the linear sequence. In β sheets two or more strands widely separated in the protein sequence are arranged side by side, with hydrogen bonds between the strands. Based on the orientation of the strands β sheets are of two types.

1. The antiparallel β sheet, in which neighboring hydrogen-bonded polypeptide chains run in opposite directions (Figure I.7-a).

2. The parallel β sheet, in which the hydrogen-bonded chains extend in the same direction (Figure I.7-b).

In parallel arrangement the NH group is hydrogen bonded to the CO group of the one amino acid on the adjacent strand, whereas the CO group is hydrogen bonded to the NH group on the amino acids two residues farther along the chain **[16,17]**.

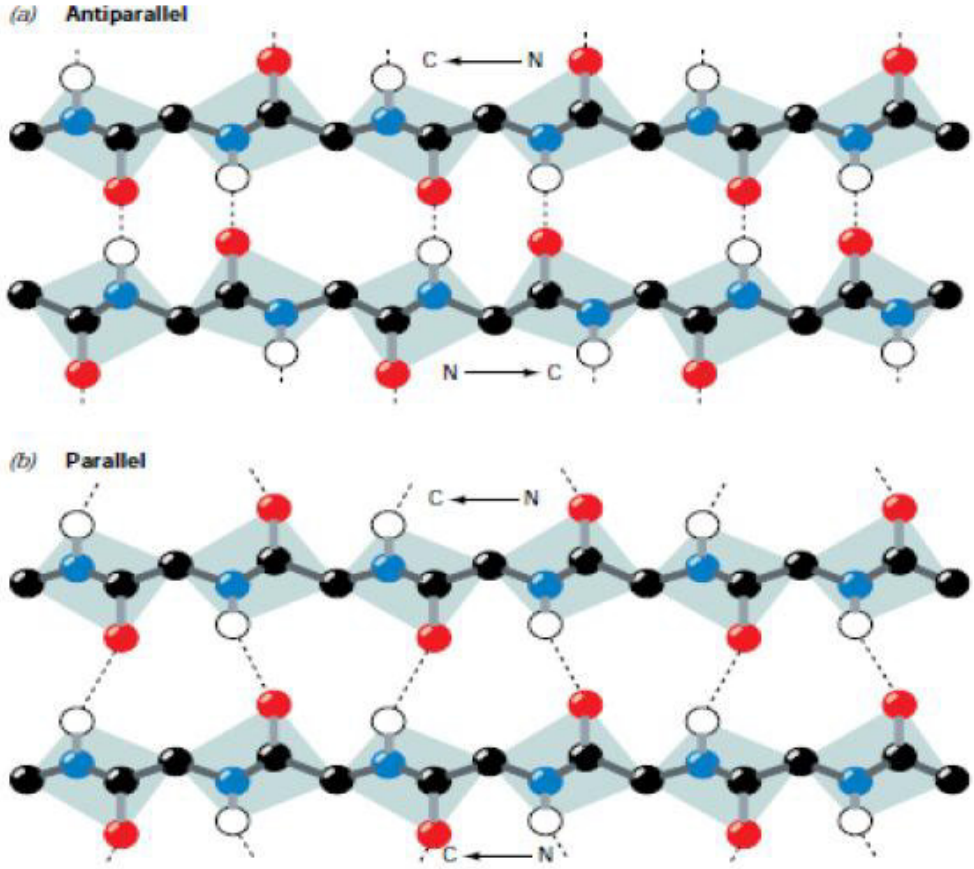

Figure I.7: Key to Structure β Sheets. (a) An antiparallel β sheet. (b) A parallel β sheet **[10]**.

I.5.3. Tertiary structure

Is the folding of a single polypeptide chain? The most important factor in determining the tertiary structure of globular proteins is the hydrophobic effect. Hydrogen bonding involving groups from both the peptide backbone and the side chains are important in

stabilizing tertiary structure **[18]**. Tertiary structure arises when various elements of secondary structure pack tightly together to form the well-defined three dimensional structures. However, the shape is maintained permanently by the intra- molecular bonds; hydrogen bond of one hydrogen atom shared by two other atoms, Van der Waals force is the weak force that incurs when two or more atoms are very close, disulphide bond which is a strong covalent bond formed between two adjacent cysteine amino acids that stabilizes the tertiary shape of a protein, and ionic bond as electrostatic interaction between oppositely charged ions (Figure I.8) **[19]**.

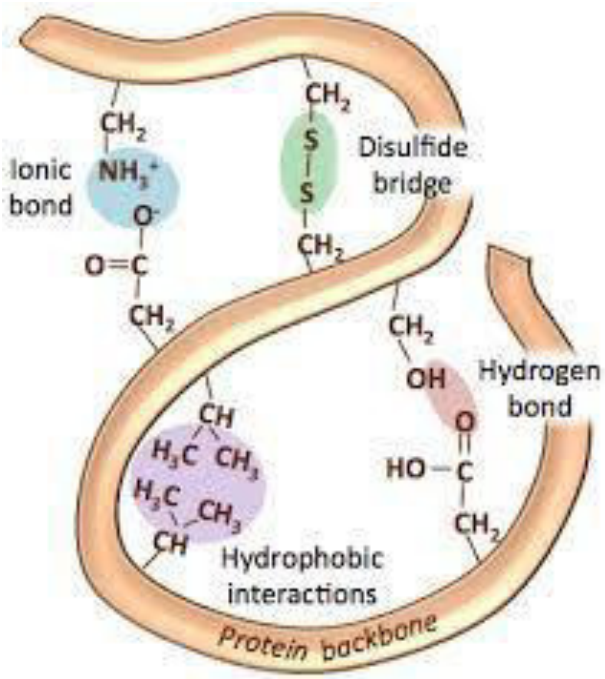

Figure I.8: Tertiary structure **[10]**.

I.5.4. Quaternary structure

In nature, some proteins form from several polypeptides. Each polypeptide chain in such a protein is called subunit. These subunits may be identical or different in their primary structure. These subunits may associate specifically to each other to form large sized complex molecule known as quaternary structure. Quaternary structure is the spatial arrangement of subunits and the nature of their contact. The same forces **i.e**. disulfide, hydrogen, hydrophobic and ionic bonds are involved in tertiary structure formation are also involved in quaternary structure to link various polypeptide chains. The simplest type of

quaternary structure is a dimer consisting of two subunits. If the two subunits or polypeptides are identical the quaternary protein is termed homodimer **[8, 20**].

I.6. Some proteins

I.6.1. Fibrinogen protein

Fibrinogen (FN) is an extracellular protein with a size of 45 nm × 9 nm× 6 nm and a weight of 340 kDa **[21]**. It is found in blood in concentrations of ≈3 mg/ml **[22**], and the isoelectric point is 5.1 FN is known to have good adsorption on various surfaces and synthetic material, especially onto hydrophobic and charged surfaces.

Fibrinogen is usually used to investigate cell adhesion due to the structural similarity with fibronectin. H. Anna Gry et *al.*, studied fibrinogen adsorption on various substrates: titanium oxide, tantalum oxide and gold. A difference between the different films was observed showing that the surface chemistry plays a large role in determining the adsorbed amount of proteins **[21]**.

I.6.2. Human serum albumin

HSA is the most abundant protein in human blood circulating at 35–45 g/L. HSA participates in multiple functions including regulation of osmotic pressure, protection against oxidative stress, and transportation of several molecules **[23]**. The HSA molecule is synthesized in the liver and it is a single peptide chain protein formed of 585 amino acids and it's presented in three homologous domains (I, II, and III) which are further divided into subdomains (A and B) of similar structural motifs, but which have different ligand-binding functions **[24]**. The HSA molecule is a 67 kDa globular protein and in the physiological environment, 68% is found in α-helix configuration. As a transport protein, HSA can easily bind to a wide range of molecules via ligands. Additionally, the HSA molecule interacts with polymeric surfaces and undergoes conformational changes upon adsorption.

I.6.3. Bovine serum albumin

Bovine Serum albumin or BSA has been one of the most extensively studied proteins for many years. It is the most abundant protein in blood plasma with a typical concentration of 50 g/L and functions as a transport protein for numerous endogenous and exogenous substances. It also plays an important role in regulating the colloid osmotic pressure of

blood, for which it provides about 80% of the osmotic pressure and is responsible for the pH maintenance in blood **[25]**. BSA is pretty much used for protein adsorption studies since its structure is close to the human serum albumin HSA structure **[26]**.

It is a good model protein to be studied because it tends to adsorb on all solid surfaces **[27]**, and since it is easily available.

It is a globular and soft protein with a flexible structure which readily changes its conformation **[28]**. It is also an amphiphilic protein due to the presence of NH_2 and COOH in its structure, and its net charge depends on the pH of the solution which determines the electrostatic state of the protein **[29]**.

BSA is generally used as a model protein in several fields of research such as, among others, molecular biology, medicine, agri-food and the environment **[30]**. The bovine serum albumin has a 76% sequence similarity with human serum albumin (HSA) **[31]**. The amino acid composition of BSA was published for the first time by J.R. Brown in 1975 **[32]** and, in 1990, Hirayama et *al.* **[33]** reviewed the primary structure of the BSA. The results obtained by the two groups are shown in Table I.1. From the amino acid assembly, it is possible to deduce the elementary composition of the protein, that is to say the number of carbon atoms, nitrogen, of oxygen and sulfur that can be found in each molecule of BSA (Table I.2).

Table I.1: The composition in amino acids of BSA protein (presence of S in the molecule) **[30]**

Amino Acids	Number of residues	
Aspartic acid	41	41
Arginine	23	26
Asparagine	13	14
Glutamic acid	59	58
Glutamie	20	21
Histidine	17	16
Lysine	59	60
Serine	28	32
Threonine	34	34
Alanine	46	48
Isoleucine	14	15
Leucine	61	65
Methionine*	04	05
Phenylalanine	27	30
Tryptophan	02	03
Tyrosine	19	21
Valine	36	38
Cysteine*	35	35
Glycine	16	17
Proline	28	28
Total	582	607
	(Brown et al. 1975)	(Hirayama et al. 1990)

Table I.2 Atomic composition of BSA protein **[30]**

Number of atoms	C	N	O	S
Brown et al. 1975	2926	779	897	39
Hirayama et al. 1990	3030	841	947	40

The BSA molecule consists of 583 amino acids, bound in a single chain cross-linked with 17 cystine residues, and has a molecular mass of 66.43 kDa (Figure I.9) **[28]**. The amino acid chain is made up of three homologous with structurally distinct domains (I, II and III), divided into nine (09) loops by the disulfide bonds and arranged in a special form of heart-shaped molecule.

Each domain consists of two sub-domains, A and B. Concerning the secondary structure of the protein; it is mainly α-helical (74%), with the remaining polypeptide chain occurring in turns and in extended or flexible regions between subdomains.

The BSA protein is a globular non-glycosylated, one of the few plasma proteins lacking carbohydrate groups, as it is synthesized in the liver without prosthetic groups or other additives **[34]**.

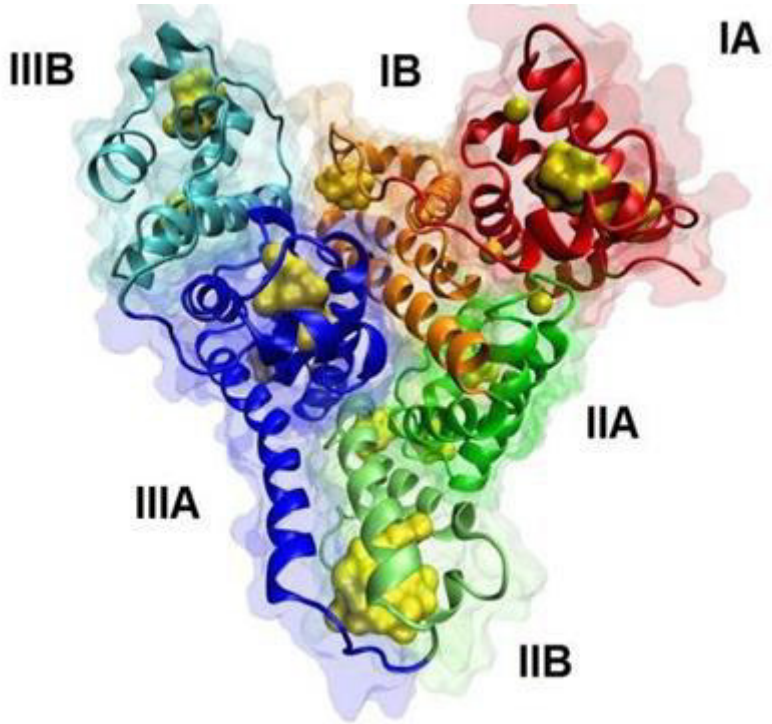

Figure I.9: Structure of BSA **[35]**

I.7. Solution pH effect on BSA form

The pH of any solution, used as a solvent for the protein, is one of the most important environment parameters that affect the structure of the protein and determines the electrostatic state of proteins.

Generally, the BSA is considered as a good model protein, to be studied because it can be attached to different solid surfaces, in several fields of research such as, molecular biology,

medicine, agri-food and the environment **[36]**. It is a soft protein, globular with the approximate shape of a prolate spheroid of dimensions 4 x 4 x 14 nm^3, with a flexible structure and it readily changes its conformation **[28,37].** Due to its low cost, wide availability and structural similarity to human serum albumin, BSA is the most widely utilized protein. The three dimensional form of the BSA undergoes radical changes depending on pH of solutions. These forms were classified according to their shapes where the "N" form is, for normal or native which is predominant in the range of pH = 8 - 4.3; "F" for fast migrating form produced abruptly at pH values less than 4.3 and up to 2.7 **[38].** The transition from form F to form E, at pH values less than 2.7 is accompanied by more expansion of the protein and a significant increase in intrinsic viscosity **[39]**. This expanded form of the BSA (form "E") morphologically resembles a sequence of balls and strings with approximate dimensions of 21 x 250 nm^2 **[25]**. These three forms are drawn and indicated in the Figure I.10 bellow**:**

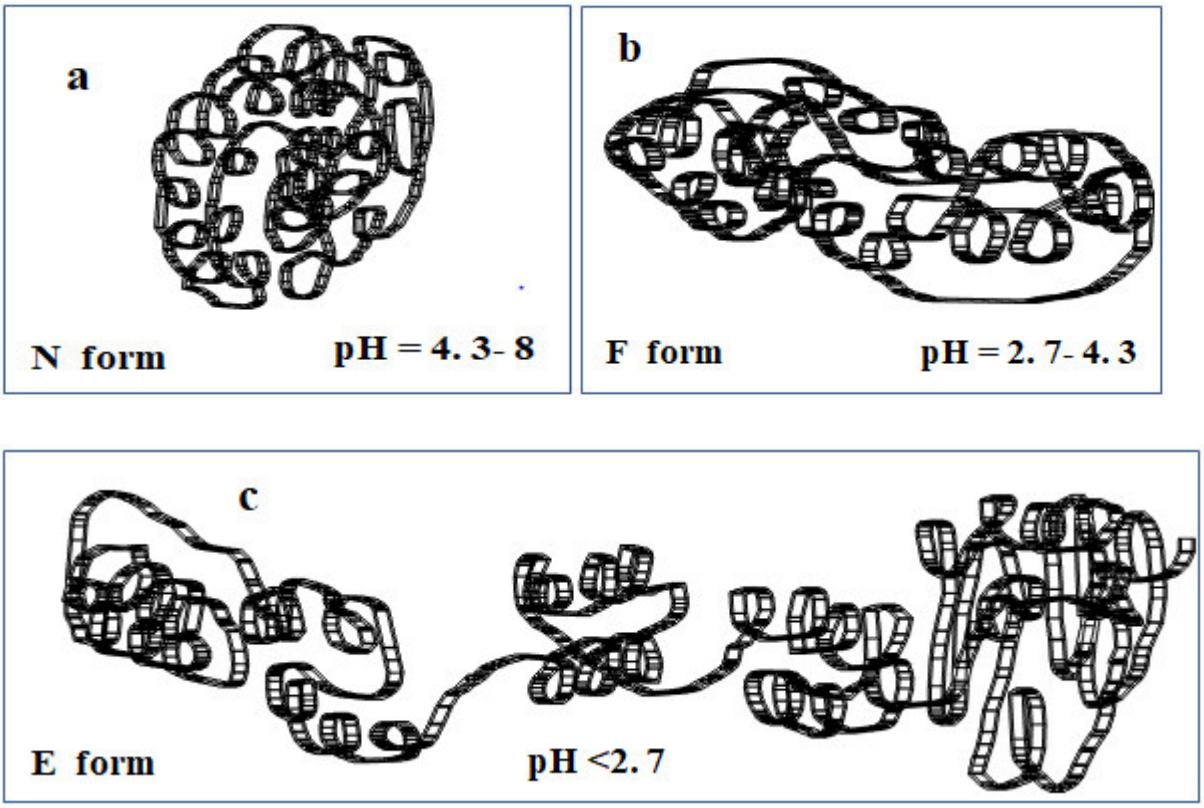

Figure I.10: A schematic diagram of conformational changes of BSA structure as a function of pH, (a) N form = Native, (b) F form = Fast and (c) E form = Expanded) **[40]**.

I.8. Titanium dioxide TiO_2

Titanium dioxide exists in several forms; the three main ones are anatase, rutile and brookite. Their corresponding crystallographic structures are shown in Figure I.11.

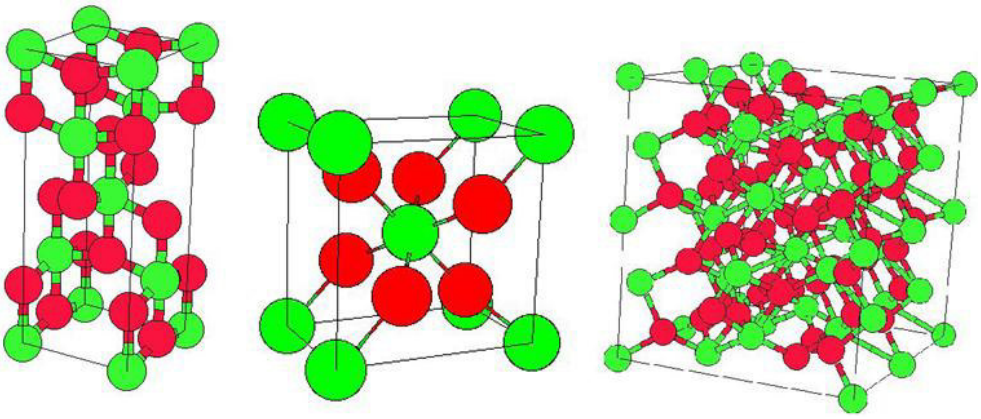

Figure I.11: Crystallographic structures of TiO_2 **[41]**

Due to a large gap, 3.2 eV for anatase and 3.0 eV for rutile **[41]**, combined with the positioning of the valence band, the holes generated are highly oxidizing. Generally, it was observed that the anatase form was significantly more active than the rutile form. Only anatase and rutile are of technological interest and they are tetragonal.

In both structures, the titanium atom is surrounded by six oxygen atoms where each one (atom) is surrounded by three titanium atoms. This material is one of essential materials in our daily life and its oldest application is UV protection thanks to its optical properties **[42]**. It is inert, non toxic and cheap material. These advantages make it one of the most used semiconductors in photocatalysis. One of its disadvantages is that this material does not adsorb the visible light because of around 3 eV properties **[43-45]**. There are researches that classify rutile as the most active photocatalyst **[46]**.

TiO_2 is in our study, to investigate the adsorption of protein, TiO_2 anatase and commercial type P25 TiO_2 was used. This latter contains two crystallite forms anatase 80% and rutile 20% **[47,48]**. It is very well characterized and is a standard and biocompatible material because these photoelectric and photochemical properties are the most interesting for many applications.

I.9. Defects of TiO_2 solid surface

As any material surface, the one of TiO_2 contains defects since it is the first contact with the exterior atmosphere that has different molecules considered as impurities when they attach to TiO_2. This surface is clearly indicated by the following figure that illustrates rutiel TiO_2 (110) face.

Oxygen vacancies, Ti interstitials, Ti vacancies, impurities, and defects at interfaces are the most konwon as point defects. Oxygen vacancies and impurities are mostly reported in literature review. Removing one of the neutral oxygen atoms from the lattice forms an oxygen vacancy, resulting in the excess electrons filling into the empty states of the Ti ions, and forming Ti3þ species. Ti interstitials are formed when Ti atoms move (migrate) from the surface to the lattice interstitial sites usually at a high temperature, or after a long time of thermal treatment **[49]**. Figure I.12 illustrates two rutile TiO_2 (110) surface models, with a number of possible defects including bridging oxygen vacancies (V_O), a bridging hydroxyl group (OH*br*), and the on-top 5f-Ti bonded O species (O_{ot}). The (1X1) surface unit cell is 2.96 Å in the '001' directionand 6.49 Å in the '110' direction **[50]**.

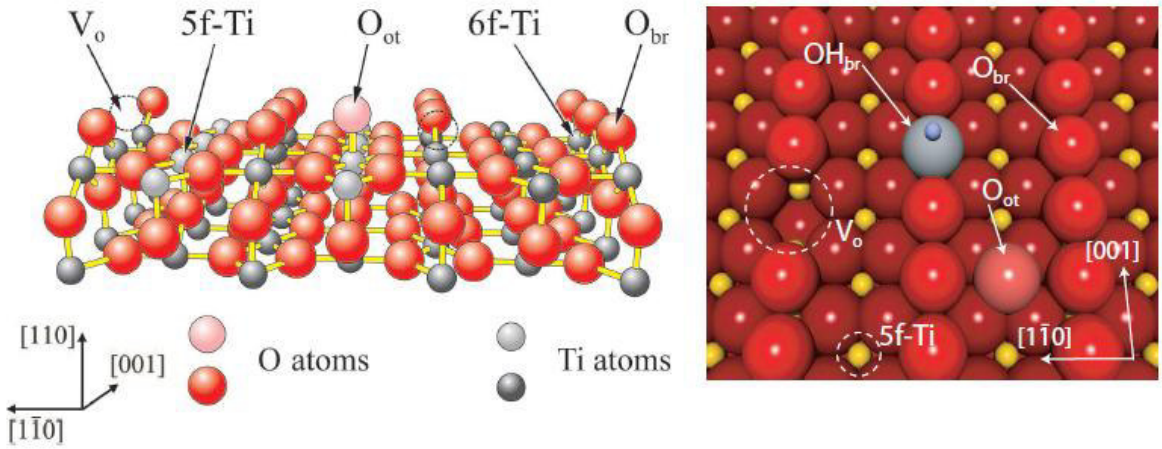

Figure I.12: Two models of the TiO_2 (110) surface. Both models show different defects and species discussed in the text. Large red balls represent O atoms, and small grey or yellow balls represent Ti atoms. Fivefold (5f-Ti) and sixfold (6f-T_i) coordinated Ti atoms, bridge bonded O species (O_{br}), single oxygen vacancies (V_o), bridging hydroxyl group (OH_{br}), and the on-top bonded O species (O_{ot}) are indicated **[50]**.

I.10. pH effect on TiO_2 surface

As we have seen before, the pH changes the protein structure and its charge. It changes also the structure and the charge of the TiO_2 surface as shown in Figure I.13.

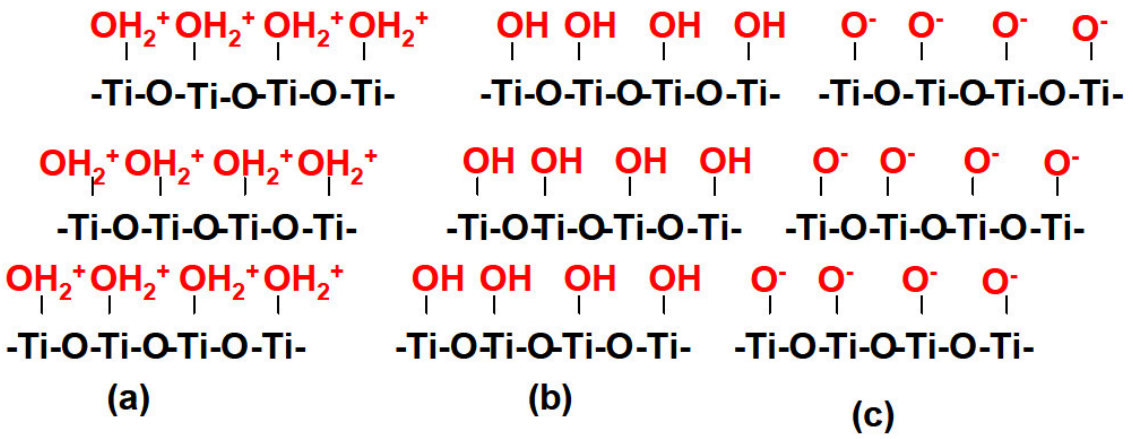

Figure I.13: Charge surface of TiO_2 at different pH. (a) pH<pHpzc, (b) pH=pHpzc and (c) pH>pHpzc **[51]**.

According to the work of A. Bouhekka **[52]**, experimentally, it was reported that the highest adsorbed amount of protein on TiO2 surface is observed using a pH between 4,5 and 5 which is very near to the zero charge of the BSA protein (4.7-4.9). Here the total charge of BSA is zero which will decrease the electrostatic interactions between BSA and titanium surface.

I.11. Protein-surface interactions under pH effect

In the Figure I.14, we clearly illustrate the interactions between the TiO2 surfaces and human serum albumin (HAS) which is recognized as a principal component of blood and the most abundant protein (very similar to BSA **[53]**) and the effect of pH. It is very clear that the optimal conditions to get a maximum of adsorbed amount of protein is using a solution of pH ranges between 4.6-5 which is near to the point of zero charge of BSA. This will strongly reduce the effect of electrostatic forces between the BSA and the surface. More addition to this pH value will not change too much the structure of BSA **[52]**.

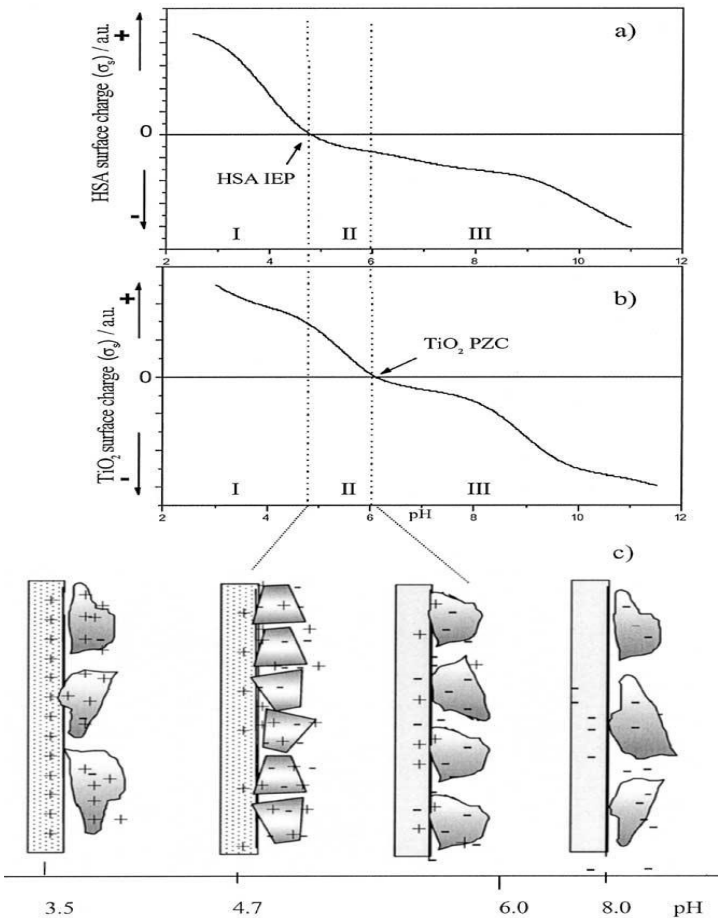

Figure I.14: Schematic representation of: The theoretical variation of the surface charge (σs) vs pH curves for (a) HAS in solution and (b) TiO_2 colloidal particles. (c) Representation of protein molecules adsorbed under different electrostatics conditions **[53]**.

I.12. Conclusion

In this part, we have dealt with the structure of proteins constituted by amino acids which make from them complex molecules usually called proteins to be studied especially when we put them in interaction with a surface considered as 2D defect for any material. This kind of study demands a lot of materials and strong theoretical background to be well understood. For this reason we are going to present, in next chapter, the details about proteins-solid surfaces interactions taking into account the previous knowledge discussed in the present chapter.

References

[1] https://byjus.com/biology/biomolecules/.

[2] https://wou.edu/chemistry/courses/online-chemistry-textbooks/ch450-and-ch451bioch -emistry-defining-life-at-the-molecular-level/chapter-2-protein-structure# C/H450-2.1.

[3] S. Cheng Li, "New approaches to protein structure prediction protein science". Doctoral thesis, Canada (2009).

[4] Wikipedia. Amino acid and peptite bond. http://en.wikipedia.org/wiki/Amino acid.

[5] D.J. Dietzen, "Amino acids, peptides, and proteins". In Principles and Applications of Molecular Diagnostics. 345-380 (2018).

[6] K.P. Gregory, G.B. Webber, E.J. Wanless and A.J. Page, "Decomposing Hofmeister effects on amino acid residues with symmetry adapted perturbation theory". Electronic Structure **5**(1), 014007 (2023).

[7] C. Bottecchia and T. Noël, "Photocatalytic modification of amino acids, peptides and Proteins". Chemistry - A European Journal **25**(1), 26-42 (2019).

[8] https://www.lkouniv.ac.in/site/writereaddata/siteContent/202003291612341624kuau m_yadav_structure_and_properties_of_proteins.pdf.

[9] I.M. Tejedor-Tejedor and M.A. Anderson, "In situ attenuated total reflection fourier transform infrared studies of the goethite (alpha-FeOOH)-aqueous solution interface". Langmuir **2,** 203-210 (1986).

[10] Y. Brahmi, "Electrostatic interactions effect on the adsorption of proteins on hydrogenated amorphous and nanocrystalline silicon at the solid/liquid interface". Doctoral thesis, University of Oran1, Algeria (2018).

[11] L. Filali, "Protein adsorption on hydrogenated silicon surfaces". Doctoral thesis, University of Oran 1, Algeria (2018).

[12] N. Chandrasekaran, "The influence of amino acid properteis on the adsorption of proteins and peptides to stainless steel surfaces", University of Canterbury, New Zealand (2014).

[13] N. Ngadi, "Mechanisms of molecular brush inhibition of protein adsorption onto stainless steel surface", University of Canterbury (2009).

[14] J. Teichroeb, "Selected experiments with proteins at Solid-Liquid interfaces", University of Waterloo, Canada (2008).

[15] G. Vallerdu, "Etude théorique de processus photophysiques dans des protéines fluorescentes", University of Paris_Sud 11, France (2009).

[16] G. Navarra, "Effects of metal ions on aggregation processes of whey proteins. Doctoral thesis, University of degli Studi Palermo, Italy (2008).

[17] https://samples.jbpub.com/9781449600914/86632_ch02_027_074.pdf.

[18] A. Gitter, "Introduction to protein structure prediction". These slides, BMI/CS 776. www.biostat.wisc.edu/bmi776/. Springer (2017).

[19] S. Issa, "Functionalization of titanium surface for dental implants design". Doctoral thesis, University Paris-Est Créteil, France (2015).

[20] X .Yu, C. Wang and Y. Li, "Classification de la structure quaternaire des protéines par composition du domaine fonctionnel". Bioinformatique BMC **7**, 1-6 (2006).

[21] A.G. Hemmersam, M. Fos, J. Chevallier and F. Besenbacher, "Adsorption of fibrinogen on tantalum oxide, titanium oxide and gold studied by the QCM-D technique". Colloids and Surfaces B: Biointerfaces **43**, 208–215 (2005).

[22] S. Herrick, O. Blanc-Brude, A. Gray and G. Laurent, "Fibrinogen". The International Journal of Biochemistry and Cell Biology **31**, 741-746 (1999).

[23] H. Westphalen, D. Kalugin and A. Abdelrasoul, "Structure, function, and adsorption of highly abundant blood proteins and its critical influence on hemodialysis patients: A critical review". Biomedical Engineering Advances **2**, 100021 (2021).

[24] A.M. Merlot, D.S. Kalinowski and D.R. Richardson, "Unraveling the mysteries of serum albumin-more than just a serum protein". Front Physiol **5**, 1-7 (2014).

[25] D.C. Carter and J.X. Ho, "Structure of serum albumin". Adv. Protein Chem. **45**, 153-203 (1994).

[26] J.J. Ramsden, "Experimental methods for investigating protein adsorption-kinetics at surfaces". Quarterly Reviews of Biophysics **27**, 41-105 (1994).

[27] K. Nakanishi, T. Sakiyama and K. Imamura, J. Biosci. Bioeng, **91**, 233-244 (2001).

[28] T. Peters Jr, "All about albumin: biochemistry, genetics, and medical applications". Academic Press, elsevier 9-75 (1995).

[29] Z.G. Peng, K. Hidajat and M.S. Uddin, "Adsorption of bovine serum albumin on nanosized magnetic particles". J. Coll. Interface. Sci. **271**, 277–283 (2004).

[30] L. Lartundo-Rojas, "Influence de l'adsorption de protéine (BSA) sur le comportement électrochimique et la composition de surface d'un alliage Fe-17Cr en solution aqueuse", University of Pierre and Marie Curie, Paris VI, France (2007).

[31] T. Peters Jr, "Serum albumin". In Advances in Protein Chemistry **37**, 161-245, **C.B. Anfinsen, J.T. Edsall and F. Richards**, editors. Academic Press, New York, (1985).

[32] J.R. Brown, "Structure of Bovine Serum Albumin", Fed. Proc. **34**, 591(1975).

[33] K. Hirayama, S. Akashi, M. Furuya and Ken-ichi Fukuhara, "Rapid confirmation and revision of the primary structure of bovine serum albumin by ESIMS and Frit-FAB LC/MS". Biochemical and Biophysical Research Communications **173**(2), 639–646 (1990).

[34] T. Topală, A. Bodoki, L. Oprean and R. Oprean, "Bovine serum albumin interactions with metal complexes". Clujul medical **87** (4), 215-219 (2014).

[35] S. Behera et *al.*, "Selective Binding of Bovine Serum Albumin (BSA): A Comprehensive Review". Biointerface Research in Applied Chemistry **13**(6), 55 (2023).

[36] D.H. Tsai, F.W. DelRio, A.M. Keene, K.M. Tyner, R.I. MacCuspie, T.J. Cho, M.R. Zachariah and V.A. Hackley, "Adsorption and conformation of serum albumin protein on gold nanoparticles investigated using dimensional measurements and in situ spectroscopic methods, Langmuir **27**, 2464–2477 (2011).

[37] M. Rabe, D. Verdes and S. Seeger, "Understanding protein adsorption phenomena at solid surfaces". Adv. Colloids Interfaces Sci. **162**, 87–106 (2011).

[38] Y. Brahmi, L. Filali, J.D. Sib, A. Bouhekka, D. Benlakehal, Y. Bouizem, A. Kebab and L. Chahed, "Conformational study of protein interactions with hydrogen-passivated amorphous silicon surfaces: effect of pH". Appl. Surf. Sci. **423**, 394–402 (2017).

[39] W.F. Harrington, P. Johnson and R.H. Ottewill, "Bovine serum albumin and its behaviour in acid solution", Biochemical **62**, 569–582 (1956).

[40] M. Tadjine, F. Bouzidi, A. Berbri, H. Nehmar and A. Bouhekka,"In situ Fourier transform infrared-attenuated total reflection spectroscopy and modeling investigation of protein adsorption: Case of expanded bovine serum albumin on titanium dioxide anatase". Biointerphases **19**(1), (2024).

[41] C. Pighini, "Synthèses de nanocristaux de TiO_2 anatase à distribution de taille contrôlée. Influence de la taille des cristallites sur le spectre Raman et étude des propriétés de surface". Doctoral thesis from University of Burgundy, France (2006).

[42] X. Chen and S. S. Mao, "Synthesis of titanium dioxide TiO_2 nanomaterials". Journal of Nanoscience and Nanotechnology **6**, 906 (2006).

[43] P.T. Spicera, O. Chaoulb, S. Tsantilisc and S.E. Pratsinisc, "Titania formation by TiCl4 gas phase oxidation". Surface Growth and Coagulation Journal of Aerosol Science **33**, 17-34 (2002).

[44] S. Yang and L. Gao, "Preparation of titanium dioxide nanocrystallite with high photocatalytic activities". Journal of the American Ceramic Society **88**, 968-970 (2005).

[45] W.S. Tang, L. Wan, K. Wei and D. Li, "Preparation of nano-TiO2 photocatalyst by hydrolyzation-precipitation method with metatitanic acid as the precursor". Journal of Materials Science **39**, 1139-1141 (2004).

[46] I. Dolamic, "Molecular insight into photocatalytic reactions by TiO2 investigated by ATR-IR spectroscopy". Doctoral thesis, University of Neuchatel, Neuchâtel (2008).

[47] Y. Bessekhouai, "Propriétés photocatalytiques de TiO_2 nanocristallins dopés par des cations (Li^+, Na^+ et K^+) et des hétérojonctions à base de sulfures et d'oxydes métalliques TiO_2 ". Pour I'obtention du grade de Docteur de l'Université de Metz (2003).

[48] W. Busayaporn, "TiO_2(110) surface structure". Student thesis, University of Manchester (2010).

[49] H. Zhao, F. Pan and Y. Li, "A review on the effects of TiO_2 surface point defects on CO_2 photoreduction with H_2O". Journal of Materiomics **3**(1), 17-32 (2017).

[50] J. Matthiesen, "The influence of point defects on TiO_2(110) surface properties". PhD thesis, University of Aarhus, Denmark (2007).

[51] J.A. Rengifo Herrera, "Preparation, characterization and photocatalytic activity of commercial TiO2 powders co-doped by N and S". Doctoral thesis, École polytechnique fédérale de Lausanne, Switzerland (2009).

[52] A. Bouhekka, "Adsorption of BSA protein on silicon, germanium and titanium dioxide investigated by in situ ATR-IR spectroscopy". Doctoral thesis, University of Oran, Algeria (2013).

[53] F.Y. Oliva, L.B. Avalle, O.R. Cámara and C.P. De Pauli, "Adsorption of human serum albumin (HSA) onto colloidal TiO2 particles". Journal of Colloid and Interface Science **261** (2), 299-311 (2003).

Chapter II

Proteins-solid surface interactions

II.1. Introduction

The comprehension of adsorption behavior of proteins on solid surfaces constitutes an important step toward development of efficient and biocompatible medical devices. Surface charge and wettability, both have been shown to influence protein adsorption attributes, including kinetics, quantities, deformation, and reversibility. However, determining the dominant interaction in these surface-induced phenomena is challenging because of the complexity of inter-related mechanisms at the liquid/solid interface **[1-3]**.
In this chapter, we will enumerate a number of mechanisms and forces that govern these interactions that take place between the protein and the surface, with an emphasis on the most relevant characteristics to this work. We will also discuss the phenomenon of protein adsorption on solid surfaces and the parameters and forces that influence this phenomenon on the protein side. The plasma surface cleaning process and methods for measuring protein adsorption will be also presented.

II.2. Phenomena of protein adsorption

Proteins are intrinsically surface-active and tend to accumulate at interfaces. When protein, in an aqueous solution, is exposed to a solid surface, it will generally tend to adsorb spontaneously at the solid-liquid interface as reported in several works **[4,5]**. The Figure II.1 clearly illustrates the different steps of this surface complex phenomenon.

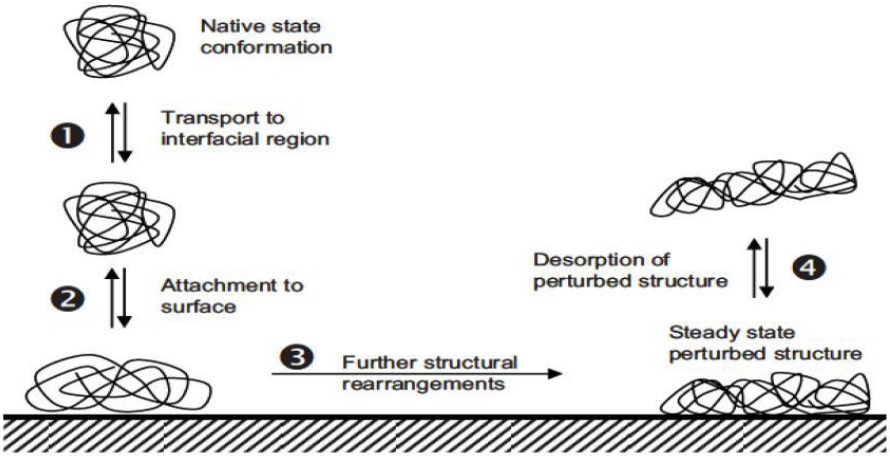

Figure II.1: Schematic representation of protein- solid surface interactions mechanism (adapted from Norde and Haynes **[6]**).

- **Step 1: Transport of a protein toward a surface:** The gradient diffusion and brownian motion are considered as the basic transport mechanisms. This explains the random movement of proteins due to the collisions and interactions with molecules of the surrounding medium such as water and salt. The concentration in the solution plays a crucial role on the rate of transport of a protein molecule towards an interface. This rate increases with increasing solution concentration of the protein and then, a higher degree of coverage is expected.

- **Step 2: Attachment of a protein at a surface:** In this step, the initial protein-surface interaction, whose strength determines the residence time of the initial proteins attachment because at the very beginning of this phenomenon, they have enough space at the surface which increases the propbability and the velocity of adsorption.

- **Step 3: Conformational changes of the protein:** This one is a time-depended structural re-arrangement of the protein on the surface. Changes and the transofrmation in conformation occur immediately during adsorption or slowly over time after the protein has sticked to the surface. These changes of conformation are suggested to be higher at low surface-coverage, usually caused by the weak protein concentration in the solution, because other molecules are believed to have an effect on the protein to adopt different conformation. The adsorption is affected by the form of protein, therefore, for proteins that are more or less rectangular in shape (with a dimension of a*b*c) is normally expected that there are two types of conformations for adsorbed protein molecules. One is called "end-on type" with the long axis and the other is called "side-on type" with the short axis perpendicular to the surface as demonstrated by the Figure II.2.

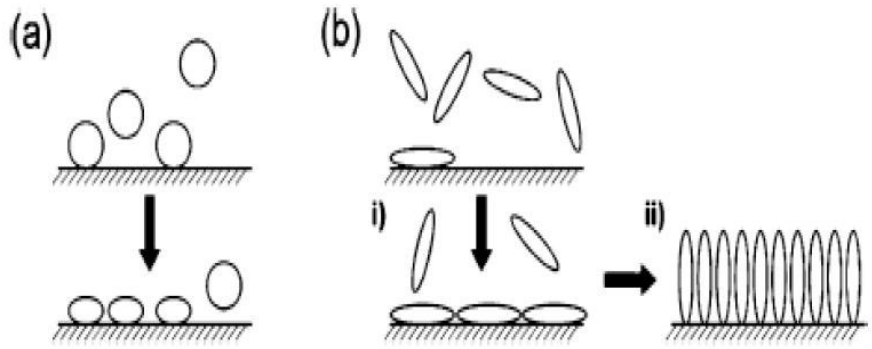

Figure II.2: Schematic illustration of (a) a globular protein, whose conformation may be distorted on interaction with the surface and (b) a rod-like protein undergoing multistage process where (i) initially the protein adsorbs with its long axis parallel to the surface and (ii) rearrangement of protein molecules occurs to increase a protein-protein interaction (reproduced from **[7]**).

- **Step 4: Detachment of a protein from the surface:** It describes the desorption process which is the opposite of adsorption. Protein adsorption is usually only partial reversible due structural changes during adsorption and they get attached with many segments to the surface. Changing pH or increasing ionic strength can desorb proteins from the surface.

- **Step 5: Transport away from the surface:** The transport away from the surface is just the reverse of step one. It could be that the desorbed protein has an altered structure compared with the native state. In many cases the desorbed proteins can adsorb again. However, in other cases the protein can recover its native conformation **[5,8]**.

II.3. Factors controlling protein adsorption

Proteins adsorption is controlled by many important environment factors like: Temperature, concentration, pH, ionic strength. The mechanism of adsorption and the bond between the protein and the surface is still not well understood right now. The form of the protein and the properties of the surface and the proteins play a fundamental role in the adsorption.

II.3.1. Influence of external parameters on protein adsorption

These parameters are: Experimental conditions, pH, ionic strength, temperature, and protein concentration.

II.3.1.1. Ionic strength

The parameter that controls the adsorption of proteins is the concentration of dissolved ions expressed by the term ionic strength. This latter basically determines the Debye length correlating **[9]** which is a measure of charge carrier's net electrostatic effect in a solution. The higher the ionic strength the shorter are the electrostatic interactions between charged molecules. This means that the adsorption of charged proteins to the oppositely charged surface gets inhibited whereas the adsorption to like charged surface gets amplified **[10**].
Lateral diffusivity of proteins decreases with the increase in ionic strength. This increases the surface pH and net protein charge at the surface **[11,12]**. In addition; a very high concentration of ions the adsorption rates are high when protein and substrate bear opposite charges since electrostatic attractions accelerate the migration towards the surface. However, the total mass load is generally observed to be maximized at the isoelectric point.

II.3.1.2. Temperature

It alters protein structure and folding that affects its adsorption at a surface. Temperature influences the equilibrium state and kinetics of protein adsorption. Increase in the temperature increases the rate of diffusion and hence favors protein adsorption.
For example, adsorption of BSA (globular protein) in a temperature range of 20 from to 40 C° increases with an increase in temperature (for pH 4 and 5) due to the increase of diffusion on adsorbent surfaces with increasing activity of protein **[13**].
However, this is not always valid, for example, native collagen (fibrillary protein) is known to be weakly surface active, a study has proved that when the temperature increases during adsorption, it helps to reduce surface tension due to a partial denaturation, and reduces protein adsorption **[14].**

II.3.1.3. Concentration of proteins

The coverage of the surface strongly depends on protein concentration in the solution. For example, at high concentration; results in an increased adsorption on surfaces leading to a quick formation of a saturated monolayer **[15,16]**. In addition to this, protein molecules tend to adsorb on the first layer and form a multilayer. The protein-protein interactions occur by hydrophobic, hydrophilic and ionic interactions or by covalent bonding. In solution, the concentration of proteins appears to have an effect on the denaturation state of a protein. At low concentrations, protein- surface interactions can be maximized by reorientation of the proteins as well as by unfolding which means denaturation and irreversible adsorption **[17]**. At higher concentrations, the supply of molecules to the surface increases and the surface will be filled with adsorbed proteins in a shorter time span. In general, small proteins adsorb more than large ones because they can fill every small empty space available at the surface. This leads to a higher mass surface density for small proteins especially at high concentration (Figure II.3) where a multistage process can occur. P. Roach et *al.* **[15]**, showed a rearrangement or orientation change for fibrinogen due to protein-protein interactions, driven by increased hydrophobic interactions between adsorbed molecules.

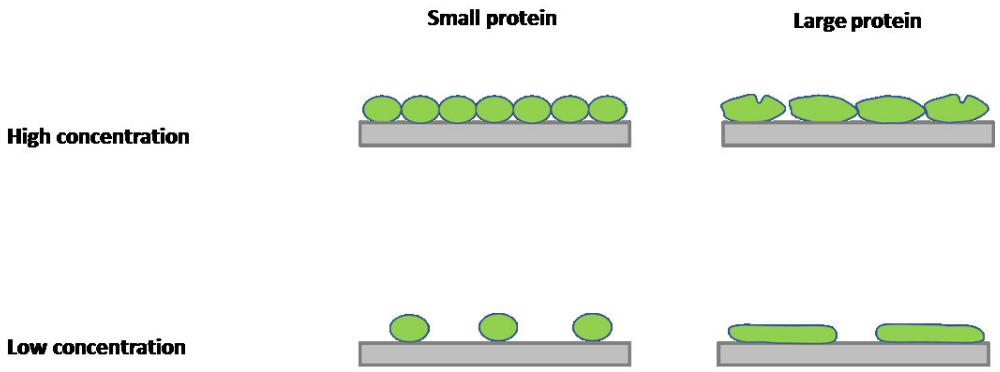

Figure II.3: Schematic representation of protein monolayer to show difference between high and low concentration on protein adsorption on flat surface **[15]**.

II.3.2. Influence of protein properties on its adsorption

The properties of proteins which affect surface activity are related to the primary structure of the protein itself, meaning that the sequence of amino acids affects protein-surface interactions these properties are listed bellow:

II.3.2.1. Size

Protein adsorption is influenced by the diffusion rate and the rate of diffusion that depends on the protein size. Smaller proteins tend to diffuse more and get adsorbed to the surface faster than larger proteins that can likely to interact with surfaces because they are able to contact the surface at more sites and hence will have more binding domains for interacting with the surfaces **[18]**.

II.3.2.2. Charge

The acid-base properties of proteins essentially depend on the number and nature of the ionizable functions of the side chains of the constituent amino acids. The proteins have acid functions and basic functions which give them an amphoteric character and they have an average net charge, which depends on the pH.

When the pH equals the isoelectric point (pI) of a protein the numbers of negative and positive charges are in balance resulting in a net neutral molecule. At low pH conditions (pH < pI), the proteins are positively charged however at high pH values (pH > pI) they are negatively charged **[10]**. On the other hand, charged amino acids are generally located on the outside of proteins and are readily available to interact with surfaces. Consequently, the charge, as well as the distribution of charge on the protein surface, can greatly influence protein adsorption. Increasing net charge on the surface of protein molecule may reduce its adsorption to the interface as charge-charge repulsions among the adsorbed molecules will increase. Also, with increasing net charge, a protein molecule can be in a more extended conformation due to intramolecular repulsions, which could lead to a decrease in adsorption due to a relatively large area required by the expanded molecule for adsorption **[19]**.

II.3.2.3. Structure stability

Less stable proteins, such as those with less of intramolecular bonds, can extend widely over a surface and, as a result, they will have much more contact points with the surface.

II.3.3. Influence of surface properties on protein adsorption

Protein–surface interactions are influenced by the protein's properties on one side and by the surface properties on the other side. The surface properties, they are frequently classified in three categories: geometric, chemical, and electrical.

II.3.3.1. Topography

Substrates with more topographical features will expose more surface area for possible interaction with proteins. For example, surfaces with grooves or pores have greater surface area compared with smooth surfaces. Other surface features, such as machine marks introduced during processing, provide additional sites for protein interaction **[18]**.

II.3.3.2. Composition

Chemical make up of a surface will determine the types of intermolecular forces governing interaction with proteins. The oxidized (passivated) surface of a metallic biomaterial exposes metal and oxygen ions. Similarly, ceramic, and some glass, surfaces comprise metal and nonmetal ions. A variety of functional species, such as amino, carbonyl, carboxyl, and aromatic groups, can be present on the surface of polymeric biomaterials. Depending on which species are exposed, biomolecules may have different affinities for various surfaces. Proteins are likely to adhere more strongly to nonpolar than to polar, to high surface tension than to surface with low tension and to charged then to uncharged substrates. Belfort et al. postulate that non-polar surfaces destabilize proteins and thereby facilitate conformational reorientations leading to strong inter protein and protein–surface interactions **[20]**.

II.3.3.3. Hydrophobic interaction

The hydrophobic or hydrophilic character of the surface has been characterized as a key parameter for the protein adsorption process, is the hydrophobic effect. It arises from the interactions of hydrogen with water.

There are numerous studies that attacked this subject, both experimentally and theoretically **[18]**. It is thought, in general, that hydrophobic surfaces cause proteins more denaturation than hydrophilic surfaces. This could be either a benefit or a hindrance for the design of biomaterials **[21]**. In general, protein molecules change their conformations to a larger

extent on hydrophobic surfaces compared to hydrophilic ones. This is because the hydrophobic part of the protein and the hydrophobic part of the surface interact with each other **[22]**.

II.4. Protein adsorption on flat surface

When a solid material is in contact with a biological medium, it becomes quickly recovered by a proteins layer **[23]**. The adsorption process consists in two steps: (i) first proteins with high affinity with the materials are adsorbed; (ii) second other biological materials are adsorbed such as cells and other proteins. The first step is in general irreversible and leads to conformational change of proteins. The adsorption mechanism is complex, depending on the properties of proteins, the surface (hydrophobicity, nano structuration, chemical functionalization…) and the surrounding medium (ionic strength, pH, solvent and temperature). The adsorption process can be divided into three steps. The first step is the transport of molecules from the liquid near to the surface (convective and the diffusion effect). Far from the surface, the convective motion dominates. Near the surface (10 μm) diffusion takes over. In second, even closer the surface the interfacial force becomes more important. The force with the longest range is the solvation force, which governs the reorganization of water to form a ramified hydrogen bond network in liquid. It has a characteristic length of about 1nm, depending on solvent polarization. Last, the electrostatic force is important. Due to the ions present in the solution, the electrostatic force has a characteristic length (Debye length), also about 1 nm. The reorganization of charges favors the interaction between protein and surface. The Van der Waals interaction is even a shorter range one, but is also important in the protein surface interaction.

II.4.1. Impact of protein structures

Protein can be described in terms of "hard" and "soft" proteins (Figure II.4). Hard proteins possess stable structure (high internal cohesion) and retain their native conformation after adsorption. They adsorb on hydrophobic interfaces under all conditions of charge interaction, and on hydrophilic surfaces only if electrostatically attracted. Examples include α-chymotrypsinogen, ribonuclease, cytochrome-c, lysozyme and β-lactoglobulin. Soft proteins lose their conformation more easily, due weakness internal cohesion **[24]**, the conformation changes after adsorption and lead to an entropy gain. This structural rearrangement allows adsorption in repulsive electrostatic condition and on hydrophilic

and hydrophobic surface, to cite a few: BSA, HSA, immunoglobulin, α-lactalbumin, β-casein and haemoglobin.

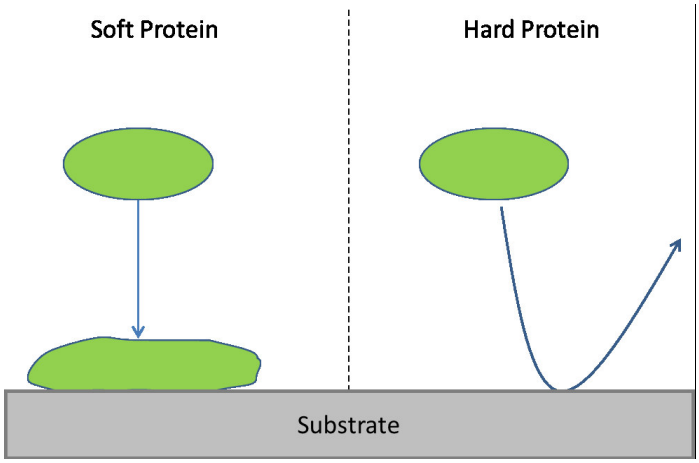

Figure II.4: Schematic representation of interaction between a surface and a hard protein and soft protein **[24]**.

II.4.2. Change of hydration state and reorganization of electric charges

Proteins possess polar and non-polar groups, thus, in an aqueous environment proteins are surrounded by counter ions (Stern layer). When proteins approach the surface; the electrical layers interact, resulting in ion redistribution. The adsorbed proteins form a compact layer where the density of charge is neutral (compensation of surface charges). Surface is covered by water molecules, which when proteins approach reorganize **[25]**. This change of hydration state, leads to an entropy gain by the release of water molecules in solution (Figure II.5). Water molecules, interacting with ions in solution (electrostatic interaction), may lead to conformational changes of proteins. The protein can expose a non-polar group to the surface during the adsorption, leads to a change in the secondary structure and a decrease in Gibbs free energy.

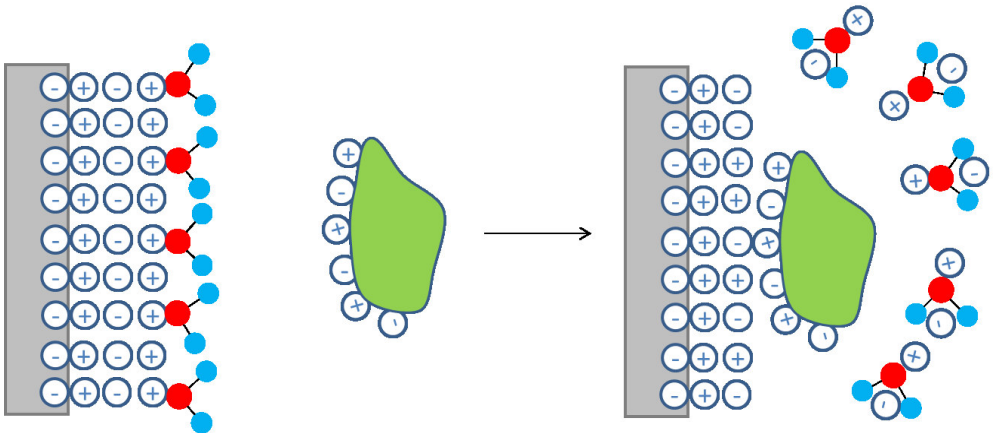

Figure II.5: Schematic representation of the change of hydration state to an interaction between negative charged surface and proteins. Ions in solution are represented by negative and positive charges **[26]**.

II.4.3. Adsorption and conformational changes of proteins

Usualy, the proteins arrive onto the considered surface from a solution with a random orientation. This latter plays a role somehow on the adsorption even it is not easy to be well controlled experimentally. The quantities of adsorbed proteins strongly depend on the pH; it is therefore likely that protein interactions play an important role. These interactions may also induce a reorientation of the adsorbed proteins. Indeed, the energy necessary to pass from one form to another is relatively low, equivalent to the dissociation of a few hydrogen bonds **[27]**.

The degree of conformational changes is determined by the native stability of the protein, the hydrophobicity and charge of the protein and the support surface. The proteins that adsorb last, will have less interactions with the surface than those adsorbed first, which is due to the steric restrictions generated by the molecules already adsorbed on the surface.

The great flexibilities and surface activities mean that the change in conformation is considered as a response of these molecules to an adaptation to their micro-environment, at the expense of an internal restructuring. Indeed, the conformational changes are more important in the case of low surface coverage by proteins**.**

II.5. Multilayer adsorption, reversibility and desorption

If the affinity between the proteins is strong enough, they can also bind to each other; this gives rise to multilayers. This phenomenon was observed during the adsorption of

transferrin on polystyrene particles **[28]**. Two behaviors were observed: part of the proteins was irreversibly adsorbed, while the other part is able to be easily desorbed. The irreversible layer would correspond to the first adsorbed layer while the second or even the third would be adsorbed reversibly. Some authors have linked the phenomenon of protein adsorption reversibility to contact time (Andrade, 1985; Norde et *al.*, 1986; Dee et *al.*, 2003; Rabe et *al.*, 2011) **[10, 29]**. They concluded that conformational changes could occur for adsorbed proteins as a function of residence time. Indeed, the more it increases, the less reversibility is likely to become totally improbable for very long times. This obviously depends on the nature of the protein, the support but also the physico-chemical conditions (pH, ionic strength).

The increase in the contact time allows the protein to generate more interactions with the chromatographic support (structural rearrangement) or to increase the phenomena of competition between the different solutes present in the medium (Figure II.6).

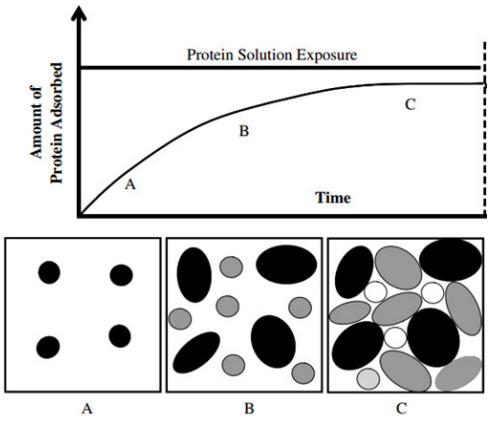

Figure II.6: Illustration of the development of an adsorbed protein layer formed when a surface is exposed to a single-component protein solution of constant concentration **[30]**.

Three steps A, B and C are shown in figure (II.6):

A: Initially, proteins adsorb randomly to the surface of the adsorbent.

B: Proteins already adsorbed (in black) begin to reorient themselves (conformational changes) by making more interactions with the support and the new molecules (in gray) adsorb on the remaining surface.

C: The last molecules that arrive will have less orientation and conformational changes due to the steric gene caused by the attached molecules. In the same context, Docoslis et *al.* (2001) **[31]** established a link between the adsorption time and the desorption efficiency of the HSA protein which was adsorbed on silica particles, for a period of 1 hour and 24

hours. It appears that the desorption takes place in greater proportions for short adsorption times. Indeed, in 24 hours the proteins have more time to explore "the most stable configurations" on the surface, desorption is therefore even more difficult.

Protein desorption then depends on:

- ✓ The properties of the protein (hard or soft: linked to the ability to conformational changes), its hydrophobicity, charge, etc.
- ✓ The hydrophobicity or hydrophilicity of the adsorbent surface
- ✓ The types of medium and properties of the resin).
- ✓ Contact time (during adsorption)
- ✓ The concentration interactions involved (electrostatic or hydrophobic depending on pH and ionic strength of the of the solution

II.6. Adsorption isotherm

Besides the different measurement techniques for measuring or quantifying protein adsorption, developing an adsorption isotherm is one of the simplest methods that can be used for studying protein adsorption **[32]**. Among these isotherms, Langmuir isotherm is the simplest and one of the widely used adsorption isotherm method. Freundlich isotherm and Brunauer-Emmett-Teller (BET) are other adsorption isotherm methods.

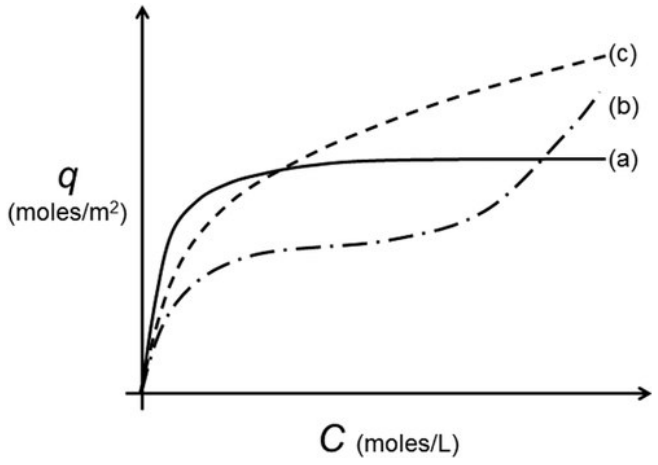

Figure II.7: Shape of different adsorption isotherms: Plot of surface concentration (q) vs solution concentration (*C*) with (a) Langmuir isotherm (———), (b) BET isotherm (-.-), (c) Freundlich isotherm (---) **[33]**.

Adsorption isotherms are constructed by plotting surface concentration of proteins at different solution concentration of proteins as shown in Figure II.7, thus it gives us an

understanding of how proteins and surfaces interact. Each adsorption models have their own characteristic shapes. Langmuir model assumes that the adsorption forms as a 'monolayer' on the homogenous surface. Freundlich model describes adsorption on heterogenous surfaces, whereas BET model describes multi-layer protein adsorption on different sites on a surface, which is usually the case **[33]**.

II.7. Plasma surface cleaning process

II.7.1. Definition of plasma

Plasma is a partially or totally ionized gas, so it generally consists of electrons, ions, atomic species or neutral molecular and photons. Plasma is often considered the fourth state of matter after the solid state, the liquid state and the gaseous state; and constitutes approximately 99% of the visible mass of the universe **[34]** as indicated in the figure II.8.

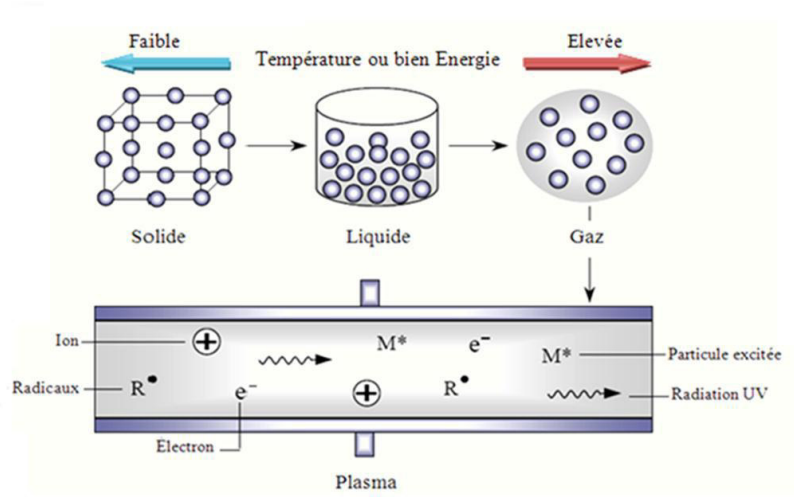

Figure II.8: Schematic representation of the four states of matter **[35]**.

It exists either in its natural state (solar crown, Sun, interior of stars, ionosphere, etc.), either in the laboratory generally produced by an electric discharge. It is a gas that contains neutral particles (atoms, molecules and free radicals), positive or negative ions and electrons.

II.7.2. Internal reflection element

Usualy germanium (Ge) and silicon (Si) are used as internal reflection elements (IREs) for FTIR-ATR on which a coating surface can be deposited. These IREs are considered as substrates that should be cleaned before using them. The cleaning techniques rely on the

same chemical principle and are based on two reactions occuring simultaneously. The UV light radiation, first, breaks down most of the chemical bonds (C-H, C-C) from organic contamination on the Ge surface **[36]**, leaving organic free radicals and excited molecules on the surface. In the case of oxygen plasma, the UV light is created through a continuous recombination process of all oxygen species involved.

Second, highly reactive oxygen species, which are either formed in the oxygen plasma or through photolysis of oxygen molecules due to UV light, bond with the remaining carbon and other organic radicals on the Ge surface, forming volatile CO, CO_2, and H_2O **[37]** resulting in a practically carbon-free surface (see Figure II.9). At the same time, a thin protective germanium (Ge) oxide film of up to 70 A° forms as a result of the oxidation of surface Ge. The newly oxidized layer consumes contaminants which have segregated to the near Ge surface region. This thin oxide layer is advantageous when using a UV light source ex situ as it acts as a passivation layer, preventing carbon from re-depositing on the Ge surface during the loading process into the vacuum system. As a final step, the passivating germanium oxide needs to be removed through an annealing step, which is usually done in situ.

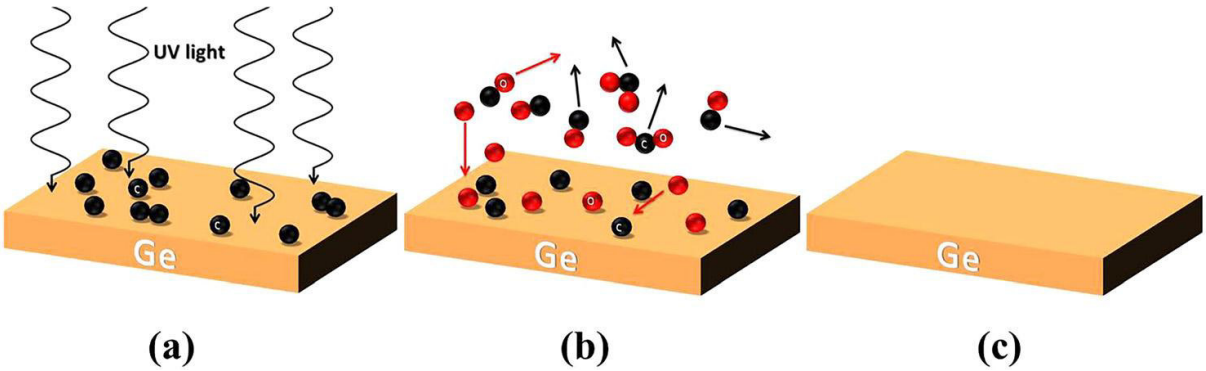

Figure II.9: (a) Ge surface with organic contamination (black). (b) Atomic oxygen (red) reacts with carbon on the surface and forms volatile CO, CO_2 and H_2O leaving behind a carbon-free Ge surface (c) **[37]**.

Both techniques of cleaning rely on the same principle; however, the creation process of the UV light radiation, that breaks down the organic bonds and the formation of the highly reactive oxygen species differ.

Oxygen plasma is created by using a radio frequency electrical excitation of a cavity containing molecular oxygen gas at some pressure in order to ionize the gas to form the plasma. Usually, an oxygen plasma consists of a variety of highly excited atomic,

molecular, ionic, and radical species (O, O^+, O^-, O_2^+, O_2^-, O_3), as well as free electrons and metastable molecules **[37]**. Molecular O_2 is usually the preferred gas to remove organic residues from wafer surfaces, due to the formation of several highly reactive oxygen species, some of which are shown below.

$$O_2 + e^- \rightarrow O_2^- \rightarrow O + O^- \quad \text{(II.1)}$$

$$e^- + O \rightarrow O^+ + 2\,e^- \quad \text{(II.2)}$$

$$e^- + O_2 \rightarrow O_2^+ + 2\,e^- \quad \text{(II.3)}$$

$$e^- + 2\,O_2 \rightarrow O_2^- + O_2 \quad \text{(II.4)}$$

$$O_2^- + O \rightarrow O_3 + e^- \quad \text{(II.5)}$$

For cleaning wafers of Ge using an ex situ UV light source, generally a low pressure Hg discharge lamp is used, due that Hg have two major emission lines at wavelengths λ_1 = 253.7 nm and λ_2=184.9 nm. These photons have energies of E_1= 472 kJ/mol and E_2 = 647 kJ/mol, respectively, and can dissociate most organic compounds (see Table II.1) **[38]**.

Table II.1: Chemical bond energies of organic molecules found on the Ge surface **[38].**

Bond	Bond energy (KJ.mol^{-1})	Bond	Bond energy (KJ.mol^{-1})
C – C	**347.7**	C = C	**607**
C – H	**413.4**	C = O	**707**
C – N	**291.6**	C – Cl	**328.4**
C = N	**791**	C – F	**441**
C – O	**351.5**		

Furthermore, the 184.8 nm wavelength is important as it is capable of dissociating O_2, leading to the formation of highly reactive ozone gas **[39]**.

$$O_2 + h\nu\ (184.8\ nm) \rightarrow 2O \quad \text{(II.6)}$$

$$O + O_2 \rightarrow O_3 \quad \text{(II.7)}$$

$$O_3 + h\nu\ (254\ nm) \rightarrow O_2 + O \quad \text{(II.8)}$$

When both wavelengths are present, highly reactive ozone is continuously created and decomposed which results in the creation of atomic oxygen a strong oxidizing agent. The major advantage of using UV light or oxygen plasma, apart from its effectiveness in completely removing any organic contamination from the Ge surface, is the economical and environmental aspects. The use of hazardous and toxic acids can be circumvented and, unlike wet-etching methods that produce a high volume of liquid hazardous waste resulting in expensive chemical disposal, excess oxygen, CO_2, and H_2O can be released directly into the atmosphere **[40]**. This cleaning method also provides the advantage that no time consuming germanium regrowth is needed to obtain a highly ordered and atomically clean Ge surface.

II.7.3. Oxygen plasma and IRE cleaning

Oxygen plasma refers to any plasma treatment performed while introducing oxygen to the plasma chamber. Oxygen is often used to clean surfaces prior to bonding. Oxygen (O_2) is the most common gas used in plasma cleaning technology due to its low cost and wide availability. Oxygen plasma is created by utilizing an oxygen source on a plasma system (Harrick machine) as shown in Figure II.10. All systems available from Plasma Etch will work with oxygen gas. An oxygen generator can be purchased and set up right in a lab. Oxygen gas is used to clean non-metal materials such as glass **[41]**, plastics, germaniun, silicon, and Teflon. Like other forms of plasma, oxygen cleans organics and is capable of surface modification by introducing some unwanted impurties.

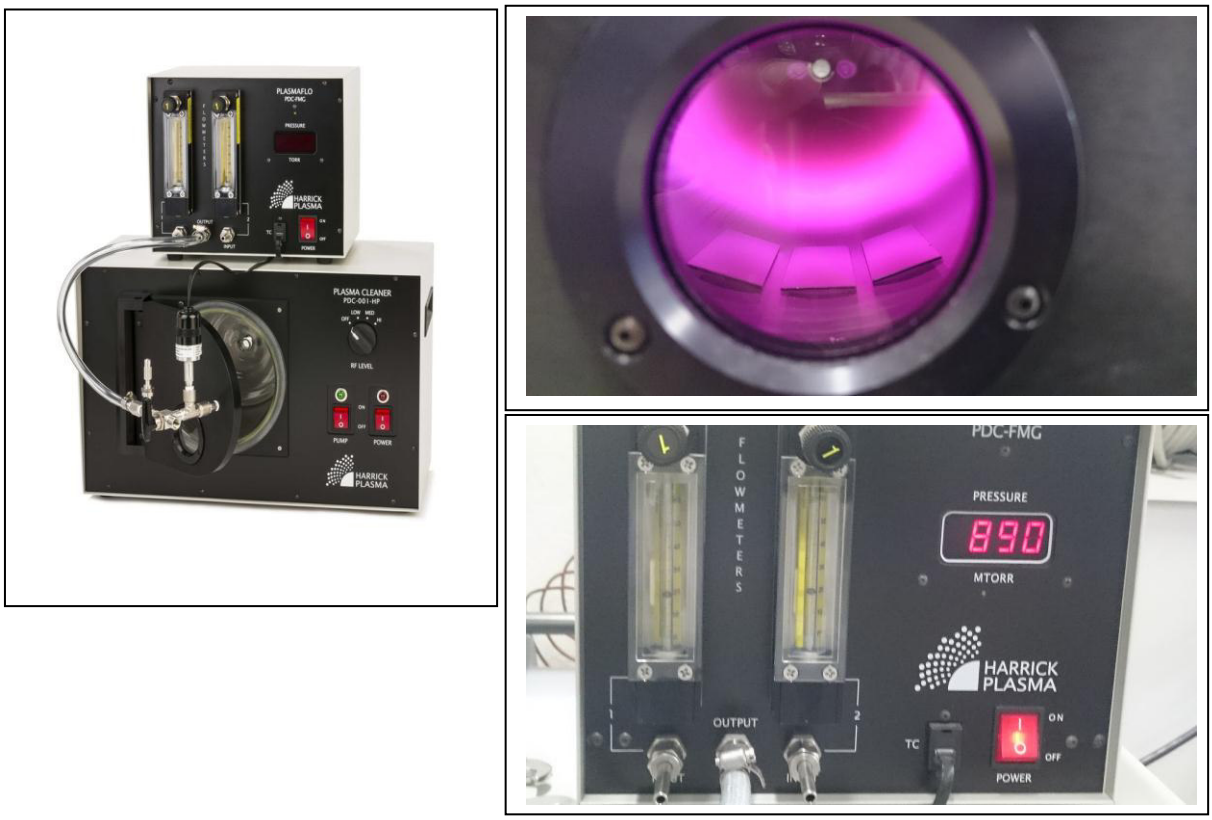

Figure II.10: (a) Harrick plasma cleaning machine **[42]**, and (b) Germanium substrates cleaned in oxygen plasma unde around 890 mtorr (pictures kindly given by A. Bouhekka **[43]**).

Before the despotion of porous TiO_2 films on germanium or silicon substrates, these latter were introduced in the harrick machine for clean under oxygen plasma at 890 mtorr of pressure as shown before.

II.8. Methods for measuring protein adsorption

Understanding protein adsorption is critical for several industrial and biomedical applications. The choice of a measurement technique strongly depends on the type of study and may involve studying adsorption kinetics, the amount of adsorbed protein, the activity and the structure of the adsorbed proteins **[44]**. Many label free approaches such as, ellipsometry, UV spectrometry, surface plasmon resonance (SPR), optical waveguide lightmode spectroscopy (OWLS), etc. have been used to study adsorption kinetics and some have also been also used to measure the thickness of the adsorbed protein layer. Spectroscopy techniques such as, X-ray photoelectron spectroscopy (XPS) has been

employed to study the composition of adsorbed protein layers. Labelled techniques such as, radiolabelling, Lowry assay, bicinchoninic acid (BCA) assay have also been employed **[45]**. Radiolabelling technique, which uses radio isotopes for labelling proteins was one of the widely used method for measuring adsorption and has been used since 1980.

Lowry and BCA assay measures protein adsorption based on absorption spectra. Fluorescence measurements of adsorption can be performed using fluorescein isothiocyanate (FITC) labels and microscopy techniques **[46]**. Techniques such as total internal reflection fluorescence (TIRF) and Förster resonance energy transfer (FRET) have been used for measuring protein adsorption. TIRF has been used to investigate protein adsorption kinetics and FRET has been used for studying protein folding/unfolding **[10]**. On the other hand, to study the structure of adsorbed proteins and its conformational changes upon adsorption, infrared spectroscopy (IR), attenuated total internal reflectance-infrared spectroscopy (ATR-IR) and circular dichroism (CD) spectroscopy has been used **[47]**. Atomic force microscopy (AFM) has also been used to study protein adsorption by imaging of the adsorbed protein and can provide information, such as the height of the protein.

II.8.1. Attenuated total reflection FTIR-ATR spectroscopy

One of the most important techniques that can be useful to investigate the solid-liquid interface is ATR spectroscopy which is a nondestructive technique used to study surface layers with thicknesses ranging from hundreds of Angstrom units to tens of micrometers. This technique was developed in the past 60 years, gained wide acceptance in the field of physicochemical studies. ATR spectroscopy can be used to investigate thin films on transparent or absorbing substrates; and to study the adsorption, catalysis and diffusion. The absence of scattering in the case of ATR provides one with a unique opportunity to record the spectra of powders, fibers, pastes, and other dispersed media. The simplicity of sample preparation allows one to study biological and medical objects in vivo **[48]**. Attenuated total reflectance (ATR) spectroscopy utilizes the phenomenon of total internal reflection (Figure II.11): A beam of radiation entering a internally refracting element (IRE) will undergo total internal reflection when the angle of incidence at the interface between the sample and IRE is greater than the critical angle, where the latter is a function of the refractive indexes of the two surfaces **[49]**:

$$\sin\theta_c = \frac{n_2}{n_1} \qquad \text{(II.1)}$$

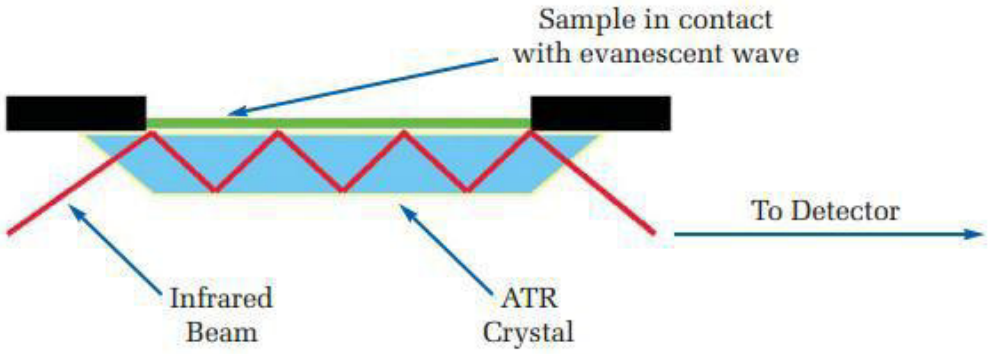

Figure II.11: A multiple reflection ATR system **[49]**.

According to Snell's law, the refractive indexes of the medium 2 must be smaller than that of medium 1. When the light undergoes total reflection at the interface of the two mediums, an electric field is formed at the reflection points which then penetrate into the rare medium. This electric field is referred to as evanescent field which is derived from the Latin root evanescere, meaning "to tend to vanish or pass away like a vapor" **[50]**.

II.8.2. FTIR Spectroscopy and protein structure

Fourier transform infrared spectroscopy is a good technique that can be applied to study the secondary structure of globular proteins **[51]**. Its applications to determine the structure of the protein is based on the assessment of amide bands. Kumosinski et *al.* **[52]** demonstrated that the results concerning the secondary structure of 14 proteins using FTIR spectroscopy and X-ray crystallographic data were in good agreement. The FTIR has many advantages, over other techniques, in studying protein and the major one is the lack of dependence on the physical state of the sample (gas, aqueous or organic solution, hydrated film, inhomogeneous suspension, or solid). The FTIR spectroscopy has been used several years ago to analyze the proteins structure and it is extensively reviewed. This method (FTIR) is particularly suitable for the study of adsorbed proteins on surfaces **[53]**. FTIR was applied to investigate the loss of secondary structure during insulin unfolding on a model lipid-water interface, adsorbed proteins on silica surfaces **[54]**, different clay surfaces, interface of oil-water, air water interface, and brushite. The conformation of adsorbed protein depends on properties of the surface **[55]**.

II.8.3. FTIR spectrum of protein

The absorption bands in FTIR spectroscopy measurements are sensitive to bond angles in the molecules and hydrogen bands. Theoretically, any changes (intensity, shift in peak position…) are caused by an alteration (conformation) in the secondary structure of the protein. Each type of secondary structure absorbs at a specific frequency in the FTIR spectrum **[56]**. The amide groups of proteins exhibit vibrational modes in the infrared region, which give rise to the amide bands A, B, and I-VII **[57]**. The amide IV-VII bands are not very important in mid-infrared region due to their low intensities. The amide I, amide II and amide III are the most important bands that can be applied to determine secondary structure of proteins **[58]**.

II.8.4. The correspondence between protein secondary structure and amide bonds

The most important point in the interpretation of proteins infrared spectra is to involve the component bands to different types of secondary structures. A lot of theories and experiments have been done to correlate FTIR absorption bands of protein to the secondary structure of protein in its different states. The bands in the range 1650-1658 cm^{-1} is associated to α-helix conformers in aqueous environments. The α-helical structures overlap with those from random (unordered structure) (1645-1652 cm^{-1}) **[59]** and loops (1658-1665 cm^{-1}) **[60]**, and they occur from 1650 to 1655 cm^{-1} in soluble proteins **[61]**.

The vibration of β-sheet can be seen in the region from 1620 to 1640 cm^{-1} and its position can be affected by varying strengths of the hydrogen bonding and transition dipole coupling in different β-strands. β-turn (turn) vibration is around 1662-1690 cm^{-1}. The secondary structure of protein can be also determined from the amide II band, but the correspondence between FTIR spectra and secondary structure is more complex than in the amide I region because bands in the amide II region have not been well studied. In amide II region, bands in the range 1540-1550 cm^{-1} are regarded as α-helix and the β-sheet vibration is at the range 1520-1530 cm^{-1} **[62]**. β-turns can be seen around 1568 cm^{-1} **[63]**.

Due to their low intensity and the contribution of the side chain vibration, the FTIR spectra of the protein in the amide III region have not been fully understood yet. It was reported by Cai and Singh that α-helix bands usually appear in range 1295-1340 cm^{-1}; β-turns gives rise to bands around 1270-1295 cm^{-1}; random structure is at 1250-1270 cm^{-1}; and β-sheet is assigned from 1220 to 1250 cm^{-1}. The important assignments of FTIR bands are given in Table II.2.

Table II.2: Band assignments in the amide I region of FTIR spectrum **[45, 64].**

FTIR region	Wavenumbers (cm^{-1})	Secondary structure
Amide I	1620-1640	β-sheet
	1645-1652	Random or unordered
	1650-1658	α-helix
	1662-1690	β-turn
Amide II	1520-1530	β-sheet
	1540-1550	α-helix
	1568	β-turn

II.9. Native and unfolded states of protein

The spreading of the adsorbed protein on the surface strongly depends on the amount of protein adsorbed. If there is enough space on the surface, the protein can spread leading to the increase in contact points between it and the surface thus the adsorption will be strong. The Figure II.12 illustrates the unfolding (spreading) of adsorbed protein onto a surface.

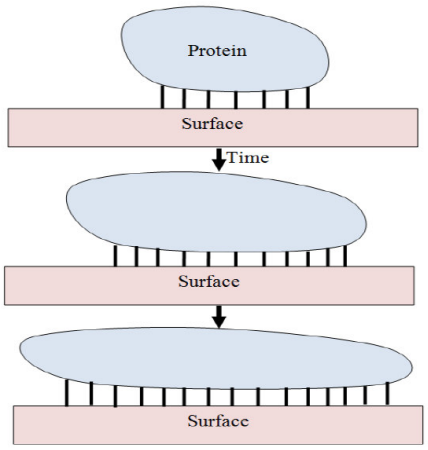

Figure II.12: Time-dependent molecular spreading of a protein on a surface **[18].**

Changing the pH of protein solution can lead to affecting strongly the structure of protein. In this case, it leads to more contact between the protein and the surface as shown in Figure II.13. This demonstrates that the footprint of protein is increased and the space between adsorbed proteins may be reduced.

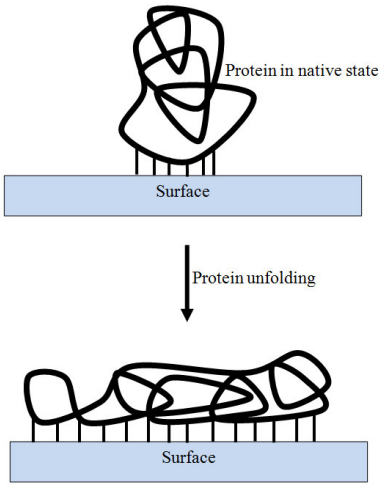

Figure II.13: Effect of protein unfolding on interaction with a surface **[18]**.

The unfolding process will be discussed in the extended model that will be discussed in the following two chapters where the determination of the surface covergaes by native and unfolding protein is an important point in this research.

II.10. Conclusion

From this chapter, we conclude that the structure of protein is very complex and the study of their adsorptions at surface still a big challenge for scientist because of the different factors that control these phenomena. The form of the protein and the properties of the surface and the proteins play a fundamental role in the adsorption.

The FTIR-ATR is a powerful technique that can be used to probe interfaces by doing in situ measurements. The next chapter will deal with in situ attenuated total reflection spectroscopy used for investigating the adsorption of protein-surfaces.

References

[1] S. Guo, D. Pranantyo, E.T. Kang, X.J. Loh, X. Zhu, D. Jańczewski and K.G. Neoh, "Dominant albumin−surface interactions under independent control of surface charge and wettability". Langmuir **34**, 1953−1966 (2018).

[2] G. Vallerdu, "Etude théorique de processus photophysiques dans des protéines fluorescentes", University of Paris_Sud 11, France (2009).

[3] G. Navarra, "Effects of metal ions on aggregation processes of whey proteins". Thesis, University of degli Studi Palermo, Italy, (2008).

[4] J.D. Andrade, editor. "Surface and interfacial aspects of biomedical polymers". New York, (1985).

[5] K. Nakanishi, T. Sakiyama and K. Imamura, "On the adsorption of proteins on solid surfaces, a common but very complicated phenomenon".J. Biosci. Bioeng, **91**(3), 233-244 (2001).

[6] W. Norde and C.A. Haynes, ACS Symposium Series **602**, 26-40 (1995).

[7] G. Jackler, R. Steitz and C. Czeslik, "Effect of temperature on the adsorption of lysozyme at the silica/water interface studied by optical and neutron reflectometry". Langmuir **18**(17), 6565-6570 (2002).

[8] W. Norde, F. MacRitchie, G. Nowicka and J. Lyklema, "Protein adsorption at solid-liquid interfaces: reversibility and conformation aspects". J. Coll. Interf. Sci. **112**, 447-456 (1986).

[9] K.L. Jones and C.R. O'Melia, "Protein and humic acid adsorption onto hydrophilic membrane surfaces: effects of pH and ionic strength". J. Memb. Sci. **165**, 31–46 (2000).

[10] M. Rabe, D. Verdes and S. Seeger, "Understanding protein adsorption phenomena at solid surfaces". Advances in Colloid and Interface Science, **162**(1), 87-106 (2011).

[11] J.J. Ramsden and J.E. Prenosil, "Effect of Ionic Strength on Protein Adsorption Kinetics". The Journal of Physical Chemistry, **98** (20), 5376-5381 (1994).

[12] S. Pasche, J. Voros, H.J. Griesser, N.D. Spencer and M. Textor, "Effects of ionic strength and surface charge on protein adsorption at PEGylated surfaces". The Journal of Physical Chemistry. B **109**(37), 17545-17552 (2005).

[13] T. Kopac, K. Bozgeyik and J. Yener, "Effect of pH and temperature on the adsorption of bovine serum albumin onto titanium dioxide". Colloids Surfaces A Physicochem. Eng. Asp. **322**, 19–28 (2008).

[14] A. Kezwon, and K. Wojciechowski, "Effect of temperature on surface tension and surface dilational rheology of type I collagen". Colloids Surfaces A Physicochem. Eng. Asp. **460**, 168–175 (2014).

[15] P. Roach, D. Farrar and C.C. Perry, "Interpretation of protein adsorption: Surface-induced conformational changes". Journal of the American Chemical Society **127**(22), 8168-8173 (2005).

[16] L. Baujard-Lamotte, S. Noinville, F. Goubard, P. Marque and E. Pauthe, "Kinetics of conformational changes of fibronectin adsorbed onto model surfaces", Colloids and Surfaces B: Biointerfaces **63,** 129-137 (2008).

[17] N. Ngadi, "Mechanisms of molecular brush inhibition of protein adsorption onto stainless steel surface", University of Canterbury (2009).

[18] K.C. Dee, D.A. Puleo and Rena Bizios, "An introduction to tissue-biomaterial interactions: Tissue-Biomaterial", Wiley (2002).

[19] S.H. Lee and E. Ruckenstein, "Adsorption of proteins onto polymeric surfaces of different hydrophilicities—a case study with bovine serum albumin". J. Colloid Interface Sci. **125**(2), 365-379 (1988).

[20] G. Anand, S. Sharma, A.K. Dutta, S.K. Kumar and G. Belfort, " Conformational transitions of adsorbed proteins on surfaces of varying polarity". Langmuir **26**, 10803-10811 (2010).

[21] Y. Brahmi, "Electrostatic interactions effect on the adsorption of proteins on hydrogenated amorphous and nanocrystalline silicon at the solid/liquid interface". Doctoral thesis, University of Oran, Algeria (2012).

[22] J. Teichroeb, "Selected experiments with proteins at solid-liquid interfaces", University of Waterloo, Canada (2008).

[23] P.E. Scopelliti, G. Bongiorno and P. Milani, "High-throughput tools for the study of protein nanostructured surface interaction". Comb. Chem. High Throughput Screen. **14**, 205–216 (2011).

[24] T. Arai and W. Norde, "The behavior of some model proteins at solid-liquid interfaces 1. Adsorption from single protein solutions". Colloids and Surfaces **51**, 1–15 (1990).

[25] T. Degabriel, "Study of the interaction between proteins and TiO_2 NPs: nature of the interfacial processes". Doctoral thesis, University of Pierre and Marie Curie, France (2015).

[26] J.B. Schlenoff, "Zwitteration: Coating surfaces with zwitterionic functionality to reduce nonspecific adsorption". Langmuir **30**, 9625–9636 (2014).

[27] J.S. Tan and P.A. Martic, "Protein adsorption and conformational change on small polymer particles". Journal of Colloid and Interface Science **136**(2), 415-431 (1990).

[28] S. Milani, F. Baldelli Bombelli, A.S. Pitek, K.A. Dawson and J. Radler, "Reversible versus irreversible binding of transferrin to polystyrene nanoparticles: soft and hard corona". ACS nano **6**(3), 2532-2541(2012).

[29] K.C. Dee, D.A. Puleo and R. Bizios, "An introduction to tissue-biomaterial interactions". Protein-Surface Interactions, John Wiley & Sons, Inc., 37-52 (2002).

[30] R.A. Latour, Biomaterials: protein-surface interactions, Encyclopedia of biomaterials and biomedical engineering **1**, 270-278 (2005).

[31] A. Docoslis, W. Wu, R.F. Giese, C.J. Van Oss, "Influence of macroscopic and microscopic interactions on kinetic rate constants. III. Determination of von Smoluchowski's f-factor for HSA adsorption onto various metal oxide microparticles, using the extended DLVO approach". Colloids and Surfaces B: Biointerfaces **22**(3), 205-217 (2001).

[32] C.M. Alves, R.L. Reis and J.A. Hunt, "The competitive adsorption of human proteins onto natural-based biomaterials. J. R. Soc. Interface, **7**(50), 1367-1377 (2010).

[33] R.A. Latour, "The Langmuir isotherm: A commonly applied but misleading approach for the analysis of protein adsorption behavior". Journal of Biomedical Materials Research Part A **103**(3), 949-958 (2015).

[34] T. Lehner, " L'état de plasma : le feu de l'univers". 268 pages, Vuibert, Paris, France (2004).

[35] P. Fauchais, "Plasma thermiques: Aspects fondamentaux". Les techniques de l'ingénieur Dossier D 2 810 (2007).

[36] S.R. Amy, Y.J. Chabal, F. Amy, A. Kahn, C. Krugg and P. Kirsch, "Wet chemical cleaning of germanium surfaces for growth of high-k dielectrics", Mater. Res. Soc. Symp. Proc. **917**, 0917 E01 (2006).

[37] A. Pizzi and K.L. Mittal, "Handbook of adhesive technology, revised and expanded" (Marcel Dekker Inc., New York) 1024 pages, (2003).

[38] P. Ponath, A.B. Posadas and A.A. Demkov, "Ge(001) surface cleaning methods for device integration". Appl. Phys. Rev. **4**, 021308 (2017)

[39] X.J. Zhang, G. Xue, A. Agarwal, R. Tsu, M.A. Hasan, J.E. Greene and A. Rockett, "Thermal desorption of ultraviolet–ozone oxidized Ge(001) for substrate cleaning," J. Vac. Sci. Technol. A **11**, 2553 (1993).

[40] A. Belkind and S. Gershman, "Plasma cleaning of surfaces", Vac. Coat. Technol. **11**, 46–57 (2008).

[41] https://www.plasmaetch.com/oxygen-plasma-treatment.php.

[42] https://www.google.com/search?sxsrf=AB5stBhtwjCZO4w2JRwGtkYtj8q9lzjkeA:1690467095980&q=Harrick+plasma+machine&tbm=isch&source=lnms&sa=X&ved=2ahUK Ewic7onWiKAAxV5U6QEHVp7A4MQ0pQJegQIDRAB&biw=1366&bih.

[43] A. Bouhekka, "Adsorption of BSA protein on silicon, germanium and titanium dioxide investigated by in situ ATR-IR spectroscopy". Doctoral thesis, University of Oran, Algeria (2013).

[44] D.A.B. Puleo and Rena Bizios, "Biological interactions on materials surfaces: Understanding and controlling protein, cell, and tissue responses". Springer Science and Business Media, 429 (2009).

[45] J. Saikia, M. Yazdimamaghani, S.P. Hadipour Moghaddam and H. Ghandehari, **"**Differential protein adsorption and cellular uptake of silica nanoparticles based on size and porosity". ACS applied materials & interfaces **8** (50), 34820-34832 (2016).

[46] K.F.A.Clancy, S. Dery, V. Laforte, P. Shetty, D. Juncker and D.V. Nicolau, "Protein microarray spots are modulated by patterning method, surface chemistry and processing conditions". Biosensors and Bioelectronics **130**, 397-407 (2019).

[47] M.C. L.Martins, S.R. Sousa, J.C. Antunes and M.A. Barbosa, "Protein adsorption characterization". In Nanotechnology in Regenerative Medicine: Methods and Protocols, M. Navarro and J. A. Planell. Eds. Humana Press: Totowa, NJ, 141-161 (2012).

[48] S.D. Stuchebryukov, "Attenuated total refection spectroscopy under conditions weak absorption: New method for determination of integrated intensities". Protection of Metals and Physical Chemistry of Surfaces **46** (3), 366–374 (2010).

[49] B. Stuart, "Infrared spectroscopy: fundamentals and applications", Book (2004).

[50] F.M. Mirabella, "Principles, theory, and practice of internal reflection Spectroscopy". F.M. Mirabella (edit.), In: Internal Reflection Spectroscopy: Theory and Applications, New York: Marcel Dekker, 17–52 (2002).

[51] A. Barth and C. Zscherp, "What vibrations tell us about proteins?. Quarterly Reviews of Biophysics **35**, 369-430 (2002).

[52] T.F. Kumosinki and J.J. Unruh, "Quantization of the global secondary structure of globular proteins by FTIR spectroscopy: comparison with X-ray crystallographic structure". Talanta, **43** 199-219 (1996).

[53] J. Gray, "The interaction of protein with solid surface". Current Opinion in Structural Biology **14,** 110-115 (2004).

[54] C.E. Giacomelli, M.G.E.G. Bremer and W. Norde, "ATR-FTIR study of IgG adsorbed on different silica surface". Journal of Colloid interface Science **220**, 13-23 (1999).

[55] S. Tunc, M.F. Maitz, G. Steiner, L. Vázquez, M.T. Pham and R. Salzer, "In situ conformational analysis of fibrinogen adsorbed on Si surfaces". Colloids and Surfaces B: Biointerfaces **42**, 219-225 (2005).

[56] M. Jackson and H.H. Mantsch, "The use and misuse of FTIR spectroscopy in the determination of protein structure". Critical Reviews in Biochemistry and Molecular Biology **30**, 95-120 (1995).

[57] S. Krimm and J. Bandekar, Vibrational spectroscopy and conformation of peptides, polypeptides, and proteins. Advances in Protein Chemistry **38**, 181-364 (1986).

[58] K. Griebenow, A.M. Santos and K.G. Carrasquillo, "Secondary structure of proteins in the amorphous dehydrated state probed by FTIR spectroscopy. Dehydration-induced structural changes and their prevention". The Internet Journal of Vibrational Spectroscopy **3**(1), 2005.

[59] P.I. Haris and F. Seveercan, "FTIR spectroscopic characterization of protein structure in aqueous and non-aqueous media. Journal of Molecular Catalysis B: Enzymatic **7**, 207-221 (1999).

[60] R. Khurana and A.L. Fink, "Do parallel beta-helix proteins have a unique fourier transform infrared spectrum". Biophysical Journal **78**, 994-1000 (2000).

[61] J. Buijs and W. Norde, "Changes in the secondary structure of adsorbed IgG and F(ab)2 studied by FTIR spectroscopy". Langmuir **12**, 1605-1613 (1996).

[62] J.O. Speare and T.S. Rush, "IR spectra of cytochrome c denatured with deuterated guanidine hydrochloride show increase in β sheet". Biopolymers **72**, 193-204 (2003).

[63] D.J. Lacey, N. Wellner, F. Beaudoin, J.A. Napier and P.R. Shewry, "Secondary structure of oleosins in oil bodies isolated from seeds of safflower (Carthamus tinctorius L.) and sunflower (Helianthus annuus L.)". Biochemical Journal **334**, 469-477 (1998).

[64] Y. Zheng, "Analysis of vaccine: Structure, storage, moisture, and classification by infrared technology". Doctoral thesis, BioCentrum-DTU, Technical University of Denmark, Denmark, (2006).

Chapter III

In situ ATR-FTIR and two state kinetics model of BSA adsorption on TiO_2 surface

III.1. Introduction

Infrared spectroscopy is one of the most widely techniques used for identification of chemical compounds and materials, including liquids, solid substances and gases, through their ability to characterize absorption of infrared radiation **[1,2].**

Knowledge about solid-liquid interface is so important and plays a fundamental role in nature and technology especially in the field of metal oxide-aqueous solution interfaces that have attracted great attention because of their importance in several fields ranging from heterogeneous catalysis, atmospheric chemistry, corrosion, implants and adhesion to metal oxide crystal growth **[3-6]**. By measuring the intensity of the transmitted light as a function of wavelength, ATR-IR spectroscopy can provide a spectrum that contains information about the functional groups and chemical bonds present in the sample. This is valuable for identifying compounds, determining their concentrations, and studying chemical reactions. ATR-IR is a non-destructive and relatively quick method for obtaining structural and compositional information about a wide range of materials. However using ATR-IR for investigating proteins adsorption in water solution is a challenge because of the absorption of water in the same region of proteins as we will see in the next parts of this manuscript **[7].** However, spectroscopy of surface is not enough to get all necessary information about proteins adsorptions due to the complexity of the system being studied. For this reason sometimes modeling still have its great value to determine and complete the experimental studies.

III.2. Materials and methods

III.2.1. TiO_2 thin film preparation on germanium substrate

The experiments were carried out using commercial type TiO_2 anatase (Sigma-Aldrich Chemie GmbH) with an average particle size less than 25 nm (specific surface area 200–220 m^2/g, density: 3.9 g/ml at 25 °C). The porous films were formed by suspending 20 mg of TiO_2 anatase in 10 ml of purified water (Milli-Q, Millipore) water (18 MΩ cm) and sonicated for 30 min. The films were prepared by dropping the slurry onto a Ge internal reflection element (IRE, 52 mm x 20 mm x 1 mm, Komlas GmbH). The IRE was first cleaned, before film deposition, with ethanol and then put in air plasma for around 15 min. The solvent was evaporated using the spin coating technique (1000 rotation per minute) where twelve successive spin coatings were applied with 2.25 min between the individual ones. Then the samples were put in an oven to be dried at 80 °C for some hours. After this

step of drying the film was ready for use. A fresh catalyst sample was prepared for every experiment, and results were reproducible on different catalyst films. Bovine serum albumin protein (BSA, Sigma-Aldrich) (68 kDa, solubility 1g in 25 ml of H_2O) was used to prepare a BSA solution of 10^{-6} mol/l in the experiments under different pH values **[8,9]**.

III.2.2. In situ attenuated total reflection infrared spectroscopy

Attenuated total reflection infrared (ATR-IR) spectroscopy is a powerful and a well-established experimental method to investigate processes taking place at solid-liquid interfaces **[10–14].** ATR spectra were recorded with a dedicated flow-through cell, fabricated from a Teflon piece and a fused silica plate (45 mm x 35 mm x 3 mm). The cell contains two holes for the inlet and outlet (36 mm apart) and a flat (1 mm) viton seal. It was mounted on an attachment for ATR measurements within the sample compartment of a Bruker Equinox 55 FTIR spectrometer equipped with a narrowband MCT detector. All the spectra were recorded at a room temperature at a resolution of 4 cm^{-1} **[8]**.

III.3. ATR-FTIR results

III.3.1. The pH effect on the adsorption of BSA onto TiO_2 anatase

The pH of any solution used as a solvent for the protein is one of the most important environment parameters that affect the structure of the protein and thus the adsorption is affected too. Figure III.1 clearly shows that IR spectrum is sensitive to the structure of the protein. In addition, this figure elucidates the effect of pH on the adsorption of BSA onto TiO_2 anatase surface. For a pH around 10, the adsorption is very weak even it does not exist because the negative charge is unfavorable for the adsorption due to the repulsion of the adsorbed proteins **[15,16].** At this basic pH the shape of the BSA is not well known. But one of the most important factors can effects on the adsorption is the electrostatic forces between TiO_2 surface and BSA **[17,18].** For a pH near to the PZC of BSA (PZC = 4.8) or the one of TiO_2 the amount of adsorbed protein is maximal because the repulsive interactions are weak. A weak adsorption is observed when using an acidic solution of pH lower than 2 due the changes of protein structure (Expanded form) that takes more space on the surface and that is why the amount of adsorbed protein is reduced.

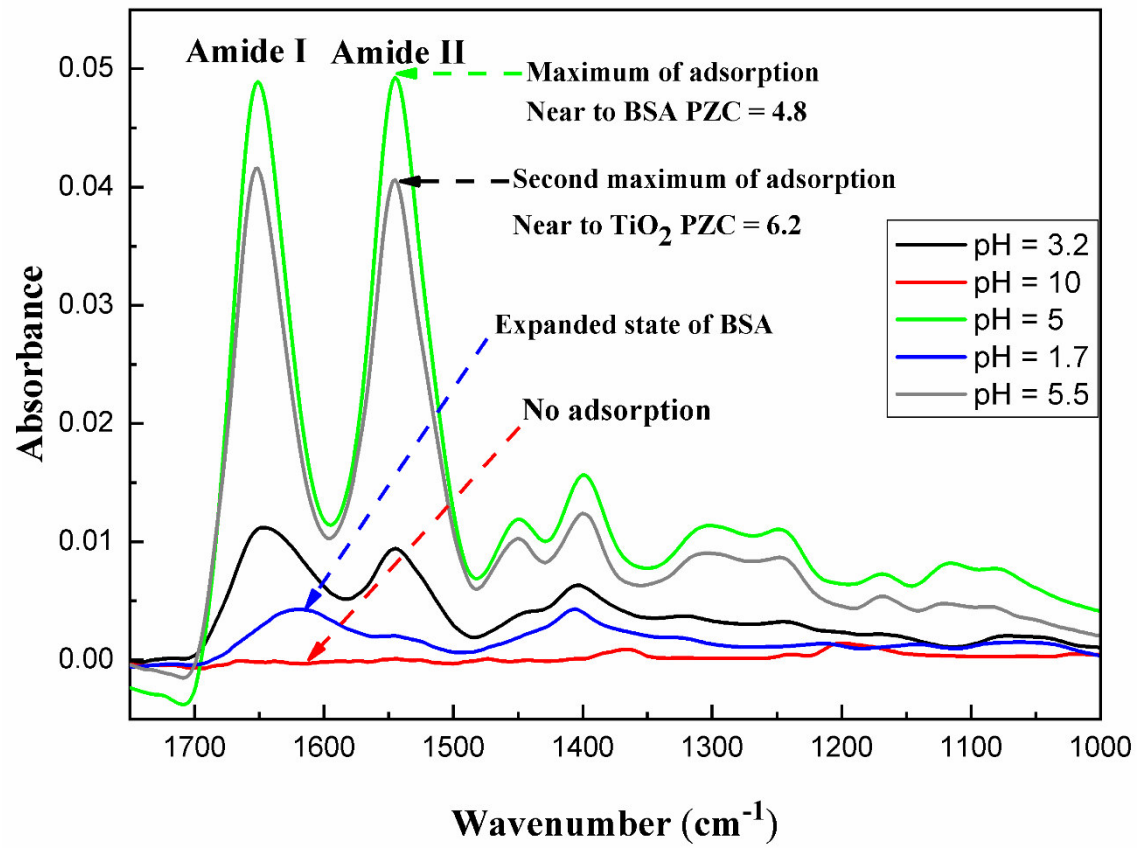

Figure III.1: The equilibrium spectra of BSA protein adsorption onto TiO_2 anatase thin films surface under various pH values (water is used as a solvent at 10^{-6} mol/l of BSA concentration).

Figure III.2.a shows the evolution of in situ FTIR-ATR spectra of expanded BSA (E form) adsorbed on TiO_2 anatase as a function of time. Regardless of the low amount of protein adsorbed, it is clear that adsorption is very rapid at the beginning. With time, the system evolves towards an equilibrium at around 80 min as illustrated in Figure III.2.b. It was then rinsed with the corresponding solution at the same pH and no changes were observed which strongly means that BSA in its E form is strongly bound to the surface.

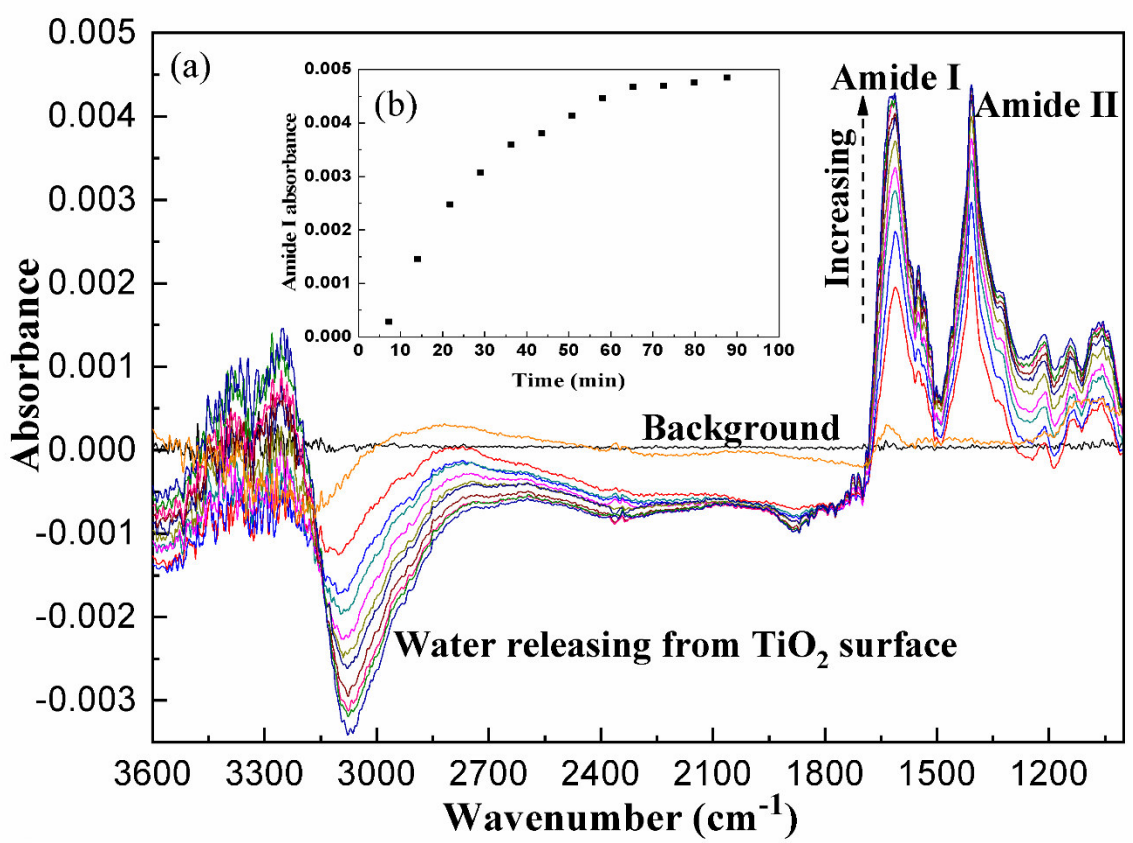

Figure III.2: (a) ATR-IR spectra collected in situ recorded during adsorption of BSA protein onto TiO_2 anatase surface at pH = 1.7 where the difference between each two successive spectra was around 7.5 min. (b) Absorbance variation of amide I band versus time and the difference between the first spectrum and background was taken as the origin of time (Experiments were done by A. Bouhekka who kindly gave these graphs).

The normalization of Figure III.2.b leads to the full surface coverage (θ %) as shown in Figure III.3 which clearly shows that the saturation of the surface was reached after around 80 min. This equilibrium is reached rather quickly and the graph shows that after 60 min the surface is almost full and no enough space left for other proteins to be adsorbed.

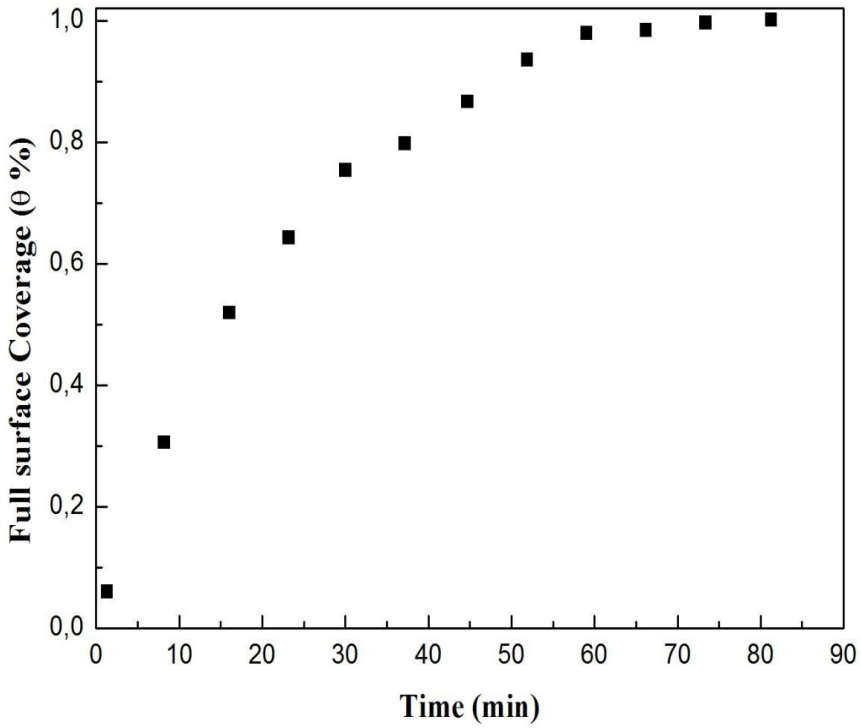

Figure III.3: The normalized absorption intensity of amide I (full surface coverage (Θ)) of BSA adsorbed onto TiO_2 anatase surface versus time at pH = 1.7.

III.4. Kinetics model of BSA protein adsorption at a solid surface

As the mechanisms behind protein adsorption events strongly affect the adsorption kinetics, the majority of models developed in this field are 'kinetic models' which are usually expressed through rate equations. In general it is rather uncomplicated to construct a kinetic model by using terms that represent the mathematical translation of adsorption phenomena such as structural rearrangements, lateral interactions, cooperative effects or overshooting.

The easiest way is to start with a reference model, for instance the Langmuir´s one, which is successively modified or extended **[19,20]**.

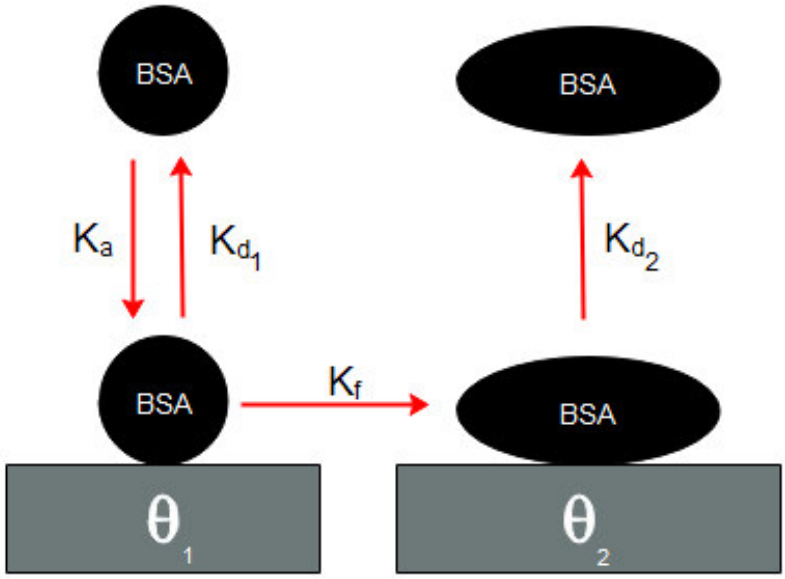

Figure III.4: A schematic illustrating the adsorption model of BSA protein on a solid surface presented in terms of the dependence of relative surface coverage by BSA.

From Figure III.4, the surface concentration of BSA in terms of its relative surface coverage Θ, the two-step (native Θ_1 and unfolding Θ_2) BSA adsorption kinetic model can be formulated as **[21,22]**. Usually, the unfolding state strongly depends on the adsorption parameters especially the pH of solution and concentration. This state is not well known and it could be slightly different from the native therefore desorption is possible ($K_{d_2} \neq 0$) and the improved model is given below:

$$\frac{d\Theta_1}{dt} = K_a C_0(1-\Theta_1-\Theta_2) - (K_{d_1}+K_f)\Theta_1 \quad \text{(III.1)}$$

$$\frac{d\Theta_2}{dt} = K_f\Theta_1 - K_{d_2}\Theta_2 \quad \text{(III.2)}$$

$$\frac{d\Theta}{dt} = \frac{d\Theta_1}{dt} + \frac{d\Theta_2}{dt} = K_a C_0(1-\Theta) - K_{d_1}\Theta_1 - K_{d_2}\Theta_2 \quad \text{(III.3)}$$

Where:

Θ_1, Θ_2 are the fractions of surface area occupied by protein in native and unfolding states, respectively. $\Theta = \Theta_1 + \Theta_2$ is the full surface coverage. K_a, K_f, K_{d_1} and K_{d_2} are the rate

constants of adsorption, transformation and desorption from native and unfolding states, respectively.

This relation is valid at any time (t) and satisfies the initial conditions $\Theta = 0$ at t = 0 s (and accordingly $\Theta_1 = \Theta_2 = 0$).

The mathematical solutions of the Eqs. (III.1)- (III.3) are indicated below:

$$\Theta_1(t) = -\frac{1}{2}\frac{K_a C_0[(\Phi K_{d_2} - \sigma\alpha)e^{-\frac{(\beta-\alpha)t}{2}} + (\Phi K_{d_2} + \sigma\alpha)e^{-\frac{(\beta+\alpha)t}{2}} - 2\Phi K_{d_2}]}{\Phi\delta} \quad \text{(III.4)}$$

$$\Theta_2(t) = -\frac{1}{2}\frac{K_a K_f C_0[(\Phi + \beta\alpha)e^{-\frac{(\beta-\alpha)t}{2}} + (\Phi - \beta\alpha)e^{-\frac{(\beta+\alpha)t}{2}} - 2\Phi]}{\Phi\delta} \quad \text{(III.5)}$$

$$\Theta(t) = -\frac{1}{2}\frac{K_a C_0\left[\left(\Phi(K_{d_2} + K_f) + \alpha(\beta K_f - \sigma)\right)e^{-\frac{(\beta-\alpha)t}{2}} + \left(\Phi(K_{d_2} + K_f) - \alpha(\beta K_f - \sigma)\right)e^{-\frac{(\beta+\alpha)t}{2}} - 2\Phi(K_{d_2} + K_f)\right]}{\Phi\delta} \quad \text{(III.6)}$$

Where:

$$\alpha = \sqrt{K_a^2 C_0^2 + 2K_a C_0(K_{d_1} - K_f - K_{d_2}) + (K_{d_1} + K_f - K_{d_2})^2}$$

$$\beta = K_a C_0 + K_{d_1} + K_f + K_{d_2}$$

$$\sigma = -K_{d_2}^2 + (K_a C_0 + K_{d_1} + K_f)K_{d_2} + 2K_a K_f C_0$$

$$\Phi = K_{d_2}^2 - 2(K_a C_0 + K_{d_1} + K_f)K_{d_2} + K_a^2 C_0^2 + 2K_a C_0(K_{d_1} - K_f) + (K_{d_1} + K_f)^2$$

$$\delta = (K_a C_0 + K_{d_1} + K_f)K_{d_2} + K_a K_f C_0$$

The general solution indicated above can be applied to any adsorption of any kind of protein at a solid surface if the kinetics constants are known. For BSA, the corresponding Θ_1, Θ_2 and Θ are shown on the Figure III.5 which clearly indicates that the sticking of BSA in its native state is very quickly in the beginning of the adsorption phenomenon whereas the unfolding state is very slow. When Θ_1 reaches a maximum after around (ten) 10 min it starts transforming to an unfolding state which increases. Thus the adsorbed amount of BSA in Θ_1 is reduced and in Θ_2 is increased.

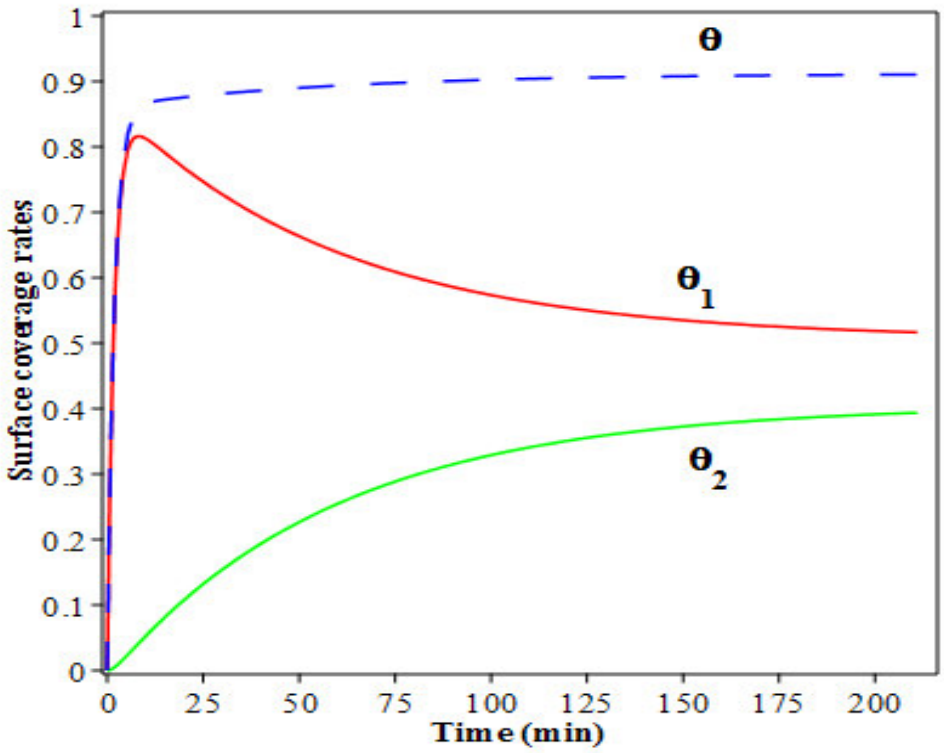

Figure III.5: The time dependence of the native (Θ_1), unfolding (Θ_2) states and full surface coverage (Θ) calculated for BSA adsorption on a gold surface using data from **[16]** where C_0 = 3 x 10^{-6} mol/l, K_a = 1.57 x 10^5 mol^{-1} l min^{-1}, K_f = 0.80 x 10^{-2} min^{-1} and K_{d_1} = 0.74 x 10^{-1} min^{-1}. K_{d_2} was chosen slightly different from K_{d_1} (K_{d_2}= 0.1 x 10^{-1} min^{-1}).

It is very clear from Figure III.5 that both stated reached equilibrium after 175 min of adsorption and no intersection between them is observed till 200 min where the amount of Θ_1 is still bigger than Θ_2.

The full surface coverage reached equilibrium of around 90% after 10 min of adsorption and still constant which strongly means that the behavior of this phenomenon is controlled by the changes between native and unfolding state plus their desorption from the surface and the total amount of adsorbed protein is constant.

Usually, the unfolding proteins Θ_2 are strongly stickled on the surface, therefore the possibility of desorption is very low, thus, one can ignore it (K_{d_2}= 0) and Eqs. (III.1) - (III.3) can be solved with the initial condition of (K_{d_2}= 0), we get the below outcomes:

$$\Theta_1(t) = \frac{K_a C_0 \alpha_1 [e^{-\frac{(\beta_1-\alpha_1)t}{2}} - e^{-\frac{(\beta_1+\alpha_1)t}{2}}]}{\Phi_1} \qquad \text{(III.7)}$$

$$\Theta_2(t) = -\frac{1}{2}\frac{K_a K_f C_0\left[(\Phi_1+\beta_1\alpha_1)e^{-\frac{(\beta_1-\alpha_1)t}{2}}+(\Phi_1-\beta_1\alpha_1)e^{-\frac{(\beta_1+\alpha_1)t}{2}}-2\Phi_1\right]}{\Phi_1\delta_1} \quad \text{(III.8)}$$

$$\Theta(t) = -\frac{1}{2}\frac{K_a C_0\left[(\Phi_1 K_f+\alpha_1(\beta_1 K_f-\sigma_1))e^{-\frac{(\beta_1-\alpha_1)t}{2}}+(\Phi_1 K_f-\alpha_1(\beta_1 K_f-\sigma_1))e^{-\frac{(\beta_1+\alpha_1)t}{2}}-2\Phi_1 K_f\right]}{\Phi_1\delta_1} \quad \text{(III.9)}$$

Where:

$$\alpha_1 = \sqrt{K_a^2 C_0^2 + 2K_a C_0(K_{d_1} - K_f) + (K_{d_1} + K_f)^2}$$

$$\beta_1 = K_a C_0 + K_{d_1} + K_f$$

$$\sigma_1 = 2K_a K_f C_0$$

$$\Phi_1 = K_a^2 C_0^2 + 2K_a C_0(K_{d_1} - K_f) + (K_{d_1} + K_f)^2$$

$$\delta_1 = K_a K_f C_0$$

Using these solutions Eq. (III.7)-(III.9) and applying them on the adsorption of bovine serum albumin (BSA) on a gold surface; the results indicated by the Figure III.6 strongly agree with those indicated by M. Dergahi et *al.* **[21]**, for time less than 60 min.

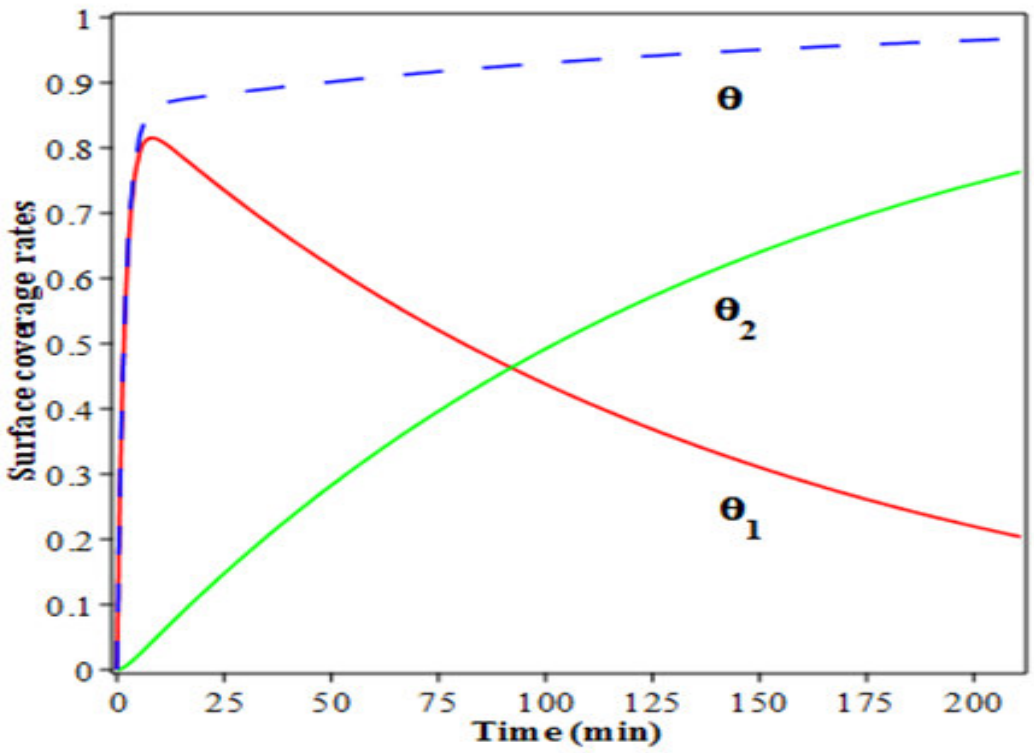

Figure III.6: The time dependence of the native (Θ_1), unfolding (Θ_2) states and full surface coverage (Θ) calculated for BSA adsorption on a gold surface using data from [16] where C_0 = 3 x 10^{-6} mol/l, K_a = 1.57 x 10^5 mol^{-1} l min^{-1}, K_f = 0.80 x 10^{-2} min^{-1} and K_{d_1} = 0.74 x 10^{-1} min^{-1}.

In general, this figure strongly shows a similar behavior as Figure III.5 excepting that equality between native and unfolding states is reached after around 85 min of adsorption and after that the amount of unfolding protein is higher than the native one.

In an adsorption experiment of protein with a concentration C_0 in a solution is adsorbed on homogeneous surface and the number of adsorbed molecules held per unit surface area at the moment is determined by the number of molecules that come to the surface from a solution and bonded on it for the same time interval Eq. (III.7) (unfold).

Proteins are irreversibly bonded on a surface with an adsorption rate constant K_a. Adsorbed native particles can transform from this state with the transformation rate constant K_f to another state if a free surface is available. Neglecting the desorption from the surface for native and unfolding states ($K_{d_1} = K_{d_2} = 0$)

The mathematical solutions of the Eqs. (III.4) - (III.6) are reduced to the followings:

$$\Theta_1(t) = \frac{K_a C_0 (-e^{-K_a C_0 t} + e^{-K_f t})}{K_a C_0 - K_f} \qquad \text{(III.10)}$$

$$\Theta_2(t) = \frac{K_f(e^{-K_a C_0 t})}{K_a C_0 - K_f} - \frac{K_a C_0 e^{-K_f t}}{K_a C_0 - K_f} + 1 \qquad \text{(III.11)}$$

$$\Theta(t) = 1 - e^{-K_a C_0 t} \qquad \text{(III.12)}$$

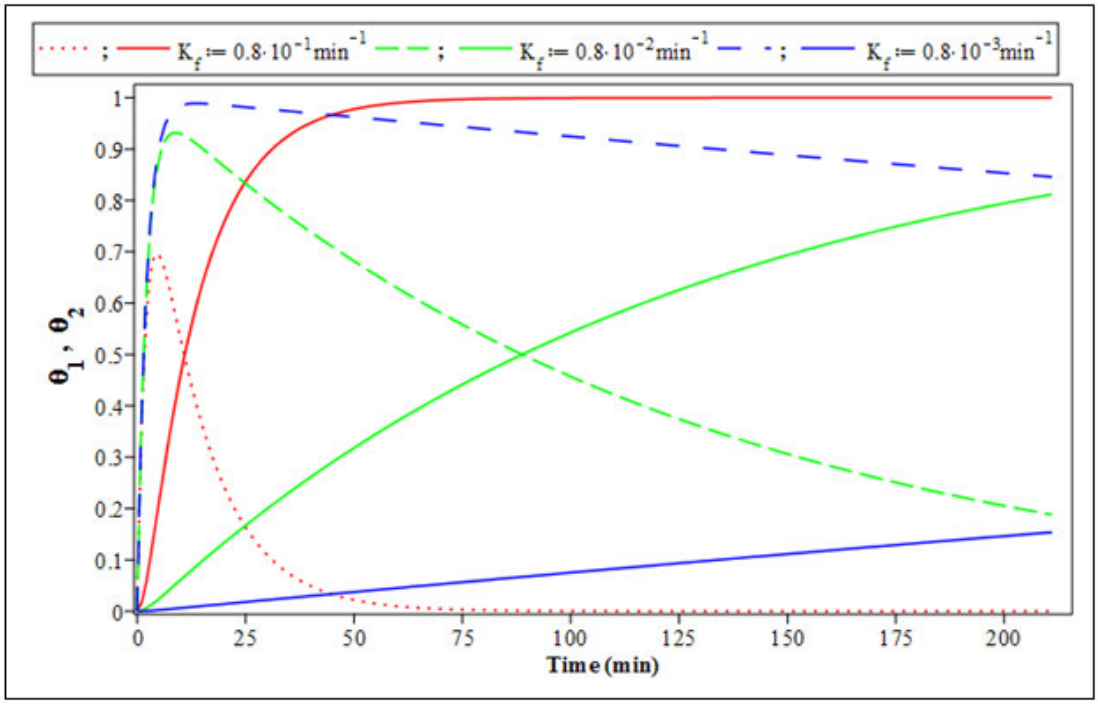

Figure III.7: The time dependence of surface coverage of BSA where (Θ_1) indicated by dashed lines (— —) and continuous lines (——) for (Θ_2) for different values of rate transformation constant K_f. The parameters used are: K_a = 1.57 x 10^5 mol^{-1} l min^{-1} and C_0 = 3 x 10^{-6} mol/l.

Figure III.7 indicates that the surface coverage Θ_1 (Eq. III.10) initially increases sharply and then reaches a maximum value of 70% at a binding time of 4.25 min, and then gradually decreases to a value of 2 % after 50 min of binding. On the other hand, the surface coverage Θ_2, (Eq. III.11) gradually increases in the entire time interval, and starts becoming predominant after 10.65 min of binding time at the transformation coefficient K_f = 0.8 x 10^{-1} min^{-1}. When we reduce a K_f = 0.8 x 10^{-2} min^{-1}. Θ_2 gradually increases in the entire time interval, and starts becoming predominant after 88 min and become majority at 200 min **[23-25]**.

This indicates that most of protein BSA that transform at longer times, when the system at acidic pH < 2.7. The transformation rate constant is smaller the surface coverage Θ_1 increases and approaches a plateau after 11 min and remains majority in a long time , so Θ_2 cannot be predominant in the system at the $K_f = 0.8 \times 10^{-3}\ min^{-1}$ and it does not exceed 14 % at a time of 200 min.

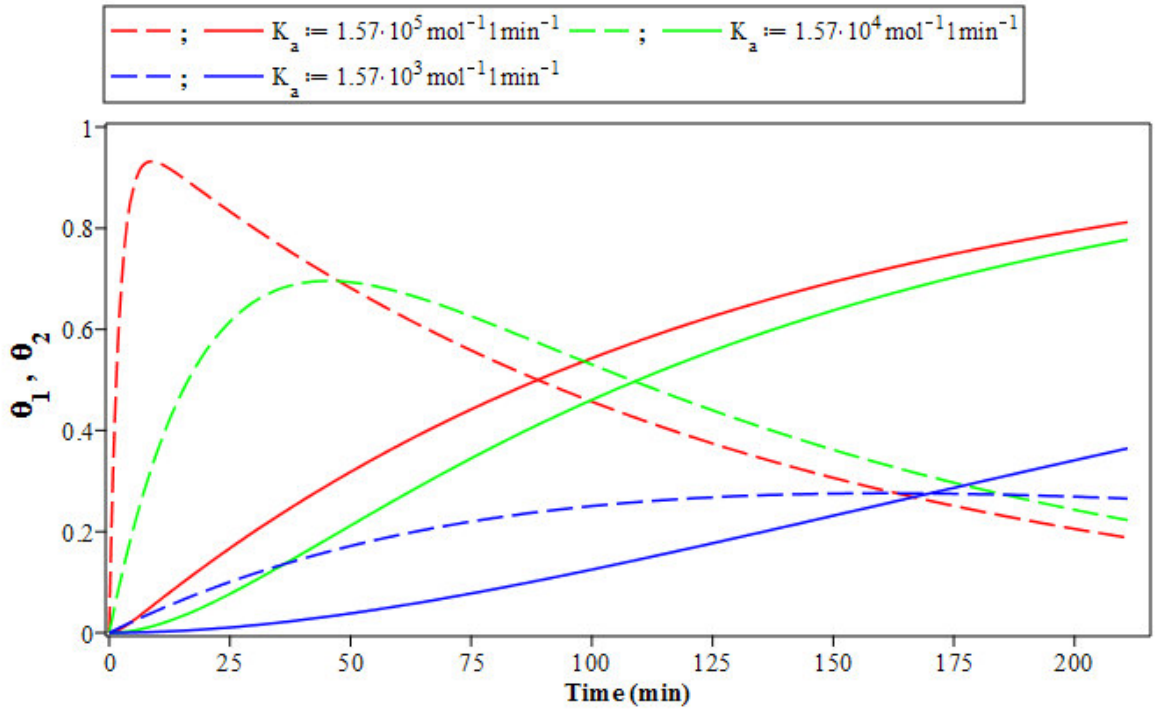

Figure III.8: The time dependence of surface coverage of BSA where (Θ_1) indicated by dashed lines (— —) and continuous lines (——) for (Θ_2) for different values of rate adsorption constant K_a. The parameters used are: $K_f = 0.8 \times 10^{-2}\ min^{-1}$ and $C_0 = 3 \times 10^{-6}$ mol/l.

Figure III.8 indicates that the surface coverage Θ_1 (Eq. III.10) initially increases sharply and then reaches a maximum value of 93% at a binding time of 08 min, and then gradually decreases to a value of 20 % after 200 min of binding. On the other hand, the surface coverage Θ_2, (Eq. III.11) gradually increases linearly in the entire time interval, and starts becoming predominant after 100 min of binding time at the adsorption coefficient $K_a = 1.57 \times 10^5\ mol^{-1}\ l\ min^{-1}$.

A high value of K_a suggests strong binding between the protein BSA and the surface. This implies that the adsorption process is favorable and efficient. In practical terms, a high K_a

indicates that even at relatively low concentrations of the protein BSA in the solution, a significant amount of protein BSA can be adsorbed onto the surface **[26,27]**.

When we reduce a K_a = 1.57 x 10^4 mol^{-1} l min^{-1} the surface coverage Θ_1 increases and approaches a maximum value of 69 % at a binding time of 44 min and then gradually decreases to a value of 24 % after 200 min of binding and the surface coverage Θ_2 starts becoming predominant after 120 min of binding time. When the adsorption coefficient K_a is smaller the surface coverage (Θ_1 and Θ_2) do not exceed to a value of 36 % at a time of 200 min**[28]**.

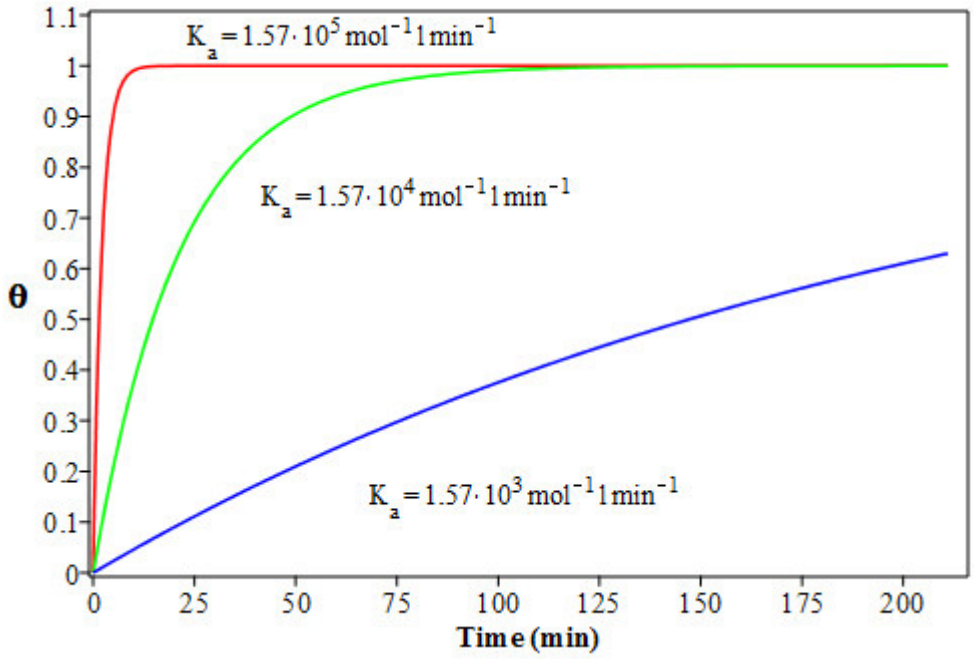

Figure III.9: The time dependence of full surface coverage of BSA (Θ) for different values of rate adsorption constant K_a. The parameters used are: K_f = 0.8 x 10^{-2} min^{-1} and C_0 = 3 x 10^{-6} mol/l.

For a three different values of rate adsorption constant K_a and taking into account the constant BSA concentration C_0 = 3 x 10^{-6} mol/l and K_f = 0.8 x 10^{-2} min^{-1}.

The results of full surface coverage are graphically presented in Figure III.9 which shows that the amount of adsorbed BSA is increased as function of rate adsorption constant K_a **[29].**

At K_a = 1.57 x 10^4 mol^{-1} l min^{-1}, the full surface coverage (Θ) increases and approaches a maximum after 100 min, but when we increase the rate adsorption constant K_a = 1.57 x

10^5 mol^{-1} l min^{-1}, Θ increases faster to surface saturation and the adsorption time is reduced to 11 min.

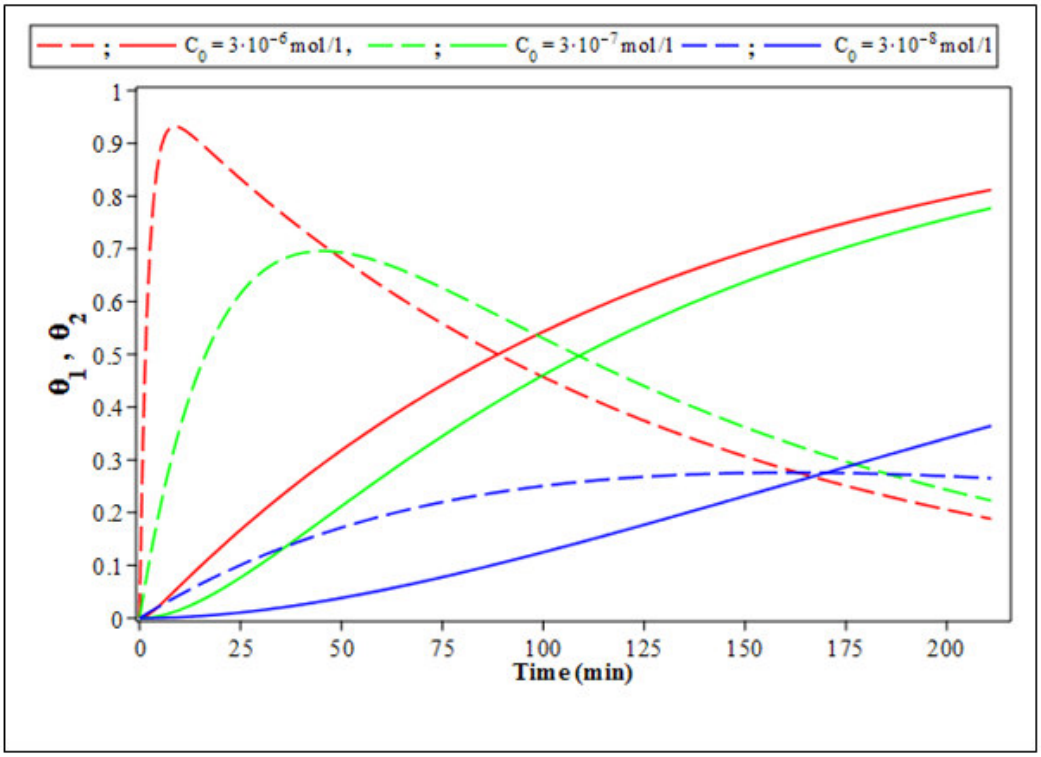

Figure III.10: The time dependence of native and unfolding states of BSA for different concentrations (same color for each value of C_0). Θ_1 dashed lines (— —) and Θ_2 continuous lines (——). The parameters used are K_a = 1.57 x 10^5 mol^{-1} l min^{-1} and K_f = 0.8 x 10^{-2} min^{-1}.

Figure III.10 shows the time dependence of surface coverage by BSA and taking into account the parameters K_a, K_f and three different BSA solution concentrations. The data in Figure III.10 demonstrate that the Θ_1 (expanding state) initial increase with in the first time of adsorption because the proteins are intrinsically surface active and tend to accumulate at interfaces. Whenever an aqueous protein solution is exposed to a solid surface, protein molecules will generally tend to adsorb spontaneously at the surface and it quickly approaches a maximum value when the concentration of the solution is higher than **[30]**, it starts gradually decreasing. On the other hand the surface coverage with a thermodynamically stable Θ_2 (unfolding state), gradually increases in the entire time interval studied. The results in Figure III.10 indicate that the transformation from the

thermodynamically unstable (Θ_1) in to the thermodynamically stable (Θ_2) adsorbed state/ transformation of BSA is rather difficult and we can't practically realize. The Figure III.10 indicates that the equilibrium on the surface native and unfolding states ($\Theta_1 = \Theta_2$) reached faster for higher concentration values.

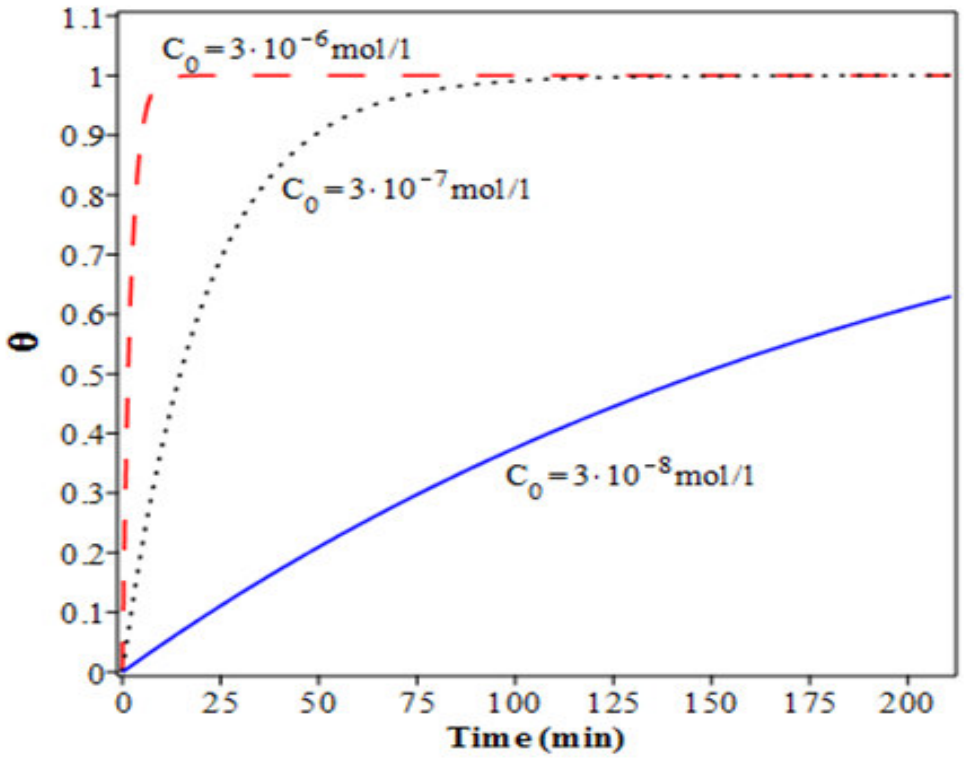

Figure III.11: The time dependence of full surface coverage of BSA (Θ) for different concentrations. The parameters used are K_a=1.57 x 10^5 mol^{-1} l min^{-1} and K_f = 0.8 x 10^{-2} min^{-1}.

This method was used to study the dynamic adsorption of BSA at surfaces as a function of various parameters K_a = 1.57 x 10^5 mol^{-1} l min^{-1} and K_f = 0.8 x 10^{-2} min^{-1} and specifically of different concentrations. It can be applied to study the expanded BSA in solution at pH = 1.7.

The results of full surface coverage are graphically presented in Figure III.11 which shows that the amount of adsorbed BSA is increased as function of protein concentration **[31]**. At C_0 = 3 x 10^{-7} mol/l, the full surface coverage (Θ) increases and approaches a maximum after 94 min, but when we increase the concentration to C_0 = 3 x 10^{-6} mol/l, Θ increases faster to surface saturation and the adsorption time is reduced to 10 min. These results

indicate that the residence time has important role in the dynamics of proteins adsorption on surface **[32]**.

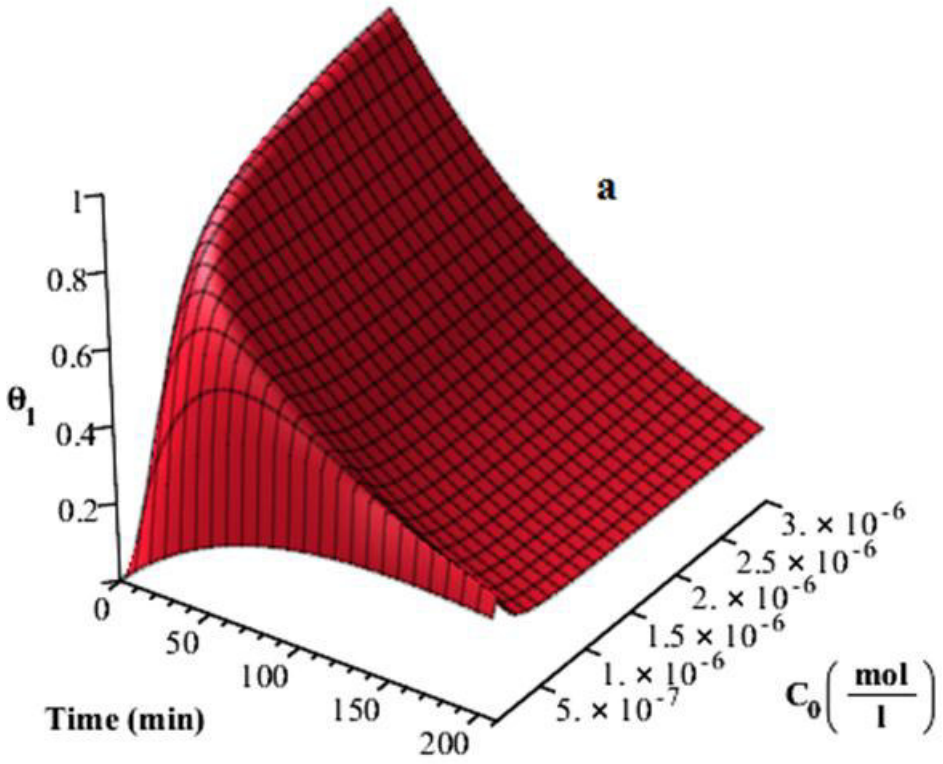

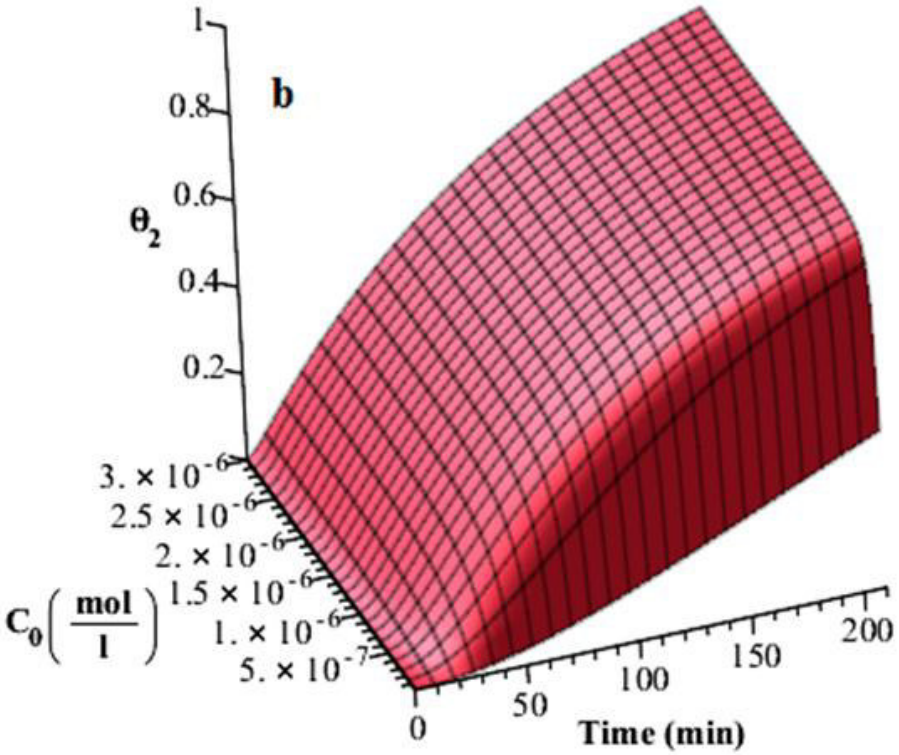

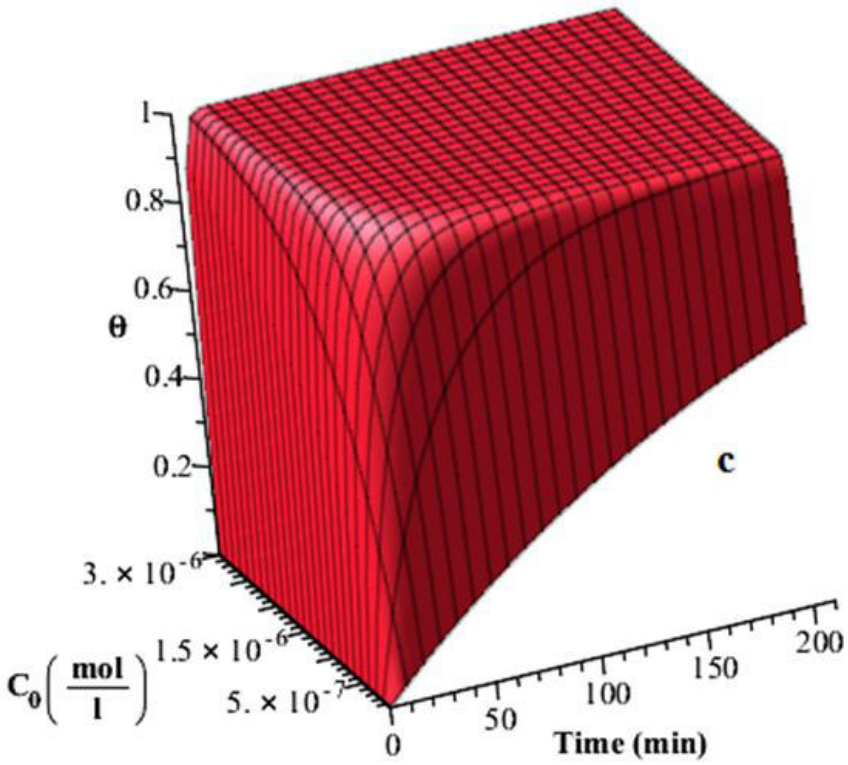

Figure III.12: Three dimensions 3D kinetic curves of: (a) the native state (Θ_1), (b) unfolding state (Θ_2) and (c) full surface coverage (Θ) versus time and concentration. The parameters used are $K_a = 1.57 \times 10^5$ mol^{-1} l min^{-1} and $K_f = 0.8 \times 10^{-2}$ min^{-1}.

To clearly illustrate the effect of concentration and time on the protein adsorption, three-dimensional plots, necessary, for Θ_1, Θ_2 and Θ were constructed showing the dependences of various concentrations C_0 with the time as shown in Figure III.12. As expected, the surface coverage of Θ_1, Θ_2 and Θ are determined by the concentration of protein BSA in a solution if the case where K_a and K_f are constants. However, although the amount of the expanding state form grows monotonically with increasing C_0 of protein in the solution, for higher concentration (3×10^{-6} mol/l), Θ_1 is dominating and reached a maximum in a short time t = 30 min afterward it will be decreasing exponentially with time. But for weak concentration (5×10^{-7} mol/l), Θ_1 reaches a maximum with coverage equal 0.4 (very weak compared to its value for higher concentration) at around t = 50 min. But a worth noting that the proteins has an important value at t = 200 min compared with other concentrations this overbalance to a strong sticking adsorption as indicated in Figure III.12 a, whereas this phenomenon is followed by the transformation to an unfolding state Θ_2 indicated in Figure III.12 b, Θ_2 is very weak at the beginning and it does not exceed 30 % for the time less

than 30 min, then it grows up till a maximum which strongly depends on the concentration of proteins in its native form (Θ_1) at the surface **[33]**.

The consequences of this behavior is that the full surface coverage (Θ) is represented by expanding state (Θ_1) up to time 90 min, because the proteins of BSA in their N form in the solution are small proteins and diffuse faster than large ones which make them the dominating species in the early adsorption stage. But over time, the fraction of the state (Θ_1) decreases until it reaches a level of around 35 % because of transformation in the state (Θ_2). Thus the unfolding state Θ_2 starts becoming predominant and it represents the majority from the full surface coverage (Θ).

The transformation of proteins to an unfolding state is not always possible, especially for solutions at pH more acidic where new can have the expanding form (E form) and practically the adsorption of proteins on a surface is almost irreversible as indicated bellow.

III.4.1. Modeling of expanded BSA protein adsorbed at pH = 1.7

At very low pH protein solution, in this case there are no different states of proteins at surface because all the molecules are unfolded into a unique state named expanded state (E state) where:

$$\Theta_1 = \Theta_2 = \Theta_E = \Theta$$

Neglecting the transformation coefficient ($K_f = 0$), the previous system becomes as follow:

$$\frac{d\Theta_1}{dt} = K_a C_0(1 - \Theta_1 - \Theta_2) \quad \text{(III.13)}$$

$$\frac{d\Theta_2}{dt} = K_f \Theta_1 = 0 \quad \text{(III.14)}$$

$$\frac{d\Theta_E}{dt} = K_a C_0(1 - \Theta_1 - \Theta_2) = \frac{d\Theta}{dt} \quad \text{(III.15)}$$

The result:

$$\Theta_E = 1 - e^{-K_a C_0 t} \quad \text{(III.16)}$$

The unfolding of protein adsorbed on a solid-surface under pH = 1.7 leads to more contact between the protein and the surface. This means that the rate constant for the transformation will be very small (negligible) and the space between adsorbed proteins will be reduced **[34]**.

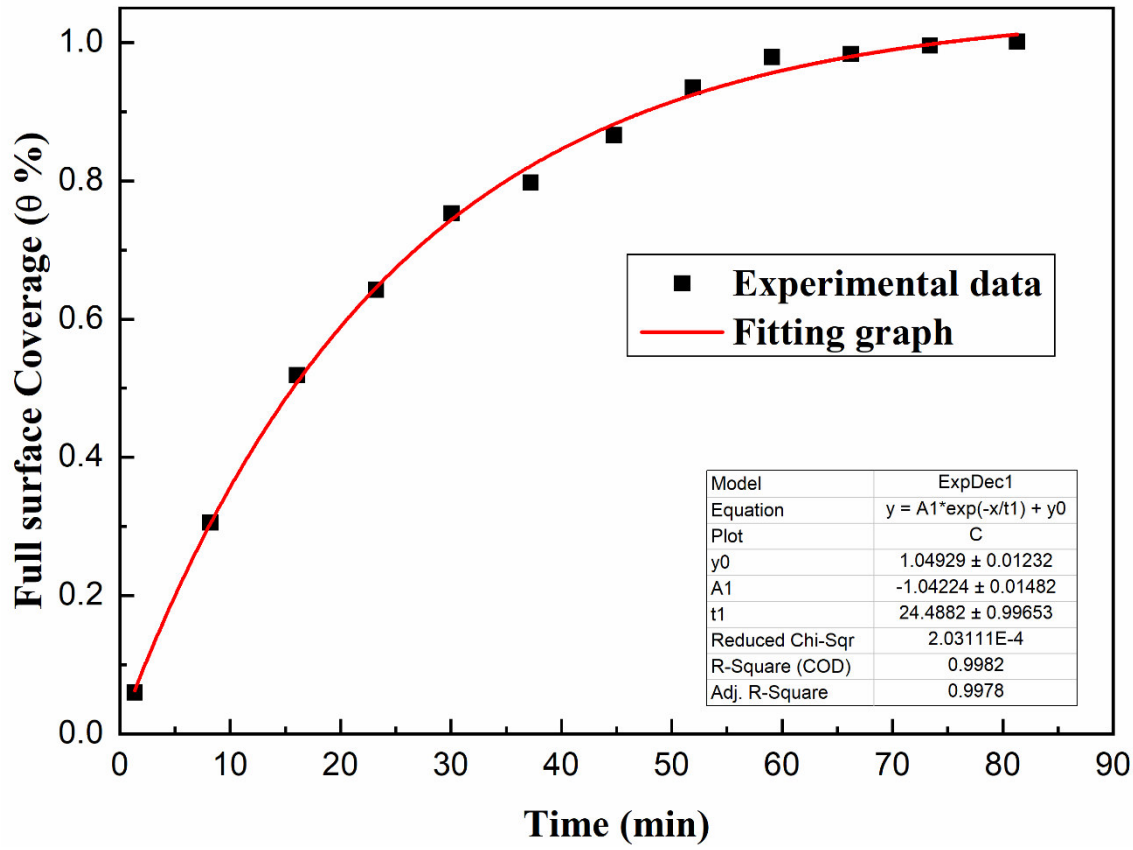

Figure III.13: Fitting of experimental data of the full surface coverage of BSA protein adsorbed onto TiO_2 anatase surface at pH = 1.7.

One of the most important points in this work is to compare the experimental data of ART-FTIR and the theoretical model as indicated clearly by Figure III.13. The mathematical equation of this fitting which leads to a good coincidence between the two graphs is given by Eqs. (III.17):

$$\Theta(t) = (1.0492 \pm 0.01232) - (1.0422 \pm 0.01482)\ \exp\left(\frac{-t}{24{,}488}\right) \qquad \text{(III.17)}$$

Finally, a comparison of Eqs. (III.16) and (III.17) for a concentration $C_{0\ exp} = 10^{-6}$ mol/l indicates the value of the adsorption rate constant $K_{a\ exp} = (0.04083 \pm 0.99653) \times 10^{6}$ mol^{-1} l min^{-1}.

III.5. Conclusion

The present chapter indicated that the surface of any solid material plays a crucial role in the determination of the rate coverage of adsorbed bio-molecules. The expanded BSA protein at TiO_2 anatase surface was studied using FTIR-ART and the two states model where the findings strongly showed that the amount and kinetic of adsorption were different from those of BSA adsorbed under other pH values at similar surfaces. The

application of mathematical model on the experimental results allowed us to determine the rate constant of adsorption (K_a) of expanded BSA protein. This method can be applied on other proteins adsorbed at different pH values taking into account their corresponding kinetics parameters. The equilibrium between native and unfolding states of adsorbed proteins can be determined using the analytical solution, presented in this part, which is considered as one of the most important points of this work. This knowledge cannot be evaluated using experimental methods especially for weak signals.

References

[1] https://niom.no/ft-ir-fourier-transform-infrared-spectroscopy.

[2] **A. Urakawa, R. Wirz, T. Bürgi, and A. Baiker**, "ATR-IR flow-through cell for concentration modulation excitation spectroscopy: diffusion experiments and simulations" J. Phys. Chem. B **107** (47), 13061-13068 (2003).

[3] **R. Wirz**, "Molecular insight into chromatographic and catalytic interfaces by in situ ATR-IR spectroscopy". Doctoral Thesis, Swiss Federal Institute of Technology (ETH) Zurich, Switzerland,(2007).

[4] **R. Wirz, T. Bürgi, W. Lindner and A. Baiker**, "Absolute configuration modulation attenuated total reflection IR Spectroscopy: An in situ method for probing chiral recognition in liquid chromatography". Analytical Chemistry **76**, 5319-5330 (2004).

[5] **B. Srour, S. Bruechert, L.A. Susana and P. Hellwig**, "Secondary structure determination by Means of ATR-FTIR spectroscopy. In book: Membrane protein structure and function characterization: Methods and protocols, 195-203 (2017).

[6] **J. Kong and S. Yu**, "Fourier transform infrared spectroscopic analysis of protein secondary structures". Acta biochimica and biophysica Sinica, **39** (8), 549-559 (2007).

[7] **Z.H. Lee et *al.***, "Determination of protein secondary structures using FTIR spectroscopy". Application Development & Support Centre, Shimadzu (Asia Pacific) Pte Ltd, Singapore. ITS Student from Nanyang Technological University, Singapore, Application news, N^0-AD-0178 (2018).

[8] **A. Bouhekka and T. Bürgi**, "Photodegradation of adsorbed bovine serum albumin on TiO_2 anatase investigated by In-Situ ATR-IR spectroscopy, Acta. Chimica Slovenica, **59**, 841–847 (2012).

[9] **A. Bouhekka**, "Adsorption of BSA protein on silicon, germanium and titanium dioxide investigated by in situ ATR-IR spectroscopy". Doctoral thesis, University of Oran, Algeria (2013).

[10] **S.J. Hug and B. Sulzberger**, "In situ fourier transform infrared spectroscopic evidence for the formation of several different surface complexes of oxalate on TiO_2 in the aqueous phase", Langmuir **10**, 3587–3597 (1994).

[11] **T. Bürgi, R. Wirz and A. Baiker**, "In situ attenuated total reflection spectroscopy: A sensitive tool for the investigation of reduction-oxidation processes on heterogeneous Pd metal catalysts", Phys. Chem. B **107**, 6774–6781 (2003).

[12] **T. Bürgi, and A. Baiker**, "Attenuated total reflection infrared spectroscopy of solid catalysts functioning in the presence of liquid-phase reactants". Adv. Catal. **50**, 227–283 (2006).

[13] **B.E. Givens, N.D. Diklich, J. Fiegel and V.H. Grassian**, "Adsorption of bovine serum albumin on silicon dioxide nanoparticles: Impact of pH on nanoparticle–protein interactions". Biointerphases **12**, 02D404 (2017).

[14] **A. Bouhekka and T. Bürgi**, "In situ ATR-IR spectroscopy study of adsorbed protein: visible light denaturation of bovine serum albumin on TiO_2", Appl. Surf. Sci. **261** 369–374 (2012).

[15] **M.E. Lienqueo, A. Mahn, J.C. Salgado and J.A. Asenjo**, "Current insights on protein behaviour in hydrophobic interaction chromatography", Chromatogr. B. **849**, 53–68 (2007).

[16] **F. Xia, D. Negrath and S.M. Cramer**, "Effect of pH changes on water release values in hydrophobic interaction chromatographic systems", Chromatogr. A. **1079**, 229–235 (2005).

[17] **F.Y. Oliva, L.B. Avalle, O.R. Camara and C.P. De Pauli**, "Adsorption of human serum albumin (HSA) onto colloidal TiO_2 particles". Colloid and Interface Sci. **261**, 299–311 (2003).

[18] **R. Huber and S. Stoll**, "Protein affinity for TiO2 and CeO2 manufactured nanoparticles. From ultra-pure water to biological media", Colloids Surf. A Physicochem. Eng. Asp. **553**, 425– 431 (2018).

[19] **J. Kim**, "Mathematical modeling approaches to describe the dynamics of protein adsorption at solid interfaces", Colloids Surf. B. Biointerfaces **162**, 370–379 (2018).

[20] **J. Zhou, M. Wang, B. Zhang, and Q. Zhang**, "Metal coordination assisted thermo-sensitive magnetic imprinted microspheres for selective adsorption and efficient elution of proteins", Colloids Surf. A Physicochem. Eng. Asp. **612**, 125981 (2021).

[21] **M. Dargahi and S. Omanovic**, "A comparative PM-IRRAS and ellipsometry study of the adsorptive behaviour of bovine serum albumin on a gold surface", Colloids Surf. B Biointerfaces **116**, 383–388 (2014).

[22] **M. Dargahi, A.L.J. Olsson, N. Tufenkji and R. Gaudreault**, "Green technology tannin-based corrosion inhibitor for protection of mild steel", Corrosion **71**, 1321–1329 (2015).

[23] **V.P. Zhdanov and B. Kasemo**, "Monte Carlo simulation of the kinetics of protein adsorption". Proteins: Structure, Function, and Bioinformatics **30**(2), 177-182 (1998).

[24] **V.P. Zhdanov and B. Kasemo**,"Monte Carlo simulation of denaturation of adsorbed Proteins". Proteins: Structure, Function, and Bioinformatics **30** (2), 168-176 (1998).

[25] **N. Willem**, "Adsorption of proteins at solid-liquid interfaces". Cells and Materials, **5** (1), 9 (1995).

[26] **M. Rabe et *al.***, "Surface organization and cooperativity during nonspecific protein adsorption events". J. Phys. Chem. B, **112**, 13971–13980 (2008).

[27] **F. Felsovalyi** ,"Mechanistic Study of the Adsorption and Desorption of Proteins on Silic". Doctoral thesis, University of Columbia (2012).

[28] **X. Wu, P. Hao, F. He, Z. Yao and X. Zhang**, "Molecular dynamics simulations of BSA absorptions on pure and formate contaminated rutile (110) surface". Applied Surface Science, **533**, 147574 (2020).

[29] **A. Docoslis et *al.*** , "Measurements of the kinetic constants of protein adsorption onto silica particles". Colloids and Surfaces B: Biointerfaces 13.2: 83-104 (1999).

[30] **S.J. McClellan, E.I. Franses**, "Adsorption of bovine serum albumin at solid/aqueous interfaces". Colloids Surf. A Physicochem. Eng. Asp. **260**, 265–275 (2005).

[31] **D. Vitasari, P. Grassia and P. Martin**,"Simulation of dynamics of adsorption of mixed protein-surfactant on a bubble surface", Colloids Surf. A Physicochem. Eng. Asp. **438**, 63–76(2013).

[32] **K.M. Yeung, Z.J. Lu and N.H. Cheung**, "Adsorption of bovine serum albumin on fused silica: elucidation of protein–protein interactions by single-molecule fluorescence microscopy". Colloids Surf. B Biointerfaces **69**, 246–250 (2009).

[33] **B.A. Snopok, and E.V. Kostyukevich**," Kinetic studies of protein–surface interactions: A two-stage model of surface-induced protein transitions in adsorbed biofilms". Analytical Biochemistry **348,** 222–231 (2006).

[34] **M. Tadjine, F. Bouzidi, A. Berbri, H. Nehmar and A. Bouhekka**,"In situ fourier transform infrared-attenuated total reflection spectroscopy and modeling investigation of protein adsorption: Case of expanded bovine serum albumin on titanium dioxide anatase". Biointerphases **19** (1), (2024).

Chapter IV

The effect of available space during unfolding process: A comparison study

IV.1. Introduction

Progress on understanding protein adsorption has been considerable over the past few years but the concept of interfacial adsorption behavior of proteins remains unclear. This is largely because of the higher complexity of protein adsorption that poses a lot of experimental difficulties such as varying molecular weight, charge and structural forms of proteins. Theoretical understanding of proteins and their intrinsic processes have been studied previously **[1,2]**. The interaction of the proteins with solid surfaces is not only a fundamental phenomenon but is also a key phenomenon to several important and novel applications, as mentioned earlier. The interaction of proteins with the surfaces involves both the binding and unfolding of proteins **[3-5**]. The desire to control, predict and understand the protein adsorption on surface has been the ultimate goal of Chapter 4 of this thesis. This also involved goals of studying surface coverage and kinetic details of the protein-surface interactions taking into account several factors such as available space and the equilibriums between adsorption, desorption and unfolding process.

IV.2. The effect of concentration and adsorption rate constant in case of equilibrium between adsorption and desorption

In the field of protein adsorption studies, the primary objective is to understand the behavior of proteins in close proximity to or deposited onto the surface. This includes their behavior as individual species and as a component in an ensemble. Given the considerable albeit not unlimited technical opportunities to date, large amounts of experimental data are available.

However, techniques allowing a direct observation of the undisturbed adsorption of proteins in molecular dimensions are still far from being mature. Thus, experimental data typically contain macroscopic information resulting from the individual behaviors of one or several proteins. At this point the design of a model that mathematically describes the experimental data is an efficient way to unravel or confirm mechanistic details of the adsorption process **[6,7**]. A model always opens the opportunity to 'play' with different ideas or to test different sets of parameters which in the end helps to argue what is possible and what is not. However, models are typically restricted to the experimental limits in which their hypotheses can be tested and generalization to other systems must be done with care. There are two main directions for developing mathematical model description in the field of protein adsorption. Kinetic models on the one hand describe the events and

phenomena during the course of adsorption or desorption. They typically start with an empty surface and model the adsorption kinetics until surface saturation is reached. Often the desorption process upon rinsing the surface with protein buffer is also included **[8,9]**.

Here we are interested to study some particular cases during the adsorption of proteins at solid surface. We can apply the following approximations to the adsorption kinetic model A described previously in chapter III, where we consider the following conditions: ($K_a = K_f + K_{d_1}$) and ($K_{d_2} = K_f$).

As it was reported in chapter III, The mathematical solutions of the Eqs. (III.1)- (III.3) are indicated below:

$$\Theta_1(t) = -\frac{1}{4}\frac{K_a C_0[(\Phi_2 - \sigma_2\alpha_2)e^{-\frac{(\beta_2-\alpha_2)t}{2}} + (\Phi_2 + \sigma_2\alpha_2)e^{-\frac{(\beta_2+\alpha_2)t}{2}} - 2\Phi_2]}{\Phi_2\delta_2} \quad \text{(IV.1)}$$

$$\Theta_2(t) = -\frac{1}{4}\frac{K_a C_0[(\Phi_2 + \beta_2\alpha_2)e^{-\frac{(\beta_2-\alpha_2)t}{2}} + (\Phi_2 - \beta_2\alpha_2)e^{-\frac{(\beta_2+\alpha_2)t}{2}} - 2\Phi_2]}{\Phi_2\delta_2} \quad \text{(IV.2)}$$

$$\Theta(t) = -\frac{1}{4}\frac{K_a C_0(2\Phi_2 + \alpha_2(\beta_2 - \sigma_2))e^{-\frac{(\beta_2-\alpha_2)t}{2}} + (2\Phi_2 - \alpha_2(\beta_2 - \sigma_2))e^{-\frac{(\beta_2+\alpha_2)t}{2}} - 4\Phi_2]}{\Phi_2\delta_2} \quad \text{(IV.3)}$$

Where:

$$\alpha_2 = \sqrt{K_a^2 C_0^2 + 2K_a C_0(K_{d_1} - 2K_f) + {K_{d_1}}^2}$$

$$\beta_2 = K_a C_0 + K_a + K_f$$

$$\sigma_2 = 3K_a C_0 + K_{d_1}$$

$$\Phi_2 = K_a^2 C_0^2 + 2K_a C_0(K_{d_1} - 2K_f) + {K_{d_1}}^2$$

$$\delta_2 = K_a C_0 + \frac{K_a}{2}$$

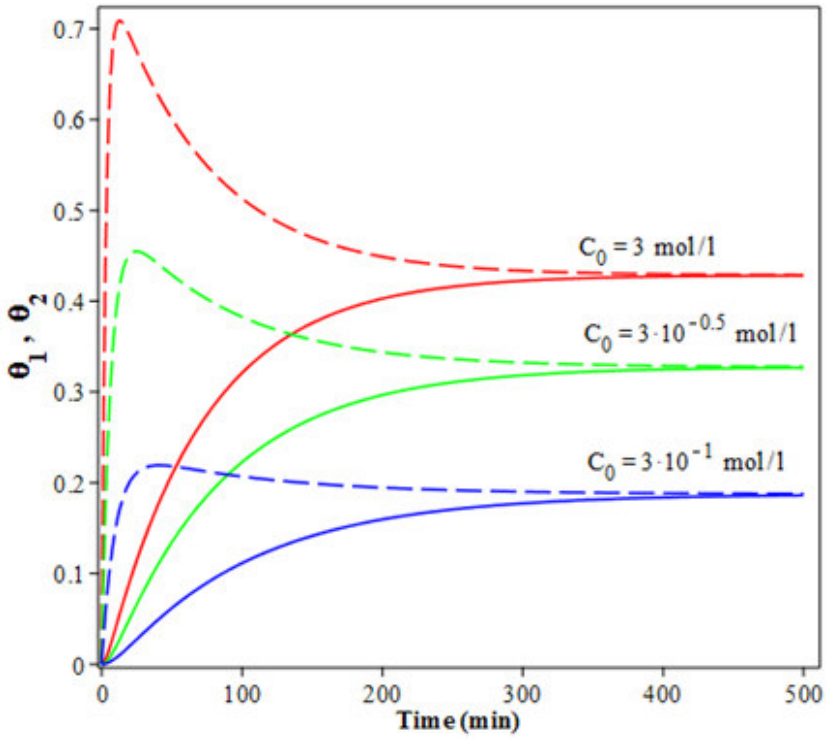

Figure IV.1: The time dependence of native and unfolding states of BSA for different concentrations (same color for each value of C_0).$\Theta_1$dashed lines (— —) and $\Theta_2$continuous lines (——). The parameters used are$K_a = K_f + K_{d_1} = 0.082$ mol^{-1} l min^{-1}, $K_{d_2} = K_f = 0.8 \times 10^{-2} min^{-1}$ and $K_{d_1} = 0.74 \times 10^{-1} min^{-1}$ **[10]**.

Figure IV.1shows the time dependence of surface coverage by BSA and taking into account the parameters K_a, K_f, $K_{d_1}$and three different BSA solution concentrations.

The graph in Figure IV.1 indicates that the surface coverage Θ_1(Eq. IV.1) initially increases sharply and then reaches a maximum value of 71% at a binding time of 13 min, and then gradually decreases to a the equilibrium on the surface native and unfolding states ($\Theta_1 = \Theta_2$); the state of equilibrium on the surface reached faster a maximum value of 42% after 390 min of binding for higher concentration values $C_0 = 3$mol/l**[11,12]**.But when we decrease the concentration C_0,the equilibrium point ($\Theta_1 = \Theta_2$)gradually decreases to a value of 18 % for a period of time 460 min at concentration values $C_0 = 3 \times 10^{-1}$ mol/l.

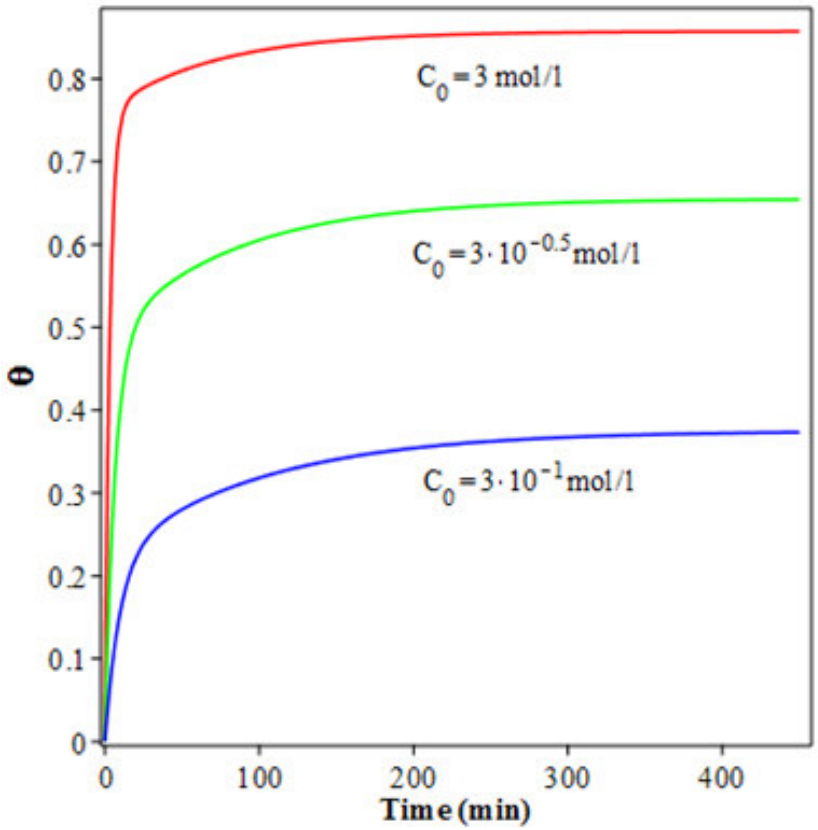

Figure IV.2: The time dependence of full surface coverage of BSA (Θ) for different concentrations. The parameters used are$K_a = K_f + K_{d_1} = 0.082$ mol^{-1} l min^{-1}, $K_{d_2} = K_f = 0.8 \times 10^{-2} min^{-1}$ and $K_{d_1} = 0.74 \times 10^{-1} min^{-1}$ **[10].**

The results of full surface coverage are graphically presented in Figure IV.2 which shows that the amount of adsorbed BSA is increased as function of protein concentration **[13]**.

AtC_0 = 3mol/l,the full surface coverage (Θ) increases and approaches a maximum value of 83 % after 100 min. In this Region I, there is ample surface available to all protein to maximize protein-surface contacts. However, in Region II, the adsorption of proteins with the surface is the maximum and this is due to the lack of vacant spaces on the surface.

When we reduce a $C_0 = 3 \times 10^{-1}$mol/l, the full surface coverage (Θ)remains fixed at a value of 37 % Despite the increase in time. These results indicate that varying the protein concentration clearly affects to the full surface coverage (Θ)percentage**[14,15]**.

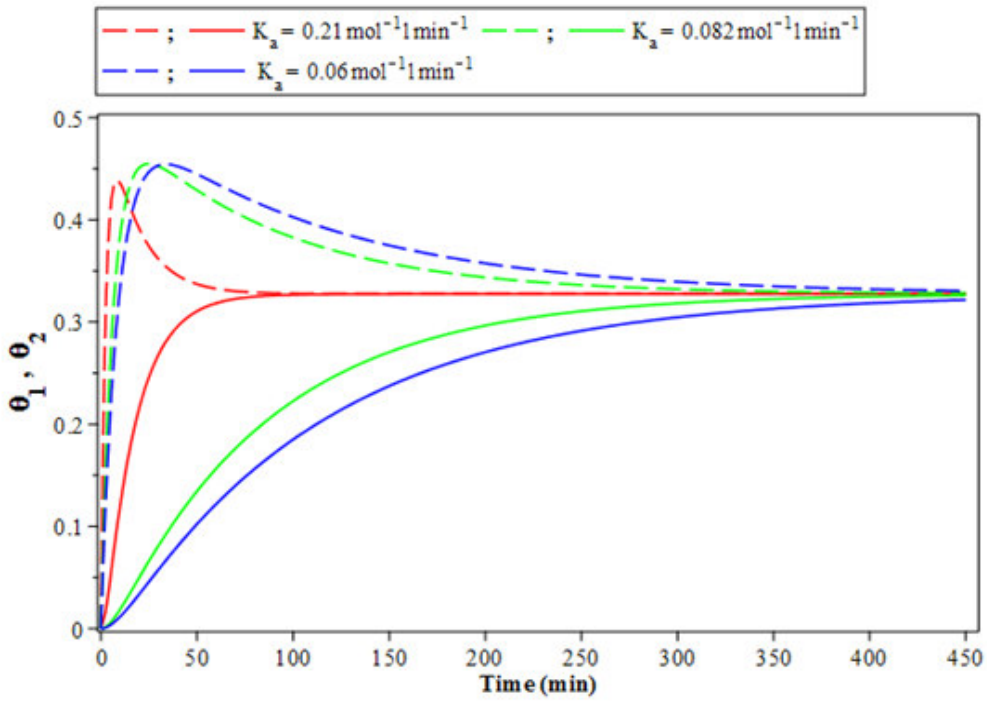

Figure IV.3: The time dependence of surface coverage of BSA where (Θ_1) indicated by dashed lines (— —) and continuous lines (——) for (Θ_2) for different values of rate adsorption constant K_a. The parameters used are: C_0 = 3 x $10^{-0.5}$ mol/l, K_a= K_f+ K_{d_1} and K_{d_2}=K_f **[10]**.

The data in Figure IV.3 indicates that the surface coverage Θ_1(Eq. IV.1) initially increases sharply and then reaches a maximum value of 45 % at a binding time of 24 min,

and then gradually decreases to a the equilibrium on the surface native and unfolding states ($\Theta_1 = \Theta_2$) reached faster a value of 32 % for higher value of rate adsorption constant K_a= 0.21 mol^{-1} l min^{-1} at a binding time of 100 min.When we reduce a K_a= 0.082 mol^{-1} l $min^{-1}$the state of equilibrium on the surface between native and unfolding states ($\Theta_1 = \Theta_2$) reached a same value 32 % a long time 420 min **[16]**.

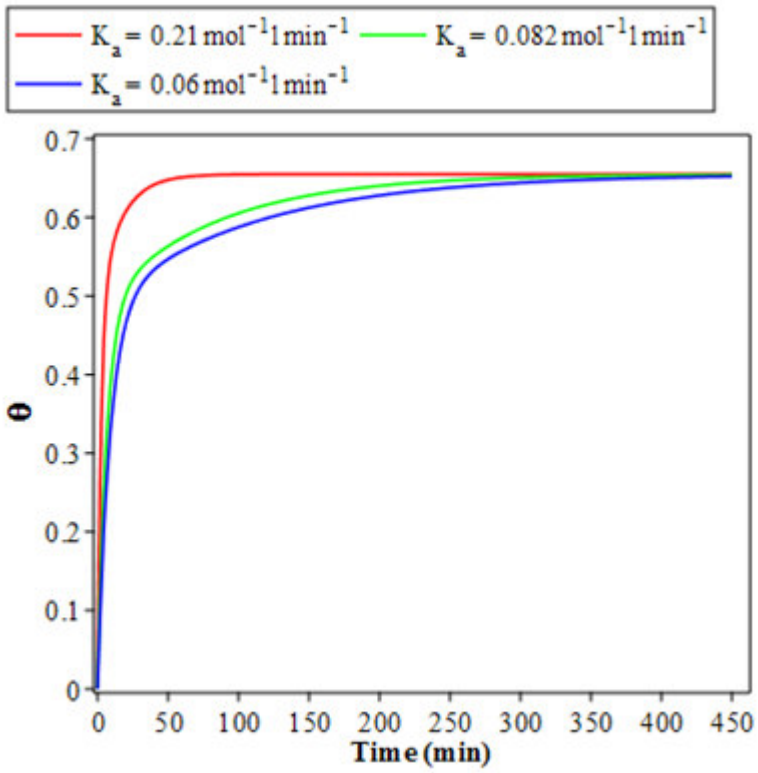

Figure IV.4: The time dependence of full surface coverage of BSA (Θ) for different values of rate adsorption constant K_a. The parameters used are: $C_0 = 3 \times 10^{-0.5}$ mol/l, $K_a = K_f + K_{d_1}$ and $K_{d_2} = K_f$ **[10]**.

The results of full surface coverage are graphically presented in Figure IV.4 which shows that the amount of adsorbed BSA is increased as function of rate adsorption constant. At $K_a = 0.06$ mol^{-1} l min^{-1}, the full surface coverage Θ increases and approaches a maximum after 350 min, but when we increase rate adsorption constant $K_a = 0.21$ mol^{-1} l min^{-1}, Θ increases faster to surface saturation and the adsorption time is reduced to 58 min. These results indicate that varying the constant adsorption rate does not affect the surface coverage percentage but indicate that the residence time has important role in the dynamics of proteins adsorption in surface saturation **[17,18]**.

IV.2.1.Case of steady state

In the following part, we want to study the model reported in chapter III in its steady state case as given bellow:

$$\frac{d\theta_1}{dt} = K_a C_0 (1-\theta_1 - \theta_2) - (K_{d_1} + K_f)\,\theta_1 = 0 \qquad \text{(IV.4)}$$

$$\frac{d\theta_2}{dt} = K_f\,\theta_1 - K_{d_2}\,\theta_2 = 0 \qquad \text{(IV.5)}$$

$$\frac{d\theta}{dt} = \frac{d\theta_1}{dt} + \frac{d\theta_2}{dt} = K_a C_0 (1-\theta_1 - \theta_2) - K_{d_1}\theta_1 - K_{d_2}\theta_2 = 0 \qquad \text{(IV.6)}$$

The solutions of these equations are indicated below:

$$\theta_1(t) = \frac{K_a K_{d_2} C_0}{K_a C_0 (K_f + K_{d_2}) + K_{d_2} (K_f + K_{d_1})} \qquad \text{(IV.7)}$$

$$\theta_2(t) = \frac{K_a K_f C_0}{K_a C_0 (K_f + K_{d_2}) + K_{d_2} (K_f + K_{d_1})} \qquad \text{(IV.8)}$$

$$\theta(t) = \frac{K_a C_0 (K_f + K_{d_2})}{K_a C_0 (K_f + K_{d_2}) + K_{d_2} (K_f + K_{d_1})} \qquad \text{(IV.9)}$$

The evolution of these solutions as a function of concentration is given in the following Figure IV.5.

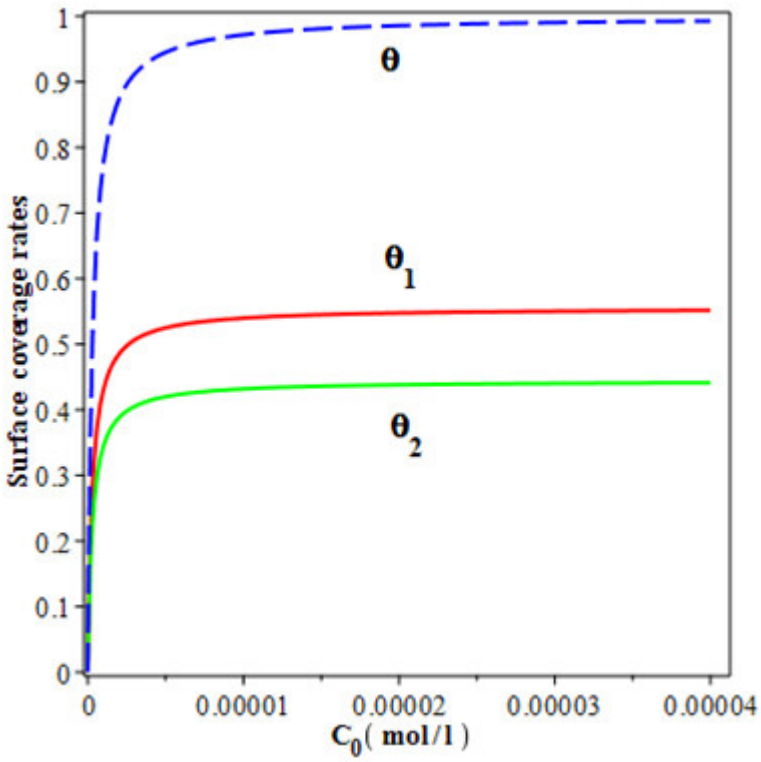

Figure IV.5: (Model A = 0). The versus concentrations of the native (Θ_1), unfolding (Θ_2) states and full surface coverage (Θ) calculated for BSA adsorption on a surface using data from [10] where, K_a=1.57 x10^5 $mol^{-1}lmin^{-1}$, K_f = 0.80 x10^{-2} min^{-1}, K_{d_1}= 0.74 x10^{-1} min^{-1} and K_{d_2}= 0.1x 10^{-1} min^{-1}.

During the first part of the kinetics, the native state Θ_1 (Eq. IV.7) initially increases sharply and then reaches a maximum value of 55% at the same time the unfolded state (Θ_2) (Eq. IV.8) increases sharply and then reaches a maximum value of 44%. But always native state Θ_1 is bigger than unfolded state (Θ_2). It's because of it the number of particles adsorbed from the surface is greater than the number of particles transform into unfold state.

The full surface coverage (Θ) (Eq.IV.9) initially increases sharply with the native state Θ_1 and unfolded state $\Theta_2$and then it reaches a maximum value of 98 % and a continuous equilibrium despite when increases the concentration C_0 **[19,20]**.

IV.2.2.Case of steady state ($K_a = K_{f+} K_{d_1}$ and $K_{d_2} = K_f$)

The previous solutions become as given by the following equations

$$\theta_1(t) = \frac{C_0}{2\,C_0 + 1} \qquad \text{(IV.10)}$$

$$\theta_2(t) = \frac{C_0}{2\,C_0 + 1} \qquad \text{(IV.11)}$$

$$\theta(t) = \frac{2\,C_0}{2\,C_0 + 1} \qquad \text{(IV.12)}$$

It is very clear that the only factor that can affect the surface coverage is the concentration of proteins in the bulk solution of protein (C_0).

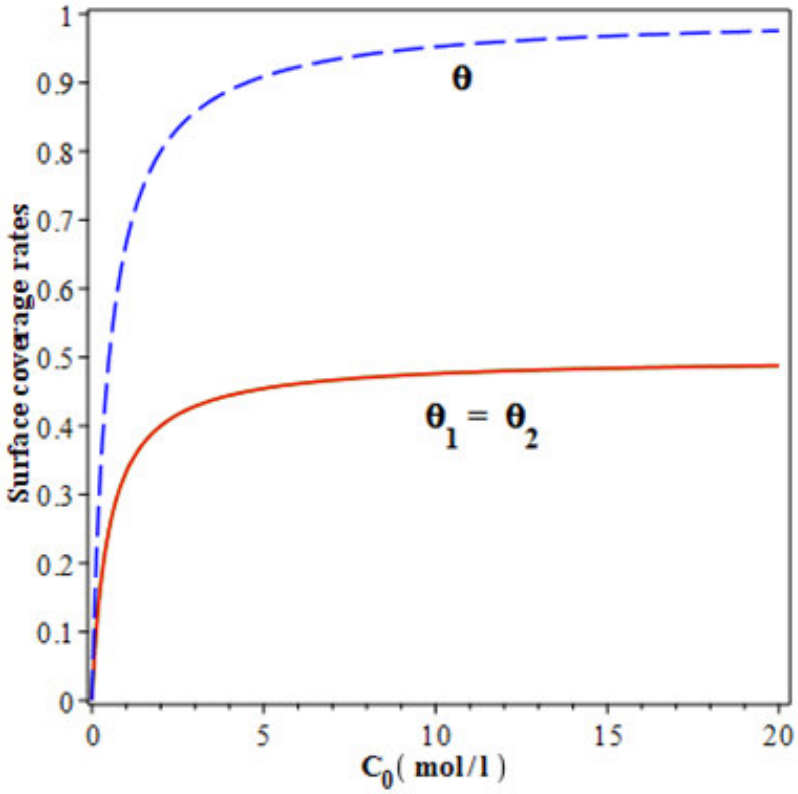

Figure IV.6: (Model A = 0). The versus concentrations of the native (Θ_1), unfolding (Θ_2) states and full surface coverage (Θ) calculated for BSA adsorption on a surface. The parameters used are $K_a = K_f + K_{d_1} = 0.082$ mol^{-1} l min^{-1}, $K_{d_2} = K_f = 0.8 \times 10^{-2}$ min^{-1} and $K_{d_1} = 0.74 \times 10^{-1}$ min^{-1} **[10].**

Figure IV.6 shows the dependence of different surface coverage (θ) of versus concentration C_0 of BSA in solution and taking into account the parameters K_a, K_f, K_{d_1} and K_{d_2}.The data in Figure IV.6indicates that the surface coverage native states and unfolding states are identical ($\Theta_1 = \Theta_2$)(Eq. IV.10, Eq. IV.11) initially increases sharply and then reaches a maximum value of 47 %, with a solution containing a single type of protein, the layer of adsorbed protein is likely to be Homogeneous. As the molecules adsorb on a clean surface if the same quantity which transform and desorb in unfolding state **[21,22]**.

The full surface coverage (θ) (Eq.IV.12), initially increases sharply and then reaches a maximum value of 96 % and a continuous equilibrium despite when increases the concentration C_0.

IV.3.The effect of available space during unfolding in the case of steady state

In a classical adsorption experiment, the protein with concentration C_0 in a solution is adsorbed on an isotropic and energetically homogeneous surface, and the number of adsorbed molecules held per unit surface area at the moment t is determined by the numbers of molecules that come to the surface from a solution and spread on it for the same time interval (Eq.IV.13). Proteins are irreversibly bonded on a surface with an adsorption rate constant K_a.

Adsorbed particles can spread (unfold) with the spreading rate constant K_f if a free surface is available (Eq. IV.14) **[6, 23, 24]**.The kinetic equations for the time evolution for both the $\Theta_1$and $\Theta_1$forms are as follows in the case of steady state:

$$\frac{d\Theta_1}{dt} = K_a C_0(1-\Theta_1 - \Theta_2) - K_f\Theta_1(1-\Theta_1 - \Theta_2) - K_{d_1}\Theta_1 = 0 \qquad \text{(IV.13)}$$

$$\frac{d\Theta_2}{dt} = K_f\Theta_1(1-\Theta_1 - \Theta_2) - K_{d_2}\Theta_2 = 0 \qquad \text{(IV.14)}$$

$$\frac{d\Theta}{dt} = \frac{d\Theta_1}{dt} + \frac{d\Theta_2}{dt} = K_a C_0(1-\Theta_1 - \Theta_2) - K_{d_1}\Theta_1 - K_{d_2}\Theta_2 = 0 \qquad \text{(IV.15)}$$

Where:

The mathematical solutions of the Eqs. (IV.13)- (IV.15) are indicated below:

$$\Theta_1(t) = \frac{-K_{d_2}(K_a C_0 + K_f + K_{d_1}) + \alpha_3}{2K_f(K_{d_1} - K_{d_2})} \qquad \text{(IV.16)}$$

$$\Theta_2(t) = \frac{((K_a C_0 + K_{d_1})K_{d_2} + K_f K_{d_1})\Theta_1(t) - K_a C_0 K_{d_2}}{(K_f\Theta_1(t) + K_{d_2})(K_{d_1} - K_{d_2})} \qquad \text{(IV.17)}$$

$$\Theta(t) = \Theta_1(t) + \frac{((K_a C_0 + K_{d_1})K_{d_2} + K_f K_{d_1})\Theta_1(t) - K_a C_0 K_{d_2}}{(K_f \Theta_1(t) + K_{d_2})(K_{d_1} - K_{d_2})} \qquad \text{(IV.18)}$$

Where:

$$\alpha_3 = \sqrt{K_{d_2}\{K_{d_2}[((K_a^2 C_0^2 + 2K_a C_0(K_{d_1} - K_f) + (K_{d_1} + K_f)^2] + 4K_a C_0 K_f K_{d_1}\}}$$

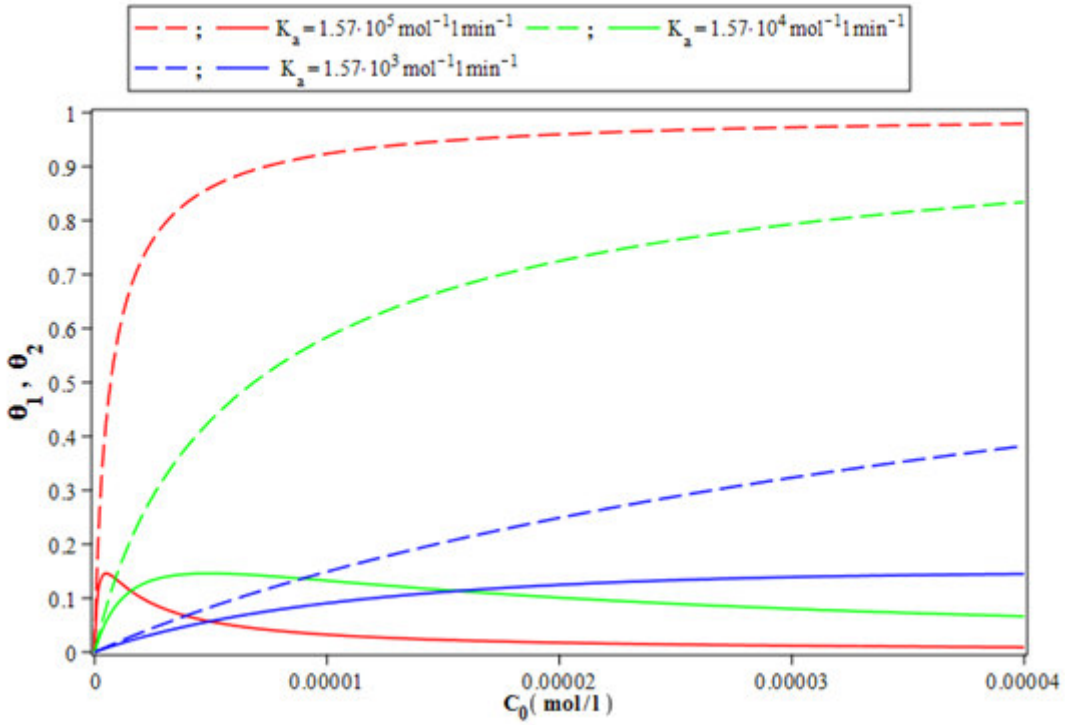

Figure IV.7: The concentration dependence of surface coverage of BSA where (Θ_1) indicated by dashed lines (— —) and continuous lines (——) for (Θ_2) for different values of rate adsorption constant K_a.The parameters used areK_f= 0.8 x $10^{-2}$$min^{-1}$, K_{d_1}= 0.74 x $10^{-1}$$min^{-1}$ and K_{d_2}= 0.1x 10^{-1} min^{-1}.

Figure IV.7 indicates that the surface coverage Θ_1(Eq. IV.16) initially increases sharply and then reaches a maximum equilibrium value of 97% at of concentration to C_0 = 0.3 x 10^{-4} mol/l. On the other hand, the surface coverage Θ_2, (Eq. IV.17) increases linearly sharply and then reaches a maximum value of 15% at of concentration to C_0 = 0.47 x 10^{-6} mol/l, and then gradually decreases to minimum value of 1% at the adsorption coefficient K_a= 1.57x 10^5 mol^{-1} l min^{-1}**[25,26]**.

When we reduce a K_a= 1.57x 10^4 mol^{-1} l $min^{-1}$the surface coverage Θ_1 increases and approaches a value of 83 % at of concentration to C_0 = 0.4 x 10^{-4} mol/l but the surface

coverage Θ_2 remains small value. We explain this result in both cases that the value of the adsorption coefficient is very large which helps the speed adsorption.

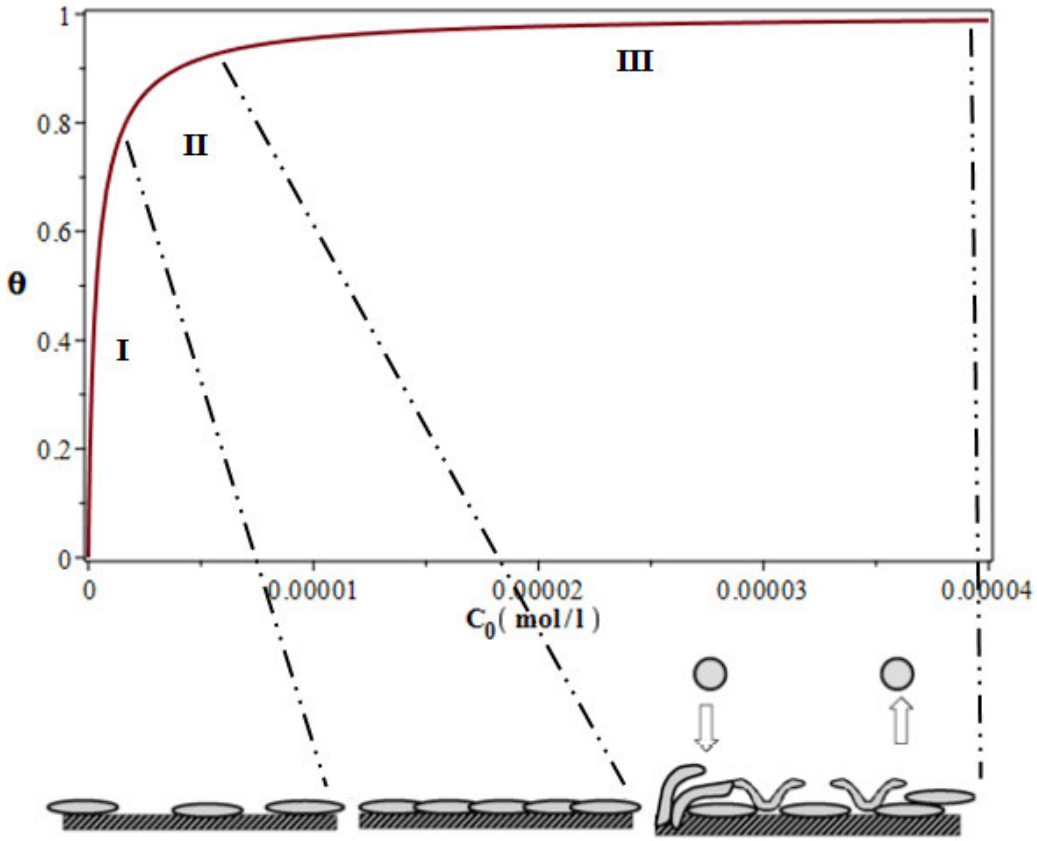

Figure IV.8: The concentration dependence of full surface coverage of BSA (Θ) for different concentrations. The parameters used areK_a= 1.57 x 10^5 mol^{-1} l min^{-1}, K_f= 0.8 x $10^{-2}min^{-1}$, K_{d_1}= 0.74 x $10^{-1}min^{-1}$ and K_{d_2}= 0.1x 10^{-1} min^{-1}.

Figure IV.8 Proposed adsorption model of the total surface coverage (eq.IV.18) Regions I, II, III represent the ascending portion, transition region and plateau, respectively, ofthe adsorption isotherm. The "elongated" structures represent unfolded protein adsorbed to the surface. In all three regions, this level of perturbation of the adsorbed state remains the same the difference comes from surface attachment sites. In regions I and II, there is ample surface available to all protein to maximize protein-surface contacts. However, in Region III, in order to maximize the number of proteins that can adsorb the number of surface attachment sites for each individual protein varies. The proteins with fewer attachments are most likely to desorb and refold into the native-like conformation **[20, 27-29]**.

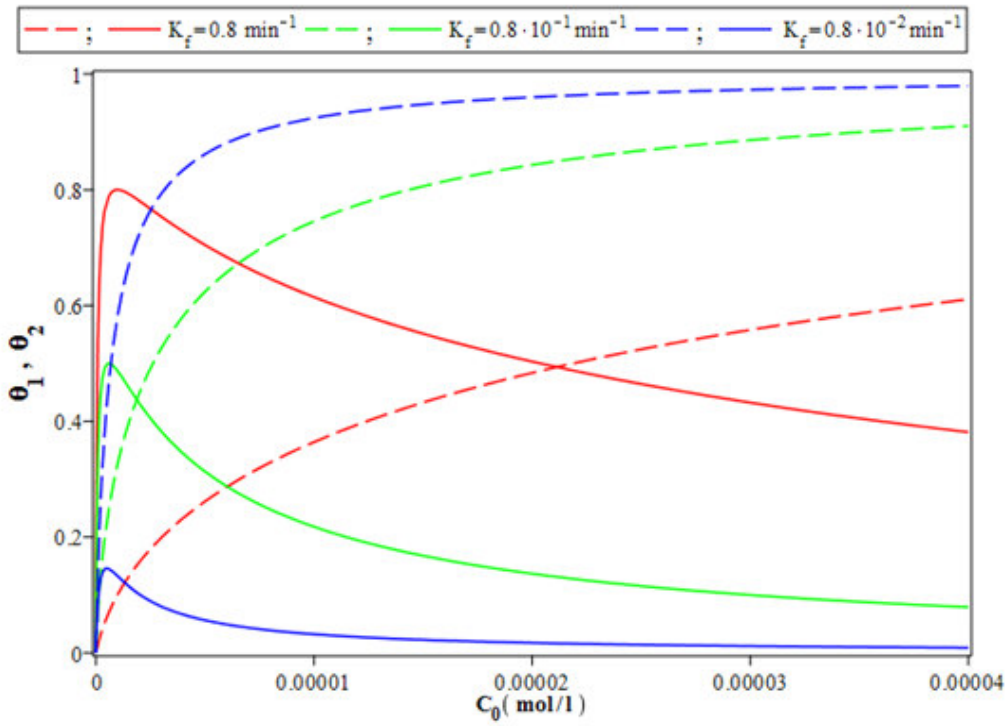

Figure IV.9: The concentration dependence of surface coverage of BSA where (Θ_1) indicated by dashed lines (— —) and continuous lines (——) for (Θ_2) for different values of rate transformation constant K_f. The parameters used areK_a = 1.57 x 10^5 mol^{-1} l min^{-1}, K_{d_1}= 0.74 x $10^{-1}$$min^{-1}$ and K_{d_2}= 0.1x 10^{-1} min^{-1}.

Figure IV.9 indicates that the surface coverage Θ_2(Eq. IV.12) initially increases sharply and then reaches a maximum value of 80% at of concentration to C_0 = 0.9 x 10^{-7} mol/l,there is ample surface available to all protein to rapidly transform from the native state $\Theta_1$to the unfolded state $\Theta_2$and this is due to the higher values transformation coefficient K_f = 0.8 min^{-1},and then gradually decreases to a value of 38 % despite increasing the concentration up to the value C_0 = 0.4 x 10^{-4} mol/l. On the other hand, the surface coverage Θ_1, (Eq. IV.11) gradually increases throughout the experience, and starts becoming predominant after the equilibrium point at the concentration C_0 = 0.21 x 10^{-4} mol/l**[30]**.

When we reduce a K_f= 0.8x $10^{-1}$$min^{-1}$the surface coverage $\Theta_2$initially increases and then reaches a value of 50% at of concentration to C_0 = 0.7 x 10^{-8}mol/land then gradually decreases to a value of 08 % to the value C_0 = 0.4 x 10^{-4} mol/l. On the other hand, the surface coverage Θ_1, gradually increases throughout the experience, and starts becoming predominant after the equilibrium point at the concentration C_0 = 0.18 x 10^{-} mol/l**[31]**.

The transformation rate constant is smaller the surface coverage Θ_1 increases and approaches a plateau value of 97 % and remains majority in a long time, so Θ_2 cannot be predominant in the system at the K_f= 0.8x 10^{-3} min^{-1} and it does not exceed 2 % at the concentration C_0 = 0.4 x 10^{-4} mol/land no intersection between them is observed where the amount of Θ_1 is still bigger than Θ_2.

IV.4.Comparison between the two models in steady state case

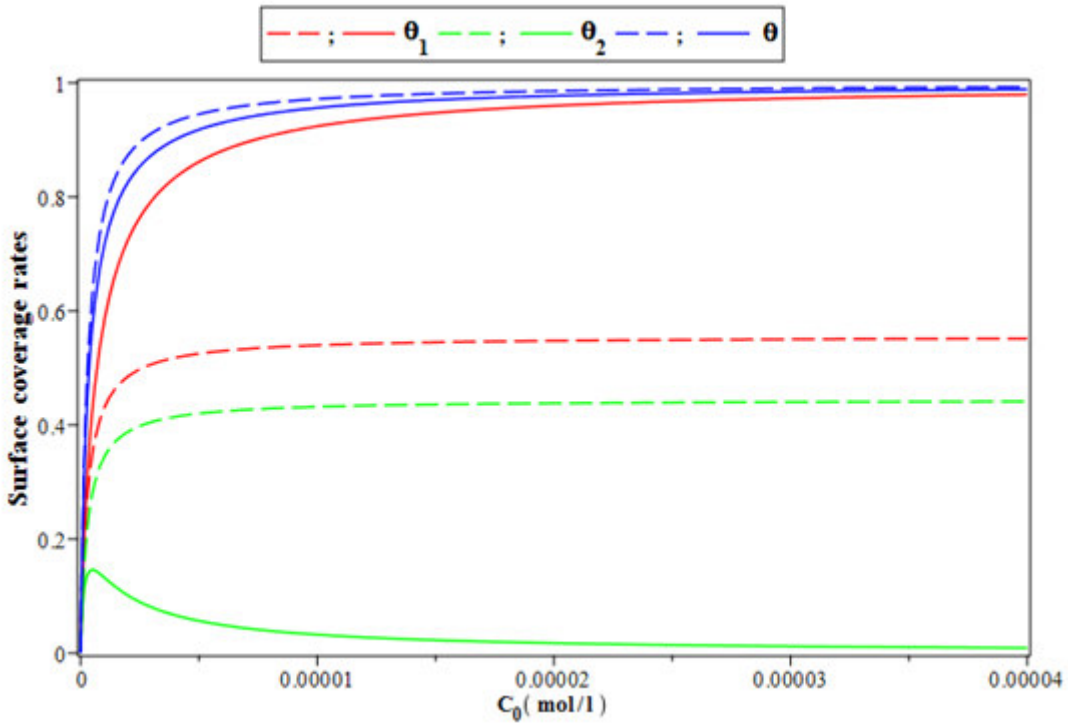

Figure IV.10: The versus concentrations of the native (Θ_1), unfolding (Θ_2) states and full surface coverage (Θ) of BSA where (Model A = 0) indicated by dashed lines (— —) and continuous lines (———) for (Model B = 0). The parameters used areK_a = 1.57 x 10^5 mol^{-1} l min^{-1},K_f= 0.8 x $10^{-2}$$min^{-1}$, K_{d_1}= 0.74 x $10^{-1}$$min^{-1}$ and K_{d_2}= 0.1x 10^{-1} min^{-1}.

The data in Figure IV.10 indicates the comparison between two models in the case of steady states. The surface coverage native states Θ_1, the Model A = 0is lower for Model B = 0and surface coverage unfolding states$\Theta_2$the Model A = 0 is bigger for Model B = 0.But the full surface coverageΘ the Model A = 0is bigger for Model B = 0, this is because Model A = 0 does not require space for adsorption**[30]**.

IV.4.1.Effect of available space in the case of time dependence of model B ($K_a = K_f + K_{d_1}$ and $K_f = K_{d_2}$)

To solve equations (IV.13-IV.15) in the case of time dependence, we need a numerical method which is used and called Runge-Kutta-Fehlberg order 4e-5e and the findings are indicated in the following graph.

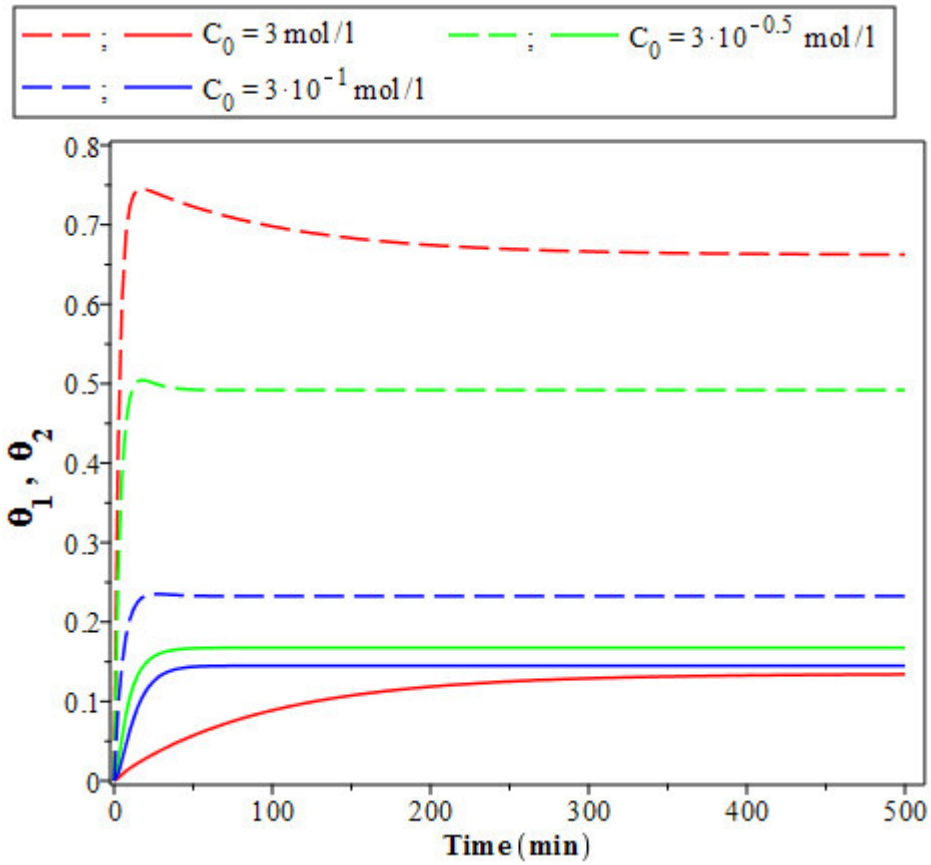

Figure IV.11: The time dependence of surface coverage of BSA where (Θ_1) indicated by dashed lines (— —) and continuous lines (——) for (Θ_2) for different concentrations (same color for each value of C_0). The parameters used are: $K_a=K_f+ K_{d_1}$= 0.082 mol^{-1} l min^{-1}, $K_{d_2}= K_f$= 0.8 x $10^{-2}min^{-1}$ and K_{d_1}= 0.74 x $10^{-1}min^{-1}$ **[10]**.

Figure IV.11 shows the time dependence of surface coverage by BSA and taking into account the parameters K_a, K_f, $K_{d_1}$and three different BSA solution concentrations.

The data in Figure IV.11indicates that the surface coverage Θ_1 initially increases sharply and then reaches a maximum value of 74% at a binding time of 17.5 min, and then gradually decreases to a value of 66 %.

The surface coverage Θ_2 gradually increases in the entire time interval and it does not exceed 14% at the higher concentration values C_0 = 3mol/l. When we decreases the concentration values $C_0 = 3\ 10^{-0.5}$mol/lthe surface coverage $\Theta_1$initially increases sharply and then reaches a maximum value of 50%at takes the same time of 17.5 minand then gradually decreases to a value of 49 % with the takes a stable state for a long time. The surface coverage Θ_2 gradually increases in the entire time interval and it does not exceed 17%**[32]**.

But when we decreases the concentration to $C_0 = 3 \times 10^{-1}$ mol/l, the adsorption of proteins on the surface is 23% Θ_1, the transformation and the desorption of proteins on the surface is 14% Θ_2.

The adsorption quantity of the native state Θ_1 is always higher than the unfolded state Θ_2 and further increases with increasing concentration value; the adsorption quantity of the native state Θ_1 is predominant.

IV.4.2.Comparison between the two models in the case of time dependence

The equations (IV.13- IV.15) given before in the case of steady state become as bellow and called model B and without space available it is named model A as presented in the previous chapter III.

$$\frac{d\Theta_1}{dt} = K_a C_0(1-\Theta_1-\Theta_2) - K_f\Theta_1(1-\Theta_1-\Theta_2) - K_{d_1}\Theta_1 \qquad \text{(IV.19)}$$

$$\frac{d\Theta_2}{dt} = K_f\Theta_1(1-\Theta_1-\Theta_2) - K_{d_2}\Theta_2 \qquad \text{(IV.20)}$$

$$\frac{d\Theta}{dt} = \frac{d\Theta_1}{dt} + \frac{d\Theta_2}{dt} = K_a C_0(1-\Theta_1-\Theta_2) - K_{d_1}\Theta_1 - K_{d_2}\Theta_2 \qquad \text{(IV.21)}$$

To solve the present coupled differential equations, one needs a numerical method as Runge-Kutta-Fehlberg order 4e-5e and the results are illustrated in the following graph Figure IV.12.

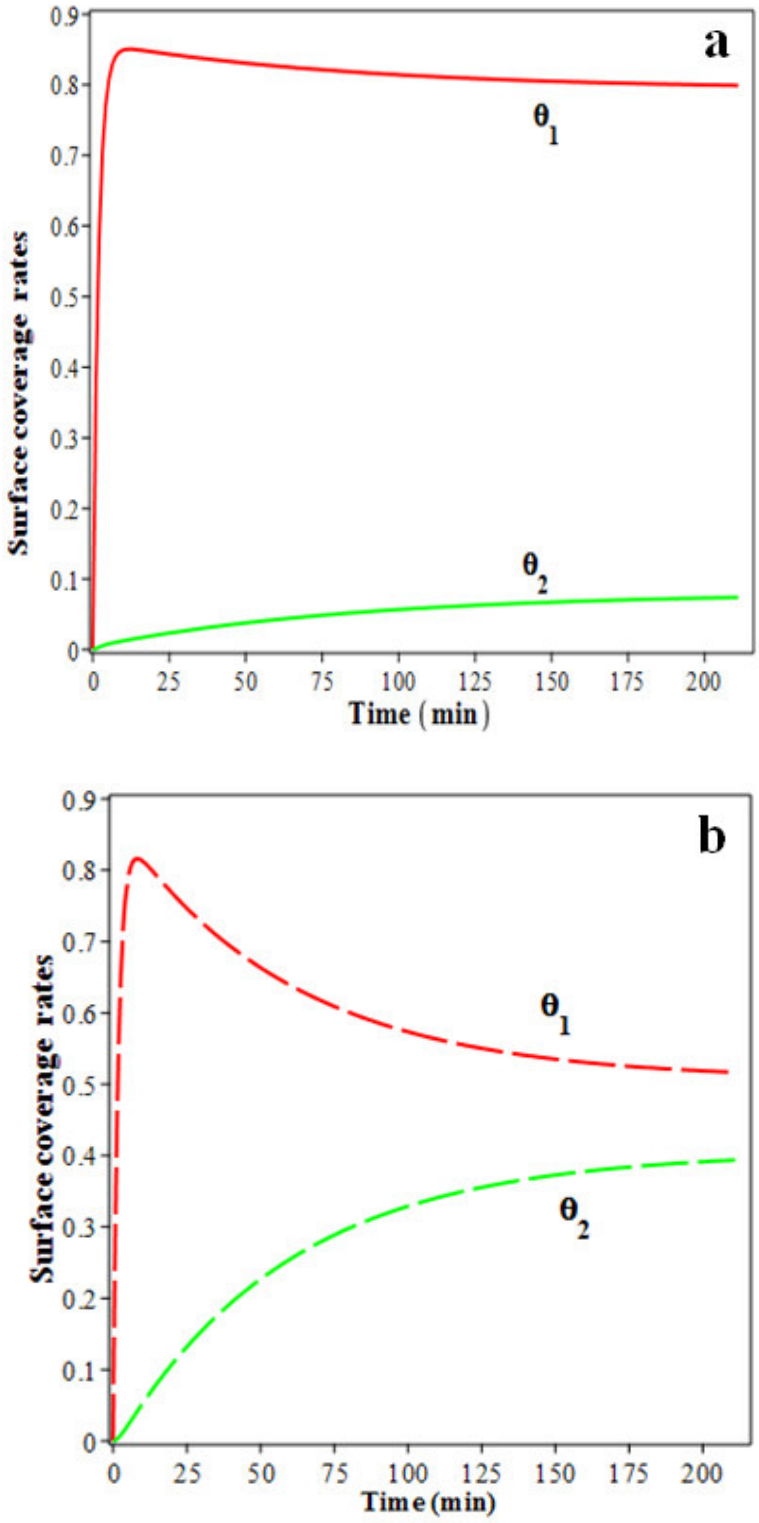

Figure IV.12: The time dependence of the native (Θ_1) andunfolding (Θ_2) states calculated for BSA adsorption on a gold surface using data from,(a)Model B VARIABLE and (b) Model A VARIABLE. The parameters used areC_0 = 3 x 10^{-6}mol/l, K_a= 1.57 x 10^5 mol^{-1} l min^{-1}, K_f = 0.8 x $10^{-2}min^{-1}$, K_{d_1}= 0.74 x $10^{-1}min^{-1}$ and K_{d_2}= 0.1x 10^{-1} min^{-1}**[33]**.

It is clear that the behavior of this phenomenon is not the same concerning native and unfolding states as indicated in Figure IV.12 where the effect of available space plays an important role in controlling this kind of unfolding at the surface.

IV.5. Application on FN adsorption and desorption processes

Taking the model of space available and in the case of $K_{d_2} = 0$ the model becomes as follow

$$\frac{d\Theta_1}{dt} = K_a C_0(1-\Theta_1-\Theta_2) - K_f\Theta_1(1-\Theta_1-\Theta_2) - K_{d_1}\Theta_1 \quad \text{(IV.22)}$$

$$\frac{d\Theta_2}{dt} = K_f\Theta_1(1-\Theta_1-\Theta_2) \quad \text{(IV.23)}$$

$$\frac{d\Theta}{dt} = \frac{d\Theta_1}{dt} + \frac{d\Theta_2}{dt} = K_a C_0(1-\Theta_1-\Theta_2) - K_{d_1}\Theta_1 \quad \text{(IV.24)}$$

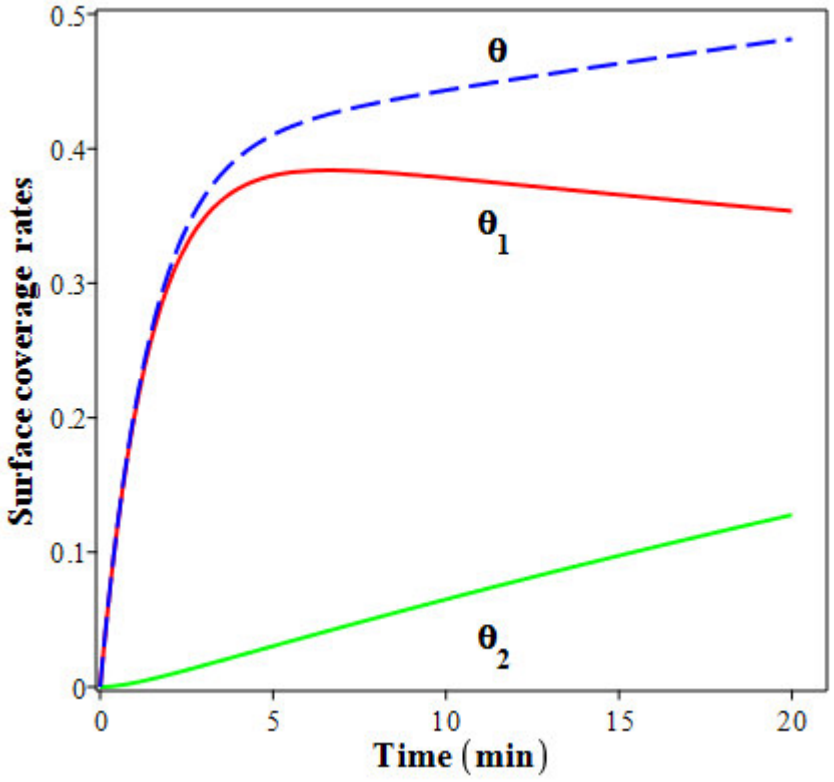

Figure IV.13: The time dependence of the native (Θ_1), unfolding (Θ_2) states and full surface coverage (Θ) calculated for FN adsorption on a surface using data from **[34]** where C_0 = 0.2g/l, K_a= 8.03 x 10^3 mol^{-1} l s^{-1}, K_f = 5.32 x 10^{-4} s^{-1} and K_{d_1} = 6.76 x 10^{-3} s^{-1}.

Jingtian Hu (2003) was obtained under experimental conditions by ESPS method and a comparison with Langmuir model was made. The rate constants for adsorption K_a = 8.03 x 10^3 mol^{-1} l s^{-1}, desorptionK_{d_1} = 6.76 x 10^{-3} s^{-1}, transform K_f= 5.32 x 10^{-4} s^{-1} andconcentration C_0 = 0.2 g/l.

We applied these measurements obtained by Jingtian Hu on model B case (K_{d_2}= 0) we obtained same results on θ_1 , θ_2 and θ inFigure IV.13. The native surface (θ_1) values first reach a peak then decrease with adsorption time, the unfolding surface (θ_2) increases with the time **[35-37].**

Because part of the protein molecules adsorption in reversible state is transformed to irreversible state, the reversible adsorption equilibrium is shifted. New protein is adsorbed from solution, which corresponds to the slight increases in total adsorption amount.

IV.6. Conclusion

The motivation for this work is to increase our understanding of the impact of various aspects of protein-surface interactions on protein stability. The ideas presented here suggest that expanding the traditional design space to include surface coverage representative of the entire adsorption isotherm yields unexpected results with respect to desorption behavior and its relationship to surface. In this chapter we compared the two models in their steady states and time dependence where the effect of available space during the unfolding process is very clear according to the findings reported here.

References

[1] N. Chandrasekaran, "The influence of amino acid properties on the adsorption of proteins and peptides to stainless steel surfaces". Doctoral thesis, University of Canterbury, New Zealand (2014).

[2] M. Malmsten, "Formation of adsorbed protein layers". Journal of Colloid and Interface Science, **207**, 186-199 (1998).

[3] R.C. Bi, Z. Dauter, E. Dodson, G. Dodson, F. Giordano, and C. Reynolds,"Insulin's structure as a modified and monomeric molecule". Biopolymers **23**,391-395 (1984).

[4] L.Lins, A. Thomasand R. Brasseur, "Analysis of accessible surface of residues in proteins". Protein Science **12**, 1406-1417 (2003).

[5] M. Lundin, Y. Hedberg, T. Jiang, G. Herting, X. Wang, E. Thormann, E. Blomberg, and I.O. Wallinder, "Adsorption and protein-induced metal release from chromium metal and stainless steel. Journal of colloid and interface science, **366**,155-164 (2012).

[6] M. Rabe, D. VerdesandS. Seeger, "Understanding protein adsorption phenomena at solid surfaces". Advances in Colloid and Interface Science, **162**, 87-106 (2011).

[7] M. Rabe, D. Verdes, J. Zimmermann and S. Seeger, "Surface organization and cooperativity during nonspecific protein adsorption events". J. Phys. Chem. B**112**, 13971–13980 (2008).

[8] F.A.M. Leermakers, M. Ballauff and O.V. Borisov,"On the mechanism of uptake of globular proteins by polyelectrolyte Brushes: A two-gradient self-consistent field analysis". Langmuir**23**, 3937-3946 (2007).

[9] K .Kubiak and P.A.Mulheran,"Molecular dynamics simulations of hen egg whitelysozymeadsorption at a charged solid surface". J. Phys. Chem. B **113**,12189–12200 (2009).

[10] M. Tadjine, F. Bouzidi, A. Berbri, H. Nehmarand A. Bouhekka,"In situ fourier transform infrared-attenuated total reflection spectroscopy and modeling investigation of protein adsorption: Case of expanded bovine serum albumin on titanium dioxide anatase.Biointerphases **19**(1), (2024).

[11 D.S. Salloum and J.B. Schlenoff, "Protein adsorption modalities on polyelectrolyte multilayers". Biomacromolecules**5**, 1089-1096 (2004).

[12] H. Hennessey, N. Afara, S. Omanovic and A.L. Padjen, "Electrochemical investigations of the interaction of C-reactive protein(CRP) with a CRP antibody chemically immobilized on a gold surface". Analytica Chimica Acta **643**, 45–53 (2009).

[13] D. Vitasari, P. Grassia and P. Martin,"Simulation of dynamics of adsorption of mixed protein-surfactant on a bubble surface", Colloids Surf. A Physicochem. Eng. Asp. **438**,63– 76 (2013).

[14] K.M. Yeung, Z.J. Lu and N.H. Cheung,"Adsorption of bovine serum albumin on fused silica: elucidation of protein–protein interactions by single-molecule fluorescence microscopy", Colloids Surf. B Biointerfaces **69**,246–250 (2009).

[15] M.M. Ouberai, Xu Kairuoand M.E. Welland, "Effect of the interplay between protein and surface on the properties of adsorbed protein layers". Biomaterials**35**, 6157– 6163 (2014).

[16] M. Rabeet al. "Surface organization and cooperativity during nonspecific protein adsorption events". J. Phys. Chem. B, **112**,13971–13980 (2008).

[17] M. Dargahi, E. Konkovand S. Omanovic, "Influence of surface charge/potential of a gold electrode on the adsorptive/desorptive behaviour of fibrinogen", ElectrochimicaActa. **174**, 1009–1016 (2015).

[18] H. Shenet al., "Single-Molecule Kinetics of Protein Adsorption on Thin Nylon-6,6 Films". Analytical Chemistry**80**, 9926-9933 (2016).

[19] A. Quinn1, H. Mantz, K. Jacobs, M. Bellionand L. Santen,"Protein adsorption kinetics in different surface potentials". Europhysics Letters **81**, 56003(2008).

[20] J.J. Gray, "L'interaction des protéines avec les surfaces solides ". Curr. Opin. Struct. Biol.**14**, 110-115 (2004).

[21] R.Mucae*t al.*,"Effects of negative and positive cooperative adsorption of proteins on hudrophobic interaction chromatography media". Journal of Chromatography A **1625** 461309(2020).

[22] R.A. LatourJr, "Biomaterials: Protein surface interactions". Encyclopedia of Biomaterials and Biomedical Engineering 270-284 (2008).

[23] B.A. Snopok and E.V. Kostyukevich,"Kinetic studies of protein–surface interactions: A two-stage model of surface-induced protein transitions in adsorbed biofilms".Analytical Biochemistry **348**, 222–231(2006).

[24] M.A. Brusatori and P.R. Van Tassel, "A kinetic model of protein adsorption/surface induced transition kinetics evaluated by the scaled particle theory". Journal of colloid and interface science **219**, 333-338(1999).

[25] I. Lundström,"Models of protein adsorption on solid surfaces".Surfactants, Adsorption, Surface Spectroscopy and Disperse Systems. Progress in Colloid and Polymer Science**70**,76-82(2007).

[26] A. Docoslis et al., "Measurements of the kinetic constants of protein adsorptionontosilica particles". Colloids and Surfaces B: Biointerfaces **13**, 83-104(1999).

[27] F. Felsovalyi, "Mechanistic study of the adsorption and desorption of proteins on silica".Doctoral thesis, University of Columbia (2012).

[28] M.F.M. Engel, C.P.M. Van Mierlo and A.J.W.G. Visser,"Kinetic and structuralcharacterization of adsorption-induced unfolding of bovine α-Lactalbumin". Journal of Biological Chemistry, **277**, 10922-10930 (2002).

[29] J.D. Andrade and V. Hlady,"Protein adsorption and materials biocompatibility: A tutorialreview and suggested hypotheses". Adv. Polym. Sci, **79**, 1-63 (1986).

[30] V.P. Zhdanov and B. Kasemo,"Monte Carlo simulation of the kinetics of protein adsorption".Proteins: Structure, Function, and Bioinformatics **30**, 177-182 (1998).

[31] N. Willem,"Adsorption of proteins at solid-liquid interfaces". Cells and Materials **5**, 9(1995).

[32] J. Kim, Mathematical modeling approaches to describe the dynamics of protein adsorption at solid interfaces, Colloids Surf. B Biointerfaces **162**, 370–379(2018).

[33] M. Dargahi and S. Omanovic,"A comparative PM-IRRAS and ellipsometry study of the adsorptive behaviour of bovine serum albumin on a gold surface", Colloids and Surfaces B: Biointerfaces**116**, 383–388 (2014).

[34] Hu Jingtianet *al*., "Estimation the kinetics parameters for non-specific adsorption of fibrinogen on quartz surface from the response of an electrode-separated piezoelectric sensor". Sensors and Actuators B: Chemical **96**, 390-398 (2003).

[35] Y.A. Mao, W.Z. Wei, H. Peng and J.Z. Zhang,"Monitoring for adsorption of humanserumalbumin and bovine serum albumin onto bare and polystyrene modified silverelectrodes by quartz crystal impedance analysis", J. Biotechnol. **89**, 1–10 (2001).

[36] F. Höök, J. Vörös, M. Rodahl, R. Kurrat, P. Bxni, J.J. Ramsden, M. Textor, N.D. Spencer, P. Tengvall, J. Gold and B. Kasemo, "A comparative study of

protein adsorption on titanium oxide surfaces using in situ ellipsometry, optical waveguide light mode spectroscopy, and quartz crystal microbalance dissipation", Colloids and Surfaces B Biointerfaces**24**,155-170 (2002).

[37] H. Jingtian et *al.*,"Bovine serum albumin adsorption on N-methyl-d-glucamine modified colloidal silica". Colloids and Surfaces A: Physicochemical and Engineering Aspects **349**, 207-213 (2009).

General conclusion and perspectives

The interactions of proteins with solid surface are one of the most important topics in physics and chemistry of surfaces. This interface is very important in many fields such as in biology and biocompatibility. However this phenomenon still not well understood because of the complex structure and the factors that can control their behavior such as: pH, concentration, temperature, the surface roughness and the charges….

To investigate the adsorption of proteins with solid surface one can use an in situ spectroscopic technique like FTIR-ATR which is a powerful instrument that can provide information about the kinetic of adsorption of the proteins over surfaces. FTIR-ATR can be used under different conditions.

In this present manuscript; we were interested to study the interactions of proteins with solid surface especially BSA at TiO_2 to determine the rate of surface coverage of proteins in its two states of adsorption native and unfolded taking into account the possible transformations and the desorption.

To achieve this goal, we extended two states kinetics model taking into account the desorption in both cases. The proposed model was applied on experimental data taken by FTIR of expanded BSA protein at the surface of TiO_2 anatase where the rate constant of adsorption was determined.

In the last part of this work, we demonstrated the effect of free available space during unfolding process and compared it with the previous model. This work clearly illustrated the complexity of the process and it gives an important value to the modeling work to complete experimental weakness.

As perspective; in the future we are interested to study the effect of other agents on adsorption like temperature.